Journal of Pyrotechnics

Issue 13, Summer 2001

CAUTION

The experimentation with, and the use of, pyrotechnic materials can be dangerous; it is felt to be important for the reader to be duly cautioned. Without the required training and experience no one should ever experiment with or use pyrotechnic materials. Also, the amount of information presented in this Journal is not a substitute for necessary training and experience.

A major effort has been undertaken to review all articles for correctness. However, it is possible that errors remain. It is the responsibility of the reader to verify any information herein before applying that information in situations where death, injury, or property damage could result.

Table of Contents

Issue 13   Summer 2001

Publication Frequency

The *Journal of Pyrotechnics* appears approximately twice annually, typically in mid-summer and mid-winter.

Subscriptions

Anyone purchasing a copy of the Journal will be given the opportunity to receive future issues on an approval basis. Any issue not desired may be returned in good condition and nothing will be owed. So long as issues are paid for, future issues will automatically be sent. In the event that no future issues are desired, this arrangement can be terminated at any time by informing the publisher. Additional discounts are available for payment in advance for issues of the *Journal of Pyrotechnics*. Contact the publisher for more information.

Back issues of the Journal will be kept in print permanently as reference material.

Evaluation of Lithium Compounds as Color Agents for Pyrotechnic Flames

Ernst-Christian Koch

Morlauterer Straße 103a, D-67567 Kaiserslautern, Germany

ABSTRACT

The obstacles to producing red colored pyrotechnic flames with lithium compounds are discussed. The principle emitter of red light in such flames is atomic lithium. Hydrogen and halogens in the flame gases are expected to have a substantial effect on the concentration of atomic lithium. The development of effective Li-based red color compositions therefore depends primarily on the proper control of the concentrations of hydrogen and halogens in the flame to maximize the formation of atomic Li. Some possible ways of doing this are proposed and are supported by thermodynamic calculations.

Keywords: lithium, pyrotechnics, red flame, color agent

Introduction

Strontium and calcium compounds yield red to orange-red pyrotechnic flames. The mechanisms leading to these colors have been described in great detail by Shimizu[1a,2] and Douda;[3,4] SrCl, SrOH, CaO, and CaCl are the main species responsible for emission in the red and orange-red regions of the visible spectrum. For as long as pyrotechnists have composed new formulas to generate red flames, the possibility of using materials other than strontium has been discussed. Although it would be advantageous to substitute the relatively expensive strontium with calcium, calcium-containing compositions yield a yellowish red that is much less useful than the purplish red of strontium.

Several other elements have been reported to yield a red flame color when introduced into the flame of a laboratory burner. These elements are listed in Table 1.

Radium is known to display a beautiful carmine flame, which can be attributed to the molecular emission of both monochloride and hydroxide,[5a] but the radioactivity of radium obviously prohibits its application as a flame colorant. Despite its radioactivity, the low natural abundance makes radium very expensive and thus would certainly rule out any application in pyrotechnics. The rare earth elements have been recently proposed to be potentially useful as color agents.[6] Among these, yttrium (Y), neodymium (Nd), praseodymium (Pr), scandium (Sc), and samarium (Sm) show molecular (monoxide) emission in the red region of the spectrum. Unfortunately, the most promising of these elements (Y and Sm) are expensive compared to strontium and calcium compounds. (The cost of $(Sm(ClO_4)_3$ is US\$5/g and that of

Table 1. Elements that Display Red Flame Colors and the Color-Emitting Species.

Element	Emitter	Main lines (nm)	Reference
Radium	RaCl, RaOH	676, 650	5a
Yttrium	YO	603,607	6,12c
Neodymium	NdO	650, 658, 660, 663	12c
Praseodymium	PrO	680–710 (broad)	12c
Scandium	ScO	603–636 (broad)	12c
Samarium	SmO	651, 652	6,12c
Lithium	Li	610, 670	3

Y(NO$_3$)$_3$·4H$_2$O is US$10/g). Even as industrial chemicals, they are still fairly expensive, for example, 5 kg lots can be found for:

99.5%	Y	US $146
99.9%	Y	US $152
99.9%	Y$_2$O$_3$	US $ 79.50
99%	Sm	US $120

In addition, these chemicals are toxic, which makes them unattractive for practical applications.

In contrast, lithium compounds are readily available, relatively economical, and show only moderate effect on either health or the environment compared to yttrium and samarium. Lithium should be a promising substitute for strontium in red pyrotechnic flames. The low atomic mass of lithium should be an advantage in items where the weight of the composition needs to be kept as low as possible. An additional advantage is the atomic/molecular weight of the corresponding emitters. Whereas SrCl—the main emitter in the red—has a molecular weight of 123.07, the atomic weight of lithium is only 6.94. This at first glance calls (regardless of any comparison of the respective emission intensity) for an increase of specific intensity ($J \cdot g^{-1} \cdot sr^{-1}$) by a factor of 17 changing from strontium to lithium. Although no exact data on specific emission intensity values for SrCl and Li are available, threshold values for the visible detection of the respective color have been reported.[18,28]

When applying a SrCl$_2$ solution to a lab burner, amounts as low as 2.4×10^{-8} g (SrCl) are said to be detectable. This corresponds to 1.94×10^{-10} moles of SrCl. In contrast, when applying LiCl to lab burner flames, amounts as low as 1.5×10^{-9} g (Li) are said to be visible with the naked eye, which corresponds to

2.16×10^{-10} moles of Li.[18,28] Thus, substitution of strontium by lithium as the desired emitter in any yet hypothetical formulation would cause a reduction in weight of the color agent by a factor of about one-tenth.

Lithium in Flames

Most chemists know that lithium compounds yield a bright scarlet flame color, similar to that produced by strontium compounds. Unfortunately, the author has not yet found any useful pyrotechnic composition showing that effect. However, most chemical reference books, as well as some monographs on energetic materials, assert the application of lithium nitrate, lithium chloride or lithium carbonate in pyrotechnics for scarlet colored flares and stars.

Although Jennings-White[7,8] gave details of a "pink" lance and of a strobe composition consisting of lithium perchlorate (LiClO$_4$) and hexamine (C$_6$H$_{12}$N$_4$), there is no indication of why only a pink—instead of a scarlet—flame color is obtained with these formulations. In addition, Chavez and coworkers[9] reported recently a "pumpkin orange" flame (with color values $x = 0.534$, $y = 0.398$) upon combustion of a composition made of ammonium perchlorate, dihydrazinotetrazine (DHT) and lithium carbonate (see Table 2).

In contrast to these disappointing attempts, combustion of several lithium compounds: (LiAlH$_4$, LiBH$_4$, LiC$_2$H$_5$) in air,[10a] as well as combustion of volatile lithium salts in methanol,[11] yield beautiful scarlet colored flames. These experiments, although not involving pyrotechnic compositions, indicate the appropriate chemistry to obtain scarlet flames with lithium.

Table 2. Lithium Compounds in Pyrotechnic Formulations.

	Weight Percent				
Application	LiClO$_4$	NH$_4$ClO$_4$	DHT	Li$_2$CO$_3$	C$_6$H$_{12}$N$_4$
Lance	75	—	—	—	25
Star	—	49.5	49.5	1.0	—
Strobe lance	50	—	—	—	50

Discussion

Introducing a lithium salt solution into the flame of a laboratory burner yields a red flame, which is due to the emission lines given in Table 1. These emissions originate from radiative transitions of gaseous atomic lithium. The main line at 670.8 nm corresponds to a $2s\,^2S_{0\frac{1}{2}}$ (ground level) – $2p\,^2P^0_{0\frac{1}{2},1\frac{1}{2}}$ (two energetically similar excited levels)[12a] transition as shown in Figure 1. (The ordinate gives the corresponding energy in units of eV; IP designates the ionization potential.)

In addition to atomic emission, lithium dimers exhibit a series of line emissions from 769.0 to 665.9 nm with the strongest line at 688.4 nm.[5b] In flame gases, however, lithium vapor is only 1% Li_2 and 99% atomic lithium according to equation 1,[13a] so that the contribution of the Li_2 emission to the red flame color would be negligible.

$$Li_{2(g)} + 110.6\ kJ \Leftrightarrow 2\ Li_{(g)} \qquad (1)$$
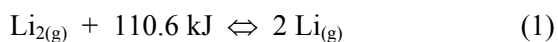
In common pyrotechnic flames these lines are superimposed on a continuum starting at 280 nm with a maximum at 400 nm, which interferes with color purity.[12b] This continuum is due to emission by $LiOH_{(g)}$ as shown in equation 2.[14]

$$Li_{(g)} + H_2O_{(g)} \Leftrightarrow LiOH_{(g)} + H_{(g)} \qquad (2)$$

Ubiquitous H_2O molecules thus scavenge lithium atoms to give thermodynamically stable $LiOH_{(g)}$.

Sodium's atomic emission is responsible for the bright yellow flame in illuminating flares and torches, but the above effect has only a minor consequence on color purity. In contrast to equation 2, sodium (equation 3) follows a different process.

$$Na_{(g)} + OH_{(g)} \Leftrightarrow NaOH_{(g)} + h\nu_{(continuum)} \qquad (3)$$

This reaction has no effect on color purity since the thermal stability of NaOH is much lower compared to LiOH, which gives rise to only trace amounts of NaOH in sodium flames. Table 3 lists the dissociation energies for gaseous alkali metal hydroxide (MOH) decomposition according to equation 4.[15a]

$$M_{(g)} + OH_{(g)} \Leftrightarrow MOH_{(g)} \qquad (4)$$

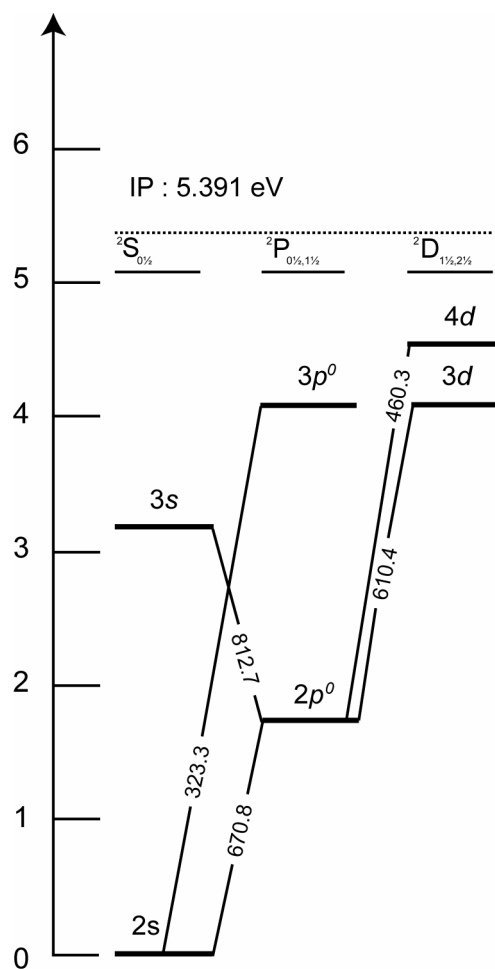*Figure 1. Atomic term diagram for lithium.*

Table 3. Dissociation Energies for Gaseous Metal Hydroxides ($MOH_{(g)}$).

Element	Dissociation Enthalpy of $MOH_{(g)}$ (kJ/mol)
Lithium	423
Sodium	322
Potassium	339
Rubidium	347
Cesium	381

As a consequence, $LiOH_{(g)}$ formation in pyrotechnic flames has to be inhibited to obtain maximum atomic emission.

It is known that the hydrogen content of flames can be determined via evaluation of Li emission intensity.[15c] In view of this, the amount of gaseous LiOH should be reduced by the introduction of hydrogen, following equation 5,[16a] that is the reverse of equation 2.

$$LiOH_{(g)} + H_{(g)} \Leftrightarrow Li_{(g)} + H_2O_{(g)} \qquad (5)$$
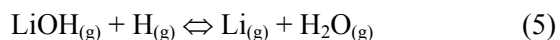
Another disturbing effect on red flame color in lithium flames is the presence of halogens, especially chlorine. From the standpoint of oxygen content, lithium perchlorate ($LiClO_4$) is superior to any other oxidizer (60.15% oxygen by weight is available for oxidation).[17] Nevertheless, flame color with $LiClO_4$ is only pale pink as has been stated above. In contrast to barium, strontium and calcium, which, in the presence of chlorine or bromine, produce relatively stable monohalide molecules that respectively emit bands in either green, red or orange-red regions of the spectrum, halogens suppress the lithium flame spectrum as has been stated in reference 18. This effect is due to the formation of lithium chloride according to equation 6, in which X is a halogen.

$$Li_{(g)} + X_{(g)} \Leftrightarrow LiX \qquad (6)$$

Lithium chloride (as well as the other halides of lithium) exhibit no lines in the visible range but show strong continuum emission with superimposed bands at 281, 285 and 290 nm.[5c] It is interesting to note that LiF has been reported to yield a bluish glow in flames, which should originate from C-type chemiluminescence,[18] but at present it is not known if this effect could be exploited pyrotechnically. It has been explained that the introduction of halogens or their precursors in lithium-containing flames depletes the LiOH content due to the reaction given in equation 7.[16b]

$$LiOH_{(g)} + X_{(g)} \Leftrightarrow LiX_{(g)} + OH_{(g)} \qquad (7)$$
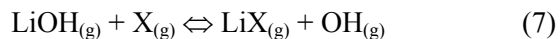
The ratio of $LiOH_{(g)}/Li_{(g)}$ itself is not changed by this reaction, but the amount that may be shifted to atomic lithium is irretrievably reduced. Thus, color purity is reduced. These findings explain the unsuccessful attempts to obtain red colored flames with traditionally formulated compositions containing lithium compounds and chemically bound halogens.

Consequences

Any discussion of the flame chemistry of lithium would be incomplete without an attempt to find a practical approach to using lithium compounds to give a red color in fireworks or even signaling applications.

The relationship between the hydrogen content of a flame and intensity of atomic emission calls for hydrogen-rich flames. Atomic hydrogen concentration is highest in flames with a less than stoichiometric oxygen/hydrogen ratio.[15b] Thus the application of hydrogen rich fuels should be helpful in obtaining strong $Li_{(g)}$ emission.

Since lithium perchlorate and also ammonium perchlorate are common oxidizers due to their readiness to yield oxygen in fireworks and pyrotechnics, a method should be found to prevent the scavenging of atomic lithium by the chlorine contained in these compositions.

Introduction of aluminum, preferably chemically bound (as in $Al(OR)_3$, where R, is an alkyl) could act as a color intensifier. Aluminum compounds are preferred over elemental aluminum since the volatility of compounds, especially metal-organic compounds, provides vaporization of aluminum within the combustion zone where it has to be supplied for further reaction with abundant halogens. With elemental aluminum, in contrast, solid-state oxidation is known to occur, which would lead mainly to a sparking flame.

Aluminum monoxide, AlO, is the main emitter in Al-containing flames, and it displays only weak continuum and spectral lines at 465, 484 and 708 nm.[1b] This is in contrast to MgO, which shows a strong continuum and thus enhances light output.

The emitters responsible for red, green and blue colors—in traditional pyrotechnic flames—are SrCl, BaCl and CuCl, respectively. These unstable compounds exist in equilibrium with the corresponding free atoms. In the presence of aluminum, chlorine is scavenged to yield AlCl.[19] This is easily explained by comparing the dissociation enthalpies of both AlCl and the previously mentioned monochlorides.[19]
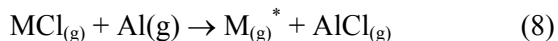
ΔH_D: AlCl: 511 kJ·mol^{-1}

ΔH_D: SrCl: 406 kJ·mol^{-1}

ΔH_D: BaCl: 436 kJ·mol^{-1}

ΔH_D: CuCl: 383 kJ·mol^{-1}

The higher dissociation enthalpy for the Al-Cl bond gives rise to the preferential formation of AlCl according to equation 8.

$$MCl_{(g)} + Al_{(g)} \rightarrow M_{(g)}{}^* + AlCl_{(g)} \qquad (8)$$

where M*, is excited Ba, Cu or Sr. Consequently, the presence of Al in the flame would reduce the concentration of the MCl molecules and thus suppress the emission of the desired colored light.

In the case of lithium, however, the presence of Al is beneficial. Lithium chloride, as with the monochlorides of Ba, Cu and Sr, has a lower dissociation enthalpy than AlCl, causing aluminum to react with gaseous LiCl to release free Li atoms.

ΔH_D: LiCl: 469 kJ·mol^{-1}

In addition, AlCl displays only lines in the ultraviolet at 261, 265 and 268 nm and no lines or continua in the visible.[20] It is not, therefore, expected to have any detrimental effect on the color purity of the flame. Similarly other elements showing ΔH_D values for their monochlorides higher than that of LiCl, and having no— or only weak—bands in the visible should be practical scavengers for Cl in Li-containing flames (e.g., ZrCl, with weak emission at 400–415 nm).[19,24]

Thermal Behavior of Lithium Compounds Suitable for Pyrotechnical Applications

In an effort to steer the development of pyrotechnics away from intuition and towards a more scientific approach, the thermal behavior of lithium compounds will now be discussed. Unless otherwise stated, the discussion will focus on the properties of the anhydrous species.

a) Lithium nitrate ($LiNO_3$), upon thermal treatment decomposes according to equation 9

$$2\, LiNO_3 \rightarrow 2\, LiNO_2 + O_2 \uparrow$$
$$\rightarrow Li_2O + N_2 + 3/2\, O_2 \qquad (9)$$
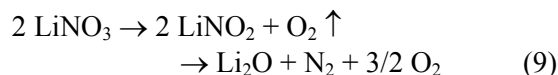
Lithium nitrate melts at 255 °C. Decomposition starts at 365 °C as slight bubbles evolve. At 472 °C the oxygen partial pressure ($p(O_2)$) equals 1 atm (101.3 kPa).[13b] Ellern[10b] summarized the heat of combustion for various $LiNO_3$/fuel mixtures. Li_2O, the main combustion product of such nitrate/fuel mixtures melts at 1570 °C. Its fugacity (vapor pressure) becomes 1 atm (101.3 kPa) at 2563 °C.[21]

b) Lithium perchlorate ($LiClO_4 \cdot 3H_2O$) loses 2 moles of H_2O between 60 and 148 °C; upon further heating, between 148 and 250 °C the last H_2O molecule is released. Oxygen evolution starts at 310 °C, and the exothermal decomposition starts at 474 °C, according to equation 10.

$$LiClO_4 \rightarrow LiCl + 2\, O_2 \qquad (10)$$
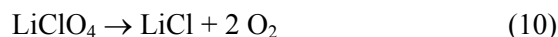
Melting occurs at 596 °C.[27] The anhydrous salt melts at 236 °C and decomposes according to equation 10 at 440 °C. Ellern[10b] summarized the heat of combustion for various stoichiometric $LiClO_4$/fuel mixtures.

c) Lithium pentandionate ($Li(C_5H_7O_2)$) is as yet a hypothetical fuel. It has been shown that the pentandionates of copper, strontium, barium, molybdenum, lanthanum, zirconium[22] and cerium[23] are suitable to impart blue, red, green, citron, pale white, dazzling white and orange colors to pyrotechnic flames in mixtures with ammonium perchlorate (AP). Since the pentandionate ligand has a large hydrogen surplus, lithium pentandionate should act as both a flame color agent and as a flame deoxidizer. Nevertheless, lithium pentandionate would require either a chlorine-free oxidizer such as TMAN (tetramethyl ammonium nitrate) or if AP were used as the oxidizer, a suitable chlorine scavenger would need to be included in the composition.

Lithium pentandionate melts at 250 °C and would presumably break down at higher temperatures to release pyrolysis products of the organic ligand including CO and alkyl fragments.

Table 4. Stoichiometry of Compositions Investigated.

Composition	Weight Percent					
	$LiClO_4$	Al	NH_4ClO_4	Mg	Li_2CO_3	$C_6H_{12}N_4$
I[8]	50	—	—	—	—	50
II	33	34	—	—	—	33
III	33	—	—	34	—	33
IV	—	—	40	35	25	—
V	—	35	40	—	25	—

d) <u>Lithium carbonate</u> (Li_2CO_3) is an anhydrous lithium salt. It melts at 723 °C and decomposes at 1300 °C to give CO_2 and lithium oxide. Application of lithium carbonate as a color agent should require both high flame temperature and excess fuel to promote the formation of atomic lithium by decomposition and reduction. As lithium carbonate is a strong base (pH 11), it is incompatible with aluminum fuel.

e) <u>Lithium oxalate</u> ($Li_2C_2O_4$) is a colorless, anhydrous crystalline substance that is soluble in water and decomposes at 590 °C according to equation 11 to give lithium carbonate whose further decomposition was described in (d).

$$Li_2C_2O_4 \rightarrow Li_2CO_3 + CO \tag{11}$$

f) <u>Lithium fluoride</u> (LiF) is a colorless, crystalline, toxic substance that is slightly soluble in water and acids, melts at 845 °C, and boils at 1680 °C. It has a substantial vapor pressure at temperatures >1100 °C.

g) <u>Lithium benzoate</u> ($C_7H_5O_2Li$) is a colorless crystalline substance that melts at temperatures >300 °C. Its metal content is very low compared to the other lithium salts mentioned (5.42%).

Although complex lithium hydrides such as $LiAlH_4$ and $LiBH_4$ are reported to give a beautiful red color upon combustion, their sensitivity towards moisture makes them too dangerous to be handled as color agents.

It is noteworthy to mention that even elemental lithium has found application in pyrotechnics. A disclosure on IR decoy flares asserts a composition consisting of hollow PTFE blocks filled with granular lithium.[29] It seems at least that the low volume-to-surface ratio of coarse lithium prevents oxidation of the complete lithium. Although no stoichiometric proportions are given in the disclosure, a lithium-rich composition should be feasible in terms of yielding both a high burn rate and a high specific IR intensity. At $\xi(Li) = 0.42$, the maximum $Li_{(g)}$ mole fraction in the combustion products is attained.[25]

Thermodynamic Calculation

To prove the prediction that aluminum should act as a beneficial additive to pyrotechnic compositions, thermodynamic calculations[25] were performed on the strobe system given by Clive Jennings-White[8] and on compositions containing either aluminum or magnesium. Although lithium carbonate and aluminum are known to be incompatible chemicals[26] due to the alkaline decomposition of aluminum, calculations were performed with Li_2CO_3/aluminum/ammonium perchlorate mixtures to confirm the capability of strong reductive fuels to yield elemental lithium from lithium carbonate and demonstrate the suppression of LiCl formation by aluminum. All stoichiometries are given in Table 4.

The mole fractions of the relevant combustion products (the sum does not add up to 1) are listed in Table 5. Composition I displays the major combustion products for the composition given by Clive Jennings-White. It is clear that almost all of the lithium is converted to LiCl, which does not emit in the visible region. Only trace amounts of elemental lithium are formed. This explains the observed pale pink color of the flame of this composition.

The addition of equivalent weight amounts of aluminum to Clive Jennings-White's composition, as shown in composition II, results in the formation of substantial amounts of elemental

Table 5. Mole Fractions of Relevant Combustion Products.

Composition	H_2	H_2O	Li	LiCl	LiOH	MgCl	AlCl	CO
I[8]	0.39965	0.00048	0.00003	0.04162	0.00004	—	—	0.35189
II	0.31870	—	0.03097	0.03976	0.00001	—	0.03153	0.26913
III	0.28125	0.00001	0.00266	0.05829	—	0.00122	—	0.13730
IV	0.04523	0.09673	0.03374	0.09539	0.07086	0.00134	—	0.07940
V	0.14580	0.02733	0.11372	0.11258	0.02257	—	0.00439	0.12325

lithium as well lithium chloride. LiOH is only present in minor amounts. Using magnesium instead of aluminum (composition III) results in one-tenth the concentration of lithium and a correspondingly larger amount of LiCl.

With lithium carbonate as a color agent, the composition with magnesium yields substantial amounts of lithium but twice as much color-interfering LiOH (composition IV). By using aluminum instead (composition V) a very high amount of elemental lithium is formed, with only a fifth as much LiOH.

Summary

Making effective lithium-based pyrotechnic red flames should not be "far from easy", as Jennings-White assumed.[7]

Several rules must be obeyed to make a successful lithium red composition. These are:

➤ The stoichiometric ratio of oxygen to hydrogen must not exceed 1.0 to favor H_2O dissociation to atomic hydrogen. To accomplish this:

• Use fuels with high hydrogen content

• Make the stoichiometry fuel rich; in other words, avoid an oxygen surplus

➤ Halogens should be avoided

• If halogens cannot be avoided, aluminum should be added to scavenge the halogen

• Each lithium compound has to be treated differently to obtain maximum color purity

Although only theoretical evidence has been given for this hypothesis, it is hoped that an experimental proof will be found soon.

A remaining problem with many lithium compounds is their high hygroscopicity, which will make practical applications difficult.

References

1) T. Shimizu, *Feuerwerk vom physikalischen Standpunkt aus*, Hower Verlag, Hamburg, 1976, [a] pp 90–99; [b] p 78.

2) T. Shimizu, *Selected Pyrotechnic publications of Dr. Takeo Shimizu, Part 3, Studies on Colored Flame Compositions of Fireworks,* Journal of Pyrotechnics, Whitewater, CO, 1999, pp 58–71.

3) B. E. Douda, *Theory of Colored Flame Production*, RDTN No. 71, 1964), U.S. Naval Ammunition Depot, Crane, IN, USA.

4) B. E. Douda, R. M. Blunt, and E. J. Blair, "Visible Radiation from Illuminating-Flare flames. Strong Emission Features", *J. Opt. Soc.*, Vol. 60, 1970, pp 1116 –1119.

5) R. W. B. Pearse and A. G. Gaydon, *The Identification of Molecular Spectra*, 4th ed., Chapman and Hall, London, 1976, [a] p 289; [b] p 201; [c] p 202.

6) B. T. Sturman, "The Rare Earth Elements as Possible Flame Color Agents", *Journal of Pyrotechnics*, No. 9, 1999, pp 57–61.

7) C. Jennings-White, "Some Esoteric Firework Materials", *Pyrotechnica*, No. XIII, 1990, pp 26–32.

8) C. Jennings-White, "Blue Strobe Light Pyrotechnic Composition", *Pyrotechnica*, No. XIV, 1992, pp 33–45.

9) D. E. Chavez, M. A. Hiskey and D. L. Naud, "High Nitrogen Fuels for Low-

Smoke Pyrotechnics", *Journal of Pyrotechnics*, No. 10, 1999, pp 17–36.

10) H. Ellern, *Military and Civilian Pyrotechnics*, Chemical Publishing Company Inc., New York, 1968, [a] p 24; [b] pp 286–287.

11) G. W. Weingart, *Pyrotechnics*, 2nd ed., 1947, p 187.

12) R. Mavrodineanu and H. Boiteux, *Flame Spectroscopy*, John Wiley & Sons, Inc., New York, London, Sydney, 1965, [a] p 370; [b] pp 368 and 371; [c] pp 391–429.

13) A. F. Hollemann, E. Wiberg and N. Wiberg, *Lehrbuch der Anorganischen Chemie*, 101, Auflage, Walter de Gruyter, Berlin, New York, 1995, [a] p 1150; [b] p 718.

14) C. J. James and T. M. Sugden, "Photometric Investigations of Alkali Metals in Hydrogen Flame Gases, III : The Source of the Alkali Metal Continuum", *Proc. Roy. Soc. London*, Vol. A 248, 1958, p 238–247.

15) A. G. Gaydon and H. G. Wolfhard, *Flames Their Structure, Radiation and Temperature*, 4th ed., Chapman and Hall, London, 1979, [a] p 354; [b] p 331; [c] p 101.

16) C. Th. Alkemade, "Fundamental Aspects of Decomposition, Atomization, and Excitation of the Sample in the Flame" in J. A. Dean, T. C. Rains (Eds.), *Flame Emission and Atomic Absorption Spectrometry, Volume 1 Theory*, Marcel Dekker, New York, London, 1969, [a] pp 121–122; [b] p 121.

17) J. Köhler and R. Meyer, *Explosivstoffe*, 9. Auflage, Wiley-VCH, Weinhein, 1998, p 194.

18) *Gmelins Handbuch der Anorganischen Chemie*, "Lithium", Lieferung 1, System-Nr. 20, Verlag Chemie, Weinheim, 1976, pp 35–36.

19) D. R. Lide, *Handbook of Physics and Chemistry*, Chemical Rubber Company, Boca Raton, 1996, pp **9**-51–56.

20) http://www.aip.org/avsguide/refguide/optic alele.html

21) M. W. Chase Jr., *NIST-JANAF Thermochemical Tables*, 4th ed., American Chemical Society, Gaithersburg, 1998.

22) J.-L. Dumont, E.P. 0252803 B1, 1987, Etienne Lacroix-Tous Artifices SA, France.

23) E. C. Koch, unpublished results, 1999.

24) R. S. Ram and P. F. Bernath, "Fourier Transform Infrared Emission Spectroscopy of the $C^4\Delta$-$X^4\Phi$ System of ZrCl", *J. Mol. Spectrosc.*, Vol. 186, 1997, pp 335–348.

25) B. J. McBride and S. Gordon, "Computer Program for calculation of Complex Chemical Equilibrium Compositions and Applications", NASA RP 1311, June 2000.

26) C. Jennings-White, "Lithium, Boron, and Calcium", *Pyrotechnica* XVII, 1997.

27) G. Krien, "Thermoanalytische Ergebnisse von pyrotechnischen Ausgangsstoffen", AZ 3.0-3/3712/75, Institut für chemisch-technische Untersuchungen CTI (today WIWEB) Swisttal Germany, p 117–119.

28) *Gmelins Handbuch der Anorganischen Chemie*, "Strontium", Lieferung 1, System-Nr. 29, Verlag Chemie, Weinheim, 1976, pp 47.

29) T. Jone, GB 2266944B, 1995, GEC-Marconi Limited, United Kingdom.

Pyrotechnic Delays and Thermal Sources

M. A. Wilson and R. J. Hancox

Pains Wessex Australia P/L, Melbourne, Australia

ABSTRACT

The technology associated with pyrotechnic delays, together with the many factors, both physical and chemical, that affect the performance of delay compositions and influence the design of delay elements have been outlined. The production of heat by thermite and thermate systems is similarly discussed.

Keywords: pyrotechnics, gassy delays, black powder, gasless delays, thermites, thermates, incendiaries, Goldschmidt reaction

Introduction

The combustion process of a pyrotechnic composition can be used to provide a time interval ranging from a few tens of milliseconds to several minutes between successive mechanical, electric or explosive events. Any composition will take a finite time to burn over a given length, but the requirements of safety, time reproducibility and ignition transfer reliability, particularly in modern military applications have resulted in the development of specific formulations known as pyrotechnic delays. Compositions of this type, when consolidated into a tube (usually by pressing the powder mixture under high loads) burn at reproducible linear rates. The assembly consisting of an ignition source, the tube, pressed composition and ignition transfer system is called a *delay element*.

A delay element can be used to provide a safety interval, for example, between the deployment and detonation of a hand grenade, to allow time for a projectile to reach its target or to form part of an electro-mechanical sequencing system for a fuze train. Pyrotechnic delays have found many applications, even in these days of cheap electronic timing systems because of their simplicity, the high degree of inherent safety, their ruggedness and reliability, and also because they do not require a power source such as a battery.

Although pyrotechnic reactions can be designed to produce diverse physical effects, including time delays, the basic combustion process is exothermic (i.e., heat is evolved). The appropriate selection of chemical ingredients can optimise heat production and because very high temperatures are produced, one or more of the reaction products will be in the liquid phase. Such specific formulations are usually known as *thermites* and can be used to cut, burn or weld metals. With controls applied to design parameters, the reaction dynamics of thermite compositions can be closely regulated, resulting in reproducible propagation velocities and very low volumes of gaseous reaction products. As a result, certain thermite type formulations, known as *'gasless' delays,* can be used in hermetically sealed systems to produce very accurate delay intervals in explosive trains. Because the chemistry of gasless delay compositions is often identical to that of thermites, both are considered together in this article.

Delay Compositions

Until World War II, Black Powder was the basis of virtually all delay elements used in munitions, whether formed into columns by a wrapping process (*Bickford or safety fuse*), coating as a paste onto hemp yarn (*quick match*) or by the more sophisticated method of pressing the material into metal tubes or channels. Black Powder, if it can be kept dry, can be used to provide quite accurate time intervals. It produces a significant volume of permanent gas during combustion (about 300 mL/g of Black Powder), and so devices containing Black Powder must be vented, otherwise, the combustion rate will
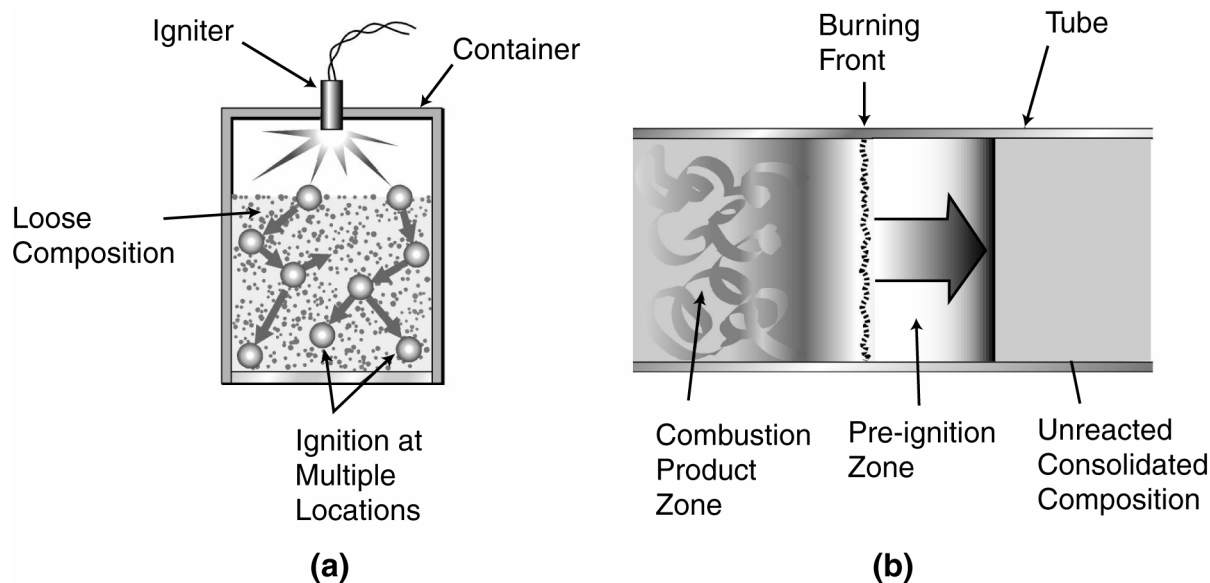
Figure 1. Combustion in the loose and consolidated states.

increase due to pressurisation, and short delay times will result. In high altitude applications where the ambient pressure is low, long delay times and possible extinguishment of the vented column are likely due to heat losses from the system. However, because the charcoal ingredient in Black Powder is somewhat hygroscopic, the delay column must be sealed from the environment during storage. Mechanical solutions to these competing requirements have increased the complexity of gas-producing (gassy) delay systems and are only partly successful.

With the development of weapons systems required to operate with high levels of performance reliability and reproducibility under a wide range of environmental conditions, the gassy delay system has been displaced by a relatively new type of composition—the gasless delay. As its name implies, the gasless delay composition produces comparatively little permanent gas during combustion. For this reason, the combustion rate is less affected by pressurisation of the burning front and as a result, the delay element can be totally sealed from its operational and storage environments. In other words, time intervals of high accuracy can be produced whether the system operates at great depths beneath the sea or in the vacuum of space. Moreover, hermetically sealed delay elements incorporating gasless delays can be stored for long

periods without deterioration due to the ingress of moisture.

However, gassy delays have not been entirely superseded. Many new formulations have been developed, resulting in delay systems that exhibit better time accuracy over their service life than the Black Powder type. The burning rate-pressure dependency of gassy delays, particularly at extremely high pressures, is still used in certain fuze systems to produce millisecond duration sequencing intervals between safety and arming events.

Combustion in Consolidated Columns

Before examining delay compositions in some detail, it is necessary to compare the mechanisms of combustion in the loose and consolidated states. Figure 1a shows a container filled with loose Black Powder. Upon initiation of the prime ignition stimulus, the grains of powder immediately beneath the stimulus are ignited. These burn, generating hot combustion products that are free to ignite surrounding grains throughout the void spaces in the filling. The low bulk density of the filling, the turbulence caused by the combustion process and the consequent ignition of Black Powder at many

sites remote from the prime stimulus means that the combustion rate is very rapid. The confinement offered by the container causes the process to occur under pressure and an explosion will generally result.

If, rather than fill the loose Black Powder into a container, it is laid out in a trail, made into a paste and coated onto a cord, or lightly stemmed into a tube, a slower burning rate generally results. In early mining operations, such arrangements were used as fuses to introduce a delay interval between ignition of the fuse and explosion of the main charge. However, combustion propagation along the fuse train is not well controlled—burning particles ejected or windborne from the trail, or flashing down the cord or tube are capable of igniting the main charge too soon—a highly dangerous situation. It was William Bickford, with the development of hemp-wrapped Black Powder fuse in the early 1800s,[1] who improved the safety of blasting operations and laid the basis for the future development of highly accurate pyrotechnic delay elements.

The combustion process shown in Figure 1b is much slower and more controlled. This is because the pyrotechnic filling has been compacted by pressing it into a tube to a density approaching its theoretical maximum (TMD), and the void spaces throughout the composition have therefore been reduced to as low a level as possible (typically 2–12% of the total volume). The void space is the total volume of the space between the ingredient particles; this is largely determined by the physical properties of the ingredients and the compaction pressure.

In a pressed composition, the products of combustion (e.g., gases and heat) are unable to travel far into the consolidated column and combustion is confined to a relatively thin propagation zone known as the *burning front*. The tube, into which the composition is pressed, not only has the function of supporting the column in a mechanical system, but also allows combustion to occur only at the burning front. Although delay compositions generally consolidate well into tubes, the risks associated with the possibility of uncontrolled burning must be considered in the design of a delay element. Adhesion failure between the composition and the delay tube wall can have serious consequences (such as a short or nonexistent delay time in a hand grenade).

As shown in Figure 1b, the plane of the burning front proceeds in a 'cigarette fashion' from left to right through the column of composition at a notionally constant speed. Immediately to the left of the burning front is the combustion product zone and to the right is the pre-ignition zone where the unreacted composition is heated by the intrusion of combustion products (gases, liquids and thermal radiation) into the consolidated column. Largely, it is the degree of pre-heating of the reactants before the arrival of the burning front that determines the rate at which the column combusts.

Burning Rate

The burning rate of a pyrotechnic composition is the speed at which the burning front proceeds along the length of the consolidated column. The burning rate can be expressed in units of length per second (*linear burning rate*), or mass consumed per second (*mass burning rate*), depending upon the application. However, it is important to understand that the measured linear burning rate is really an average value—the speed at which the burning front progresses through the column may continually increase and decrease under the influence of a wide range of factors. These are related to the properties of the composition itself and to other stimuli both internal and external to the system. For a pyrotechnic delay composition filled into a device, the cumulative effect of these influences results in a measured burning time for a particular column length—the *delay interval*.

Because the time produced by a given system is often of more direct relevance to the pyrotechnist than the length of the column, many designers and researchers have used a reciprocal unit to quantify the burning rate of pyrotechnic compositions. The *reciprocal linear burning rate* (RLBR) is expressed in units of time per (convenient) unit of length (e.g., s/cm) rather than as a speed value (cm/s or mm/s). The reader will encounter the use of both units in the literature, and it is largely a matter of personal preference as to which value is employed.

However, pyrotechnic performance characteristics, including explosives sensitiveness are related to the burning rate of a composition and therefore the two units must never be confused.

The RLBR can be used as a primary quantifier of a pyrotechnic composition. Although the burning rate will likely be altered by the combustion environment (e.g., certain mixtures burn faster under increased pressure and temperature), the RLBR value is normally determined at ambient pressure and temperature. It allows an immediate comparison to be made of the burning rates of different formulations and can also be used to predict the pyrotechnic effect likely to be produced by various formulations and composition types. For example, a flare composition that burns at a faster rate will generally produce higher luminous emission than a similar, but slower burning formulation.

Determination of Burning Rate

Often, the pyrotechnist faced with the problem of making a composition that burns at a specified rate for a particular application can physically blend two similar formulations having different RLBR values to achieve the required burning rate. Usually, the burning rate under ambient conditions can be readily determined by using one of the following techniques:

(a) Incremental Method

This is probably the most common method used to fill delay elements for applications such as hand grenades. A small mass of loose composition is loaded into the delay tube and consolidated using sufficient force to produce a high compaction pressure (typically >150 MPa). Successive increments are loaded and pressed in this way until the required column length is achieved. The mass of each increment is limited so that density variations throughout the consolidated column do not cause excessive variations in the burning rate (the interfaces between the individual increments can cause a momentary slowing of the burning rate). The column length may be increased or reduced, depending on the reaction dynamics of the system, to achieve the specified delay interval. This filling technique is time consuming and the results are somewhat dependant on operator skill levels, and therefore may not be cost effective for long (>5 s) delay intervals or the determination of the RLBR in the laboratory.

(b) Extrusion Method

A faster method for filling delays was developed in the UK in the 1960s—a length of lead tubing, which has been closed at the bottom by crimping, is volumetrically filled with loose composition. This is stemmed by hand using a wooden drift and the tube is crimped at the top. The filled tube is then passed through a set of reduction rollers in a specially designed machine until the required diameter is obtained. The first 5–10% of the extruded length is discarded from each end and the remainder is then cut into equal lengths using a sharp knife. Each length is ignited with a match and the burn time is recorded with a stopwatch or video system. The average burning time for the lengths is then calculated and (in the case of RLBR) expressed as a function of length.

The process compacts the lead-sheathed composition to about 100 MPa so that longer lengths can be loaded and subsequently pressed into delay elements, reducing the number of increments and the likelihood of burning time variations. The technique is especially applicable to the determination of the RLBR under ambient conditions because it is much quicker, cheaper and less skill dependant than the incremental method and delays of longer length can be more readily produced.

Factors Affecting Burning Rate

A wide range of factors can influence the burning rates of pyrotechnic compositions, including those intrinsic to the compositions themselves and other factors introduced by the device into which they are filled or the operational combustion environment:

- thermochemical properties of the reactants
- stoichiometry of the composition
- chemical and physical properties of the reactants; including purity, particle size and behaviour under compression

- thermal conductivity of the composition, particularly the fuel ingredient

- thermal conductivity of the tube housing the column

- thermal radiation from the reaction products and probably the infrared (IR) absorption characteristics of the composition's ingredients

- convective effects at the burning front

- volume of temporary and permanent gases produced by the composition

- pressure at the burning front

- characteristics of the condensed combustion products

- void space in the filling and consolidation pressure

- environmental effects such as the temperature of the surroundings and spin

- design of the device, particularly the end seals

- number and size of composition increments

- diameter and length of the column

- the mechanical strength of the column

- the type of ignition source

- the 'first fire' (priming composition) that might be used

While a delay composition having a fast burning rate is generally more reproducible than a slower burning formulation, the collective influence of all these factors (to a greater or lesser extent) determines the overall time interval produced by the delay element. Considering the above list, it might not seem possible that a pyrotechnic delay element could ever give a consistent time, but pyrotechnic delays are used in explosive trains to produce accurate time intervals, often under very adverse conditions. The pyrotechnist faced with designing a delay element or solving production problems with an existing system must consider all these influences to be successful.

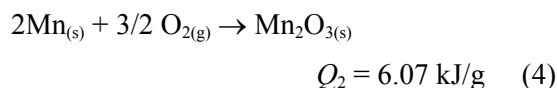**Thermochemistry and Stoichiometry**

The intrinsic burning rate of a delay composition is mainly determined by the chemical ingredients, their proportions in the composition, and also their thermochemical properties. For example, an oxidiser that decomposes exothermically (such as potassium perchlorate, $\Delta H_r^\circ = -3.7$ kJ/mol of $KClO_4$) will require less heat from the system for decomposition than an endothermic oxidiser (such as barium nitrate, $\Delta H_r^\circ = 220.0$ kJ/mole of $Ba(NO_3)_2$). This means that, all other factors remaining equal, the combustion temperature and the burning rate of the system containing the exothermic oxidiser will be greater. An oxidiser or fuel that undergoes a phase change or a phase change at higher temperature during the combustion process will remove heat from the system and slow the progression of the burning front accordingly. Chemical impurities in the ingredients, and the mere presence of the mixed ingredients themselves may lower the onset decomposition temperature of the oxidiser or alter the combustion characteristics of the fuel.[2] These factors may cause variations in performance.

To compare the relative thermal output of fuel ingredients, the Q_1 value is often used:

$$Q_1 = \frac{\Delta H_f^\circ}{mA} \tag{1}$$

where ΔH_f° is the heat of formation (enthalpy) of the oxide, A is the atomic (or molecular) weight of the fuel and m is the number of atoms of the fuel in the product molecule. For a given particle size and surface area, a fuel such as boron that produces more heat when it oxidises ($Q_1 = 58.96$ kJ/g) will react faster than a less reactive fuel such as silicon ($Q_1 = 32.40$ kJ/g). Depending on its proportion in the composition, a fuel may also combust to produce higher or lower oxides and alter the thermal output (where Q_2 is the heat of combustion per unit mass of reactants) of the combustion process. McLain[3] gives an example:

$$Mn_{(s)} + 1/2\ O_{2(g)} \rightarrow MnO_{(s)}$$
$$Q_2 = 5.43\ kJ/g \tag{2}$$

$$Mn_{(s)} + O_{2(g)} \rightarrow MnO_{2(s)}$$
$$Q_2 = 5.98\ kJ/g \tag{3}$$

$$2Mn_{(s)} + 3/2\ O_{2(g)} \rightarrow Mn_2O_{3(s)}$$

$$Q_2 = 6.07 \text{ kJ/g} \quad (4)$$
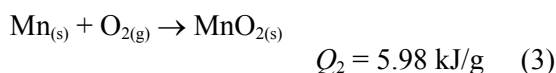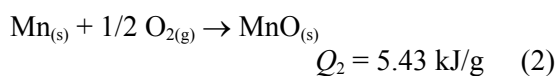
Diluents or modifiers may be added to the formulation to cause deliberate changes to the burning rate. A diluent is a material that may not take part in the combustion reaction, but which will physically separate the fuel and oxidiser and reduce their combined reactivity. It may also serve as a heat sink, removing thermal energy from the burning front and slowing the combustion reaction. Examples of diluents include kaolin, kieselguhr, chromic oxide, and magnesium oxide.

Rate modifiers usually undergo a physical or chemical change that removes heat from the system, for example by melting or decomposing to produce a gas that directly carries heat away from the burning front. Some phase change modifiers include the low melting point oxidisers, potassium nitrate and potassium dichromate and organic fuels such as lactose, which dehydrates on heating.[4] Gas producing modifiers such as sodium bicarbonate, calcium carbonate and calcium oxalate may also be used in gassy delays.

Delay compositions are generally formulated to be slightly fuel rich for two reasons:

- in gasless delays, the excess fuel is required to consume any oxygen gas that might otherwise be evolved by the reaction[5]

- excess fuel increases the combustion temperature, which leads to a higher combustion rate and improved reproducibility[3]

However, the determination of the optimum theoretical ratio of reactants for a delay formulation (particularly gasless mixtures) can be difficult for the designer because of the high combustion temperature of the burning front (approximately 2000–3000 °C). Deciding upon the actual product species existent at these temperatures can be assisted by computer codes such as the NASA-Lewis CEC76 program in which the conditions of temperature and pressure can be ascribed to the burning front to more accurately estimate the products.

Because of this difficulty, experimental techniques are commonly used to examine the effect of ingredient proportions on the burning rate of
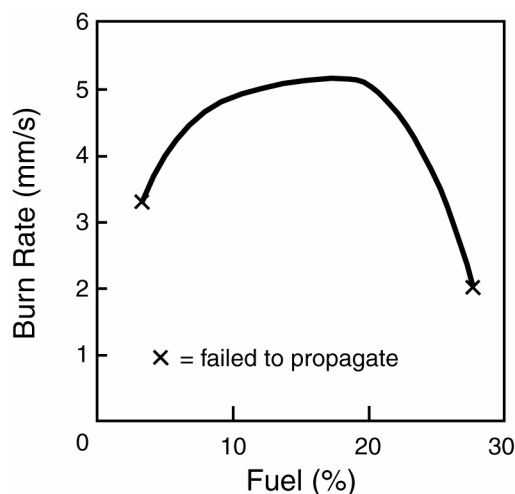

Figure 2. Burning rate vs. fuel content for a binary delay system.

the composition. For example, in binary systems several delay formulations are prepared in which the fuel/oxidiser ratio is widely varied around the stoichiometric ratio (between fuel deficient and fuel rich). A number of delay columns of set length are then prepared and ignited under ambient conditions of temperature and pressure. The burn times of the columns are then measured and converted to burning speed (or RLBR) values for each formulation. These are then plotted against fuel content to give a relationship similar to that shown in Figure 2.

When designing a delay element, it is necessary not only to select a composition having a particular burning rate, but it is equally important to ensure that the chosen formulation exhibits the required burning rate on the flat region of the burning rate vs. fuel content curve. If not, small variations in the fuel content as a result of poor mixing or ingredient segregation can significantly affect the burning rate and ultimately the time produced by the delay element. Therefore, homogeneity provided by proper ingredient preparation and mixing techniques is critically important in most delay compositions.

For formulations containing more than two ingredients, the same experimental technique is used, but the results are plotted as shown in Figure 3. This diagram shows the relative percentages of the oxidisers plotted against the per-
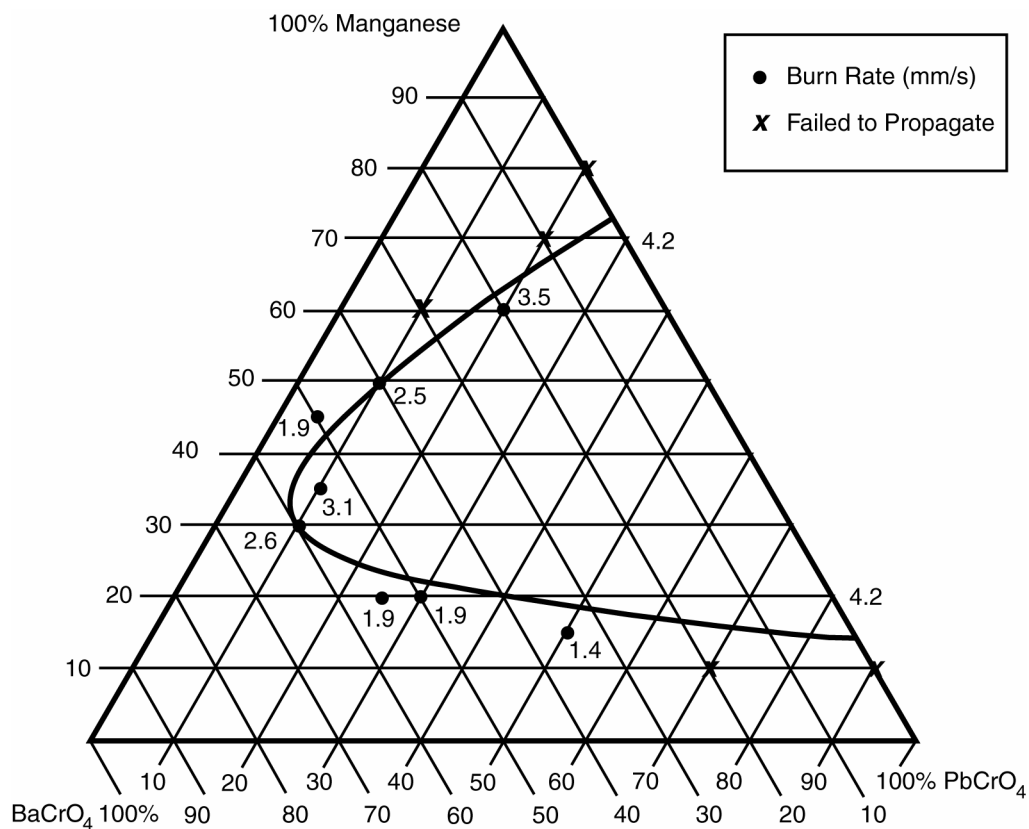
Figure 3. Burning rate vs. ingredients content for a ternary system.

centage of fuel ingredient for a manganese/barium chromate/lead chromate delay system. The method can also be used with compositions containing two fuels and a single oxidiser.

Physical Properties of the Reactants

The physical properties of the reactant chemicals can have a significant effect on the burning rate and burning rate reproducibility of a pyrotechnic delay composition. Usually, the mean particle diameter of the ingredients (particularly of the fuel component) is reduced as much as possible (often to less than 10 μm) to produce the most reproducible burning rate for a given system. Although a high surface area fuel (e.g., made by a cutting or stamping process) can be expected to burn more rapidly, fuels having a low surface area (e.g., spherical particles manufactured by an atomising process) tend to combust in a more reproducible manner—a factor essential for a delay system. Another important consideration is the particle size

distribution of the ingredients—chemicals having large particle size disparities can result in inconsistent burning, particularly if the composition is not well mixed.

Purity and Moisture

Because of the tight performance tolerances often placed upon delay systems, it is particularly important that each chemical ingredient of the composition is as pure (or as consistent) as possible. The chemicals used in pyrotechnic compositions normally contain impurities and these may produce unwanted effects such as the production of gas, catalytic effects, chemical instability or thermochemical changes, all of which can alter the burning rate. The chemical specifications usually set limits for particular impurities so that these effects are minimised.

Moisture must be eliminated from gasless delay compositions because of the numerous chemical and physical changes it is likely to cause within the system during both storage and

combustion. For example the gradual oxidation of the fuel due to the presence of moisture will alter the available fuel content of the composition, and to a lesser degree, the change of water to vapour during combustion will cool the reaction, pressurise the burning front or directly remove heat from the system. In both these circumstances the burning rate is likely to change.

Some impurities however, may provide beneficial effects such as reducing the thermal decomposition temperature of the oxidiser or assisting the combustion of the fuel and hence improve the ignition or propagation characteristics of the composition. Boron, for example normally contains about 5–10% impurities yet serves as a versatile and effective pyrotechnic fuel. Very pure boron on the other hand is relatively difficult to ignite.

Thermal Conductivity within the Column

The use of a fuel having high thermal conductivity, such as a metal powder, increases the burning rate due to preheating effects. This effect not only demonstrates that the thermal conductivity of the column is one factor controlling the burning rate[6] but also gives the pyrotechnist another means of altering the burning rate of different formulations to suit specific requirements. The appropriate selection of the fuel ingredient or the addition of a diluent to act as an insulator or heat sink will alter the conductivity of the column and as a consequence, slow the burning rate.

Similarly, the pressing load (and the flow properties of the ingredients under increased pressure) can affect the burning rate by altering the thermal conductivity of the column by bringing the ingredients into more intimate contact with each other.

Direct Heating

The reactants in the pre-ignition zone are directly heated by thermal radiation from the combustion reaction, and it is therefore likely that the infrared absorption characteristics of the ingredients will help determine the burning rate of the system.

The reactants immediately ahead of the burning front are also heated by direct contact (conduction) with the reaction products, particularly if they are in the liquid phase. Gaseous or solid products are often carried quickly away from the burning front by thermal expansion or gas flow and so have less time to transfer energy to the unreacted ingredients.

Reaction Products

The reaction products also influence the burning rate of a consolidated column of pyrotechnic composition, often long after the combustion front has passed. At the time of burning, the specific heat of the products and their physical state at the combustion temperature will influence the heating processes occurring at the front (e.g., gaseous products may pressurise the system causing an increase in the burning rate). However condensed phase products (slag), formed once the burning front has passed, may alter the dynamics of heat loss and gas flow, thereby altering the temperature and pressure at the front and therefore the propagation speed of the burning front. In some burning delay columns, slag continually accumulates until it is suddenly displaced by internal gas pressure; it then reforms with the result that the burning rate tends to be erratic. In order to minimise the problem with compositions of this type, the diameter of the delay column is often increased.

Sometimes a formulation of ingredients is deliberately chosen so that the slag quickly solidifies, rendering the column impermeable to gas flow. This isolates the burning front from external factors that may otherwise adversely affect the burning rate or even extinguish combustion. This is the so-called 'self-sealing' type of delay system that can be used underwater or in ignition transfer applications where directional projection of the reaction products is desirable. A composition that has been found to exhibit self-sealing properties is:

Manganese	34%
Barium chromate	30%
Lead chromate	36%

Void Space and Compaction Pressure

The degree of preheating of the reactants for a given system is controlled by the intrusion of the hot combustion products into the pressed column of composition. This in turn is partly

determined by the void space present in the compact. Most consolidated compositions exhibit microscopic spaces between the ingredients, even when pressed at very high loads. The reason for this is that once a certain density is achieved, no further movement of particles within the compact is possible. The total volume of the void spaces present in a composition depends on the formulation, the physical characteristics of the ingredients, including their particle size and shape and the presence of substances such as waxes or resins that can deform or flow under pressure. In delay columns, where very small particle size ingredients are normally used, the void space is generally quite low.

In spite of the low void space, delay columns are sufficiently porous for the combustion gases to flow ahead of the burning front, particularly if a pressure differential exists between one end of the column and the other. This can be demonstrated by pressing a slow burning 'gasless' delay composition into an open-ended metal tube and igniting it with the opposite end connected to a water-filled manometer. Even with no gas flow restriction at the ignition end, the manometer will soon be seen to rise, long before the burning front reaches the end of the delay column. This flow, if unhindered by a tube end closure, will heat the column, raise the temperature of the reactants and increase the burning rate. If the system is sealed and the igniter generates significant pressure, the burning rate may be further increased.

Conversely in slow burning delay systems, if one or more of the ingredients undergoes a phase change and liquefies during the preheating process, the molten material may be forced into the void space of the unreacted composition by internal pressure. This may act as a seal, reduce gas flow through the column and depress the burning rate. The burning characteristics of the system may become quite complex, particularly under pressure.

Void space clearly influences the regularity of the burning front and for this reason, pyrotechnic delays normally incorporate finely ground ingredients that are pressed at a high compaction pressure to minimise any effects related to variations in void space. The effect on the burning rate of compaction pressure and

density variations due to increment interfaces should be considered when designing a delay element.

Environmental Factors

With the composition parameters controlled as much as possible, the pyrotechnist must also consider environmental factors during the combustion period that may influence the burning rate. The ambient temperature, the thermal conductivity of the surroundings, the combustion pressure and operational factors such as acceleration or spin contribute effects that must be considered to achieve the required delay time.

When deciding on the mechanical design aspects of a delay element, the thermal output of the delay composition and its environment must be taken into account. A fast burning, hot system will be less affected by thermal losses than a slower burning, cooler composition. The faster-burning compositions can therefore be filled into small tube diameters and still yield very reproducible results, whereas the column diameter should be increased to produce similar results from a cooler system.

The temperature of the delay column, both prior to and during combustion, influences the burning rate. For military and aerospace applications, delay elements must provide an accurate time interval, which is specified to within certain limits over a set environmental temperature range, often between –40 and +60 °C. Depending on the formulation, most gasless delay compositions burn about 25% slower at the lower temperature and 25% faster at the higher temperature than they would at room temperature. Gassy delays are less affected by temperature variations because of the intrinsic removal of reaction products from the burning front.

For similar reasons, the thermal conductivity of the delay tube itself and its immediate surroundings are factors contributing to the time interval produced by the system. Highly conductive materials such as aluminium, copper or brass will transfer thermal energy along the length of the tube, heat the remaining composition and increase its burning rate. Any surrounding components in thermal contact with the delay tube may slow or even remove sufficient energy from the system to extinguish the
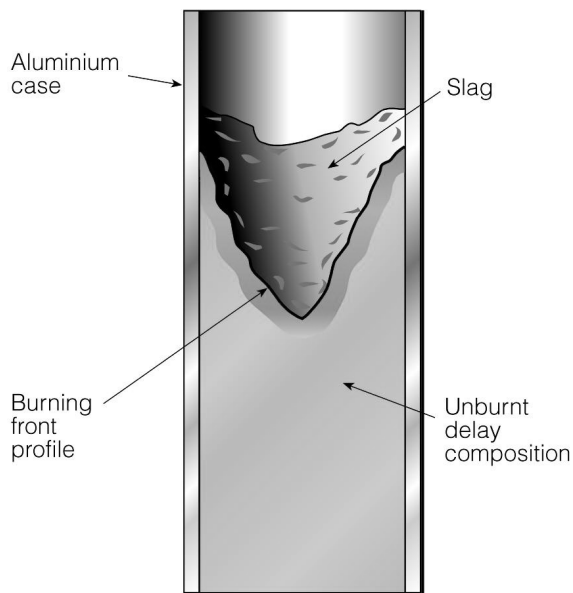
Figure 4. A delay column that has failed due to heat losses.

burning composition (Refer to Figure 4). It is normal practice to use low thermal conductivity materials such as stainless steel for the manufacture of delay tubes to reduce these effects. Aluminium alloy delay tubes can be used in slow burning systems, but the metal should be anodised to reduce surface conductivity.

Pressurization of the burning front often leads to an increase in the burning rate, although the effect is generally more pronounced with gas-producing delays. Increased pressure at the burning front confines the combustion products to the reaction zone and increases the temperature. Combustion products are forced to greater depths into the compact and this also increases the burning rate due to preheating of the delay column. Decreased pressure may have the opposite effect, particularly with gassy systems, by assisting in the removal of reaction products from the system—this causes a drop in temperature and possibly leads to propagation failure. In extreme circumstances, such as a pressure drop caused by the ejection of an igniter or sealing disc (particularly at high altitudes) can cause the entire burning front to dislodge from the column and so extinguish the delay element.

The combustion pressure may be the result of environmental conditions such as deployment altitude, the reaction products of the composition, or a deliberate attempt on the part of the pyrotechnist to improve the reproducibility of the system. Obviously if a system is designed to operate under sealed conditions, the effectiveness of the gas seals will determine the reproducibility of the delay element; one major cause of delay elements failing to produce the specified interval or standard deviation is internal gas venting to atmosphere past the environmental seals.

Longitudinal or angular acceleration might be expected to affect the burning rate, particularly if solid to liquid phase transitions are a result of the combustion process. When designing delay fuzes for gun-launched, spin-stabilised ammunition, the delay composition must be formulated and engineered to withstand the associated forces—this is mainly achieved by the choice of oxidiser, with ionic solids exhibiting better compaction and mechanical strength properties than amorphous or covalently-bonded substances. In general, gasless delays tend to burn at a slower rate under spin; this is because the molten reaction products of gasless systems are displaced from the combustion front. In projected ammunition, high acceleration forces along the line of flight can cause propagation failures for a similar reason.

Design and Manufacturing Factors

A number of design and manufacturing factors can affect the delay interval produced by a delay element:[7]

- length and diameter of the column
- the burning rate of the composition
- density of the column
- type of igniter used
- the use of a priming composition
- design of the delay element, particularly the end seal
- ignition transfer and the mechanical strength of the column

Although a pyrotechnic delay element is an inherently simple system, it often requires more

careful design and manufacturing techniques than any other type of pyrotechnic device. To achieve its performance criteria, the delay element requires close control from its inception, materials selection and preparation, mixing, pressing and final assembly as part of a pyrotechnic or explosive train.

(a) Column Length and Diameter

For a given composition with a defined burning rate, it is primarily the length of the consolidated column that determines the overall time interval produced by the system. Unfortunately, the pyrotechnist is often consulted last and is given minimal space in the item of ordnance in which to incorporate the delay element. This can mean that the preferred delay composition cannot be used because of space restrictions and so a less-than-ideal composition may have to be used in a shorter length. This requires that all the factors that affect the burning rate must be highly controlled in order to achieve a reproducible delay interval. In some instances, filled delay columns have needed to be mechanically machined to close length tolerances after pressing in order to produce the time accuracy required by modern missile systems.

The diameter of the delay column is usually chosen as a matter of space efficiency, but care should be taken to ensure that sufficient thermal energy is available to account for heat losses in the system and still maintain the reproducible propagation of the burning front. A composition, burning in a larger diameter column, has more composition per unit length and hence increased thermal energy to maintain smooth and reliable propagation.

(b) Burning Rate and Filling Density

As a general rule, the use of faster burning compositions in longer columns with greater cross-sectional area more readily meet stringent time specifications. This is because faster burning systems are less affected by thermal losses caused by conduction into the surrounding medium. A slower burning composition of the same type produces less heat per unit length and is therefore more susceptible to variations in propagation speed, particularly during the initial burning period when maximum temperature differential is experienced by the system.
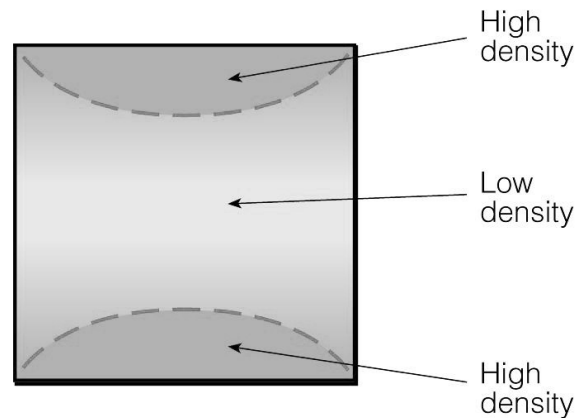
Figure 5. Density variations in a pressed column.

Gasless compositions that burn much slower than about 3–4 mm/s tend to be unreliable—this limits the practical length for an incrementally-pressed delay element to about 75 mm, or a time interval of about 25 s. For longer intervals, delay elements have sometimes been made by pressing compositions into flat 'C' sections (e.g., in early artillery rounds), by utilising the lead tube extrusion technique and pressing into long, straight tubes (for intervals of up to 30 s), or by forming the lead-sheathed composition into unpressed, spirally-wound delay elements; these can provide time delays of several minutes.

A delay column should be manufactured to ensure that the density throughout the consolidated column is as consistent as possible. Normally, a pressed pyrotechnic composition incorporates zones of density variation within the compact. In a delay element, this is highly undesirable because composition density and void space greatly influence the burning rate. The solution normally employed to produce a consistent compact is the incremental filling technique where a series of small increments of composition are pressed into the tube to form a column of the required length. However, even within each consolidated increment there are density disparities, with a zone of increased density opposite the pressing drift and reduced density in the middle of the increment (See Figure 5). As the burning front approaches and crosses each increment interface, the burning rate slows. The more increments in the column (particularly with slow burning compositions),

the more significant the time differences between delay elements can become. The lead tube extrusion process can be used to reduce delay time variations due to the effect of increment interfaces, simply because there are less interfaces over a given column length.

(c) Ignition Source

The type of ignition source can affect the manner in which a delay composition burns. For example, 'hard' igniters such as a gas-producing percussion primer or electric fuzehead may produce less reproducible combustion[8] by generating sufficient pressure to significantly increase the burning rate, disrupt the surface of the pressed composition, or even vent the system by ejecting the igniter assembly. A 'gasless' fuzehead or low gas-producing primer, although generally preferred as a 'soft' ignition source (hot particles rather than hot gases) for pyrotechnics, may not produce a consistent pressure in the *free space* incorporated between the igniter and the pressed column in a typical delay element; this will likely result in delay time variability. Both the delay composition and its igniter must be carefully matched to ensure performance reproducibility.

(d) Priming Compositions

Often when using a slow burning delay composition, the ignition surface must be primed to ensure reliable ignition transfer from the igniter. This means pressing a small increment of a faster and hotter burning formulation onto the delay column. While the actual burning time of the priming composition usually makes negligible contribution to the overall delay interval, the heat generated during its combustion will produce certain effects:

a) The delay composition may be initially 'overdriven' leading to a slightly faster burning rate during light up.

b) The heat from the priming may also help to bring the system to thermal equilibrium with its surroundings at a somewhat faster rate.

Both these effects will make a contribution to the delay interval and should be taken into account.

(e) Ignition Transfer and Sealing

While a delay element is usually a sealed unit during storage and its initial operation, it is always required to perform an additional function at the conclusion of the burning process, usually ignition transfer. This either means that a space is provided into which a loose filled ignition transfer or gas-producing composition is loaded or a tube closure seal must be disrupted to allow incandescent delay composition reaction products to exit the end of the tube. The implications of each of these situations on the burning rate of the delay column are quite different.

In the first case, gas can more readily flow through the compact and preheat the column; the burning rate can be expected to be relatively fast. But as the burning front approaches the end of the column, mechanical support for the remaining composition is diminished and it may break away due to internal gas pressure. Unless the design provides support for the end of the column, erratic and short times may result. Delay elements are often required to perform with high reliability and accuracy under extreme conditions of mechanical shock and vibration. Some delay compositions exhibit superior mechanical strength to others, with gassy delays generally exhibiting greater mechanical integrity than gasless compositions. This difference relates to the physical properties of their ingredients and the designer must consider this when choosing a composition for a particular application.

When the tube is fitted with a gas-tight base-seal, the gaseous reaction products are less able to flow through the column and the burning rate will be relatively slow. This has the advantage however that once the seal is expelled (often by melting) the high internal pressure will cause the reaction products to be ejected over large distances, providing an excellent ignition transfer stimulus. The designer must ensure that the end seal is effective throughout the time of the combustion process; otherwise uncontrolled gas leakage will result in variable delay times.

Gassy Delay Compositions

Gassy delay compositions are relatively cool systems because heat is removed from the combustion front by the gaseous reaction products. This means that the burning rate and hence the delay interval produced by the system is relatively unaffected by thermal losses to its combustion environment. Depending on the formulation, gassy compositions generate oxides of carbon and nitrogen and solid, particulate residues, producing between 200 and 400 mL of permanent gas for each gram of composition consumed. This derives from the nature of the fuels and oxidisers used in this type of composition. The fuel for a reliable gassy delay composition must meet certain requirements. It should:

- not be hygroscopic
- be chemically stable
- be compatible with the surrounding components
- be easily ignited
- consolidate well
- produce gaseous reaction products
- produce minimal solid residues that can obstruct the exit of gas and pressurise the system

The most common gassy delay composition is Black Powder, a homogeneous substance consisting of potassium nitrate, charcoal and sulphur, however the sulphurless type is usually employed in military applications due to its improved chemical compatibility. Other gassy formulations contain carbonaceous fuels such as lactose, tetranitrocarbazole (TNC), tetranitrooxanilide (TNO), ascorbic acid or chlorinated fuels such as polyvinylchloride.

Although many of the above requirements can also be placed upon the oxidisers, in practice the choice is more restricted, with potassium nitrate being mostly used. Potassium nitrate also has the advantage that it produces delay columns of high mechanical strength and it is sometimes used in conjunction with barium nitrate to make slower burning formulations.

Gasless Delay Compositions

Gasless delay systems are based on the exothermic reaction between a powdered metal and a metal oxide typical of the Goldschmidt oxidation-reduction reaction. Characteristics of the combustion process include the formation of condensed phase products and the relative regularity of the burning rate under varying pressures. While the reaction is notionally gasless, a small quantity (about 5–10 mL/g) of permanent gas (i.e., existing in the gas phase at STP) is usually formed due mainly to impurities in the chemical ingredients. However, it is important to be aware that temporary gases may be also formed during the high temperature combustion process, often resulting from the vaporisation of a portion of the metal fuel or metal oxide products or simply from the thermal expansion of air entrapped in the system. Though only temporarily in the gas phase, these species can pressurise the burning front during combustion and alter the burning rate. Although gasless delay compositions can burn in hermetically sealed systems, it is normal practice to provide a small volume, or *free space* between the igniter and the pressed column of composition to avoid excessive internal pressurisation and potential ejection of the igniter which seals the tube.

The range of fuels suitable for the manufacture of gasless delays is quite wide (Table 1),

Table 1. Some Examples of Fuels Suitable for Gasless Delay Compositions.

Fuels
Aluminium
Antimony
Boron
Chromium
Manganese
Molybdenum
Selenium
Silicon
Tellurium
Titanium
Tungsten
Zirconium
Zirconium/nickel alloy

but the choice of oxidisers (Table 2) is limited to those that produce minimal gaseous decomposition or combustion products when burnt with the selected fuel or fuels.

The range of compositions that can be formulated with these ingredients is obviously quite wide and each mixture has its own characteristics that are suitable for particular applications. Several such composition systems are shown in Table 3.

For a given application, the choice of a delay composition is determined by a range of factors, one of which is the burning rate. Table 4[5] shows how a range of burning rates might be achieved by varying the percentages of the ingredients of a particular type of delay composition.

Another of the other major considerations (particularly in applications related to safety and arming) influencing the choice of composition for a delay element is its mechanical strength as a consolidated column. A column that can be disintegrated as a result of rough handling during transport or thermal or mechanical stresses prior to or during operational deployment cannot produce a reliable delay time and the safety of the system into which it is incorporated may be compromised. Many potential gasless delay compositions formulated with the ingredients shown in Table 2 will not consolidate well. For this reason, the choice of oxidisers has largely been limited to ionic com-

Table 2. Examples of Oxidisers Suitable for Gasless Delay Compositions.

Oxidisers
Barium chromate
Barium peroxide
Bismuth oxide
Calcium chromate
Chromic oxide
Copper oxide
Iron oxide
Lead chromate
Lead oxides
Molybdenum oxide
Potassium dichromate
Potassium perchlorate
Potassium permanganate

Table 3. Typical Gasless Delay Compositions.

Barium chromate
Potassium perchlorate
Zirconium/nickel alloy

    Burning rate range = 1.7–25 mm/s

Boron
Barium chromate

    Burning rate range = 7–50 mm/s

Potassium dichromate
Boron
Silicon

    Burning rate range = 1.7–25 mm/s

Boron
Bismuth oxide
Chromic oxide

    Burning rate range = 7–50 mm/s

pounds such as barium chromate or potassium dichromate. Experience has shown that ionic solids tend to exhibit superior strength characteristics on pressing to covalently bonded substances. However, in recent years, occupational health and safety (OH&S) issues related to the use of some of the ingredients used in delay compositions has initiated research on new formulations which do not incorporate toxic or carcinogenic chemicals. Of particular concern are compounds containing bismuth, chromium(VI) or lead (i.e., the oxidisers used in most of the current gasless delay systems!)

Chemistry of Gasless Delay Compositions

Gasless delays are similar to thermites in that their combustion chemistry is based on the Goldschmidt reaction:

$$M_1 + M_2O \rightarrow M_1O + M_2 + \text{heat} \qquad (5)$$

where metal M_1 is oxidised to M_1O by a metal oxide, M_2O, which is, in turn, reduced to its metallic form M_2. Over the years, many delay compositions have been developed for particu-

Table 4. Burning Rates of a Tungsten Fueled Delay Composition System.

Ingredient	Percentage in Composition					
Tungsten (7–10 μm)	27	33	49	63	80	58
Barium chromate	58	52	41	22	12	32
Potassium perchlorate	10	10	5	5	5	5
Diatomaceous earth	5	5	5	10	3	5
RLBR (s/cm)	15.8	11.4	3.9	1.4	0.6	0.4
Equivalent burning speed (mm/s)	0.6	0.9	2.6	7.1	16.7	25.0

lar applications and some likely chemical reactions of the simpler systems are:

$$2\ Si_{(s)} + Pb_3O_{4(s)} \rightarrow 2\ SiO_{2(s)} + 3\ Pb_{(l)}$$
$$Q_2 = 1.49 \text{ kJ/g} \qquad (6)$$

$$2\ B_{(s)} + Bi_2O_{3(s)} \rightarrow B_2O_{3(s)} + 2\ Bi_{(l)}$$
$$Q_2 = 1.43 \text{ kJ/g} \qquad (7)$$
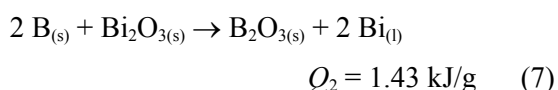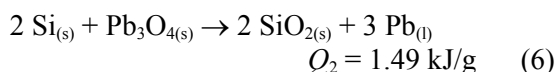
McLain[3] notes that for a boron/barium chromate system, the oxidation product at the reaction temperature might predominantly be a gaseous sub-oxide such as BO rather than the expected oxide, B_2O_3. It is probable that sub-oxides do form as a result of these notionally gasless reactions, and this further stresses the need to check theory (or assumption) with practical experimentation, particularly when attempting to determine the stoichiometry of a system prior to deciding upon ingredient formulation.

Effect of Pressure on Gasless Delay Compositions

Gassy delays, which must burn vented to the atmosphere because their burning rates are often exponentially related to increasing pressure, tend to be extinguished in low-pressure environments.

Gasless delay compositions however, will burn reliably at a relatively reproducible linear rate at both high and low pressures. Although gasless delays are normally burnt in a sealed system (that is, independent of the external en-

vironment), high internal pressures can be generated at the burning front by the hot reaction products from the igniter or from the combustion of the composition itself. Gasless delays are affected by pressure but unlike gassy systems, the burning rate usually slows at moderate to high pressures and tends to achieve a region where further pressure increase has little effect on the burning rate. In spite of this, the burning rate dependence on pressure of a sealed gasless system must still be considered if accuracy and time reproducibility are to be attained. The burning rate of most pyrotechnic compositions increases with pressure according to Vieille's law:[9]

$$R = R_oP^n \qquad (8)$$

where R is the burning rate at elevated (or reduced) pressure, P is the pressure (in atmospheres) and R_o is a constant (the burning rate at atmospheric pressure). The value n is specific to the system and varies from about 0.1–0.6, depending on the amount of gas produced by the combustion reaction. While this relationship has potential use in predicting the theoretical burning rate of pyrotechnic systems including gasless delays, the specific reaction dynamics of certain types of composition may introduce over-riding factors that, over certain pressure ranges, produce unpredictable changes in the burning rate. This means that the burning rate/pressure relationship for a particular delay formulation may need to be determined experimentally over a wide range of pressures.
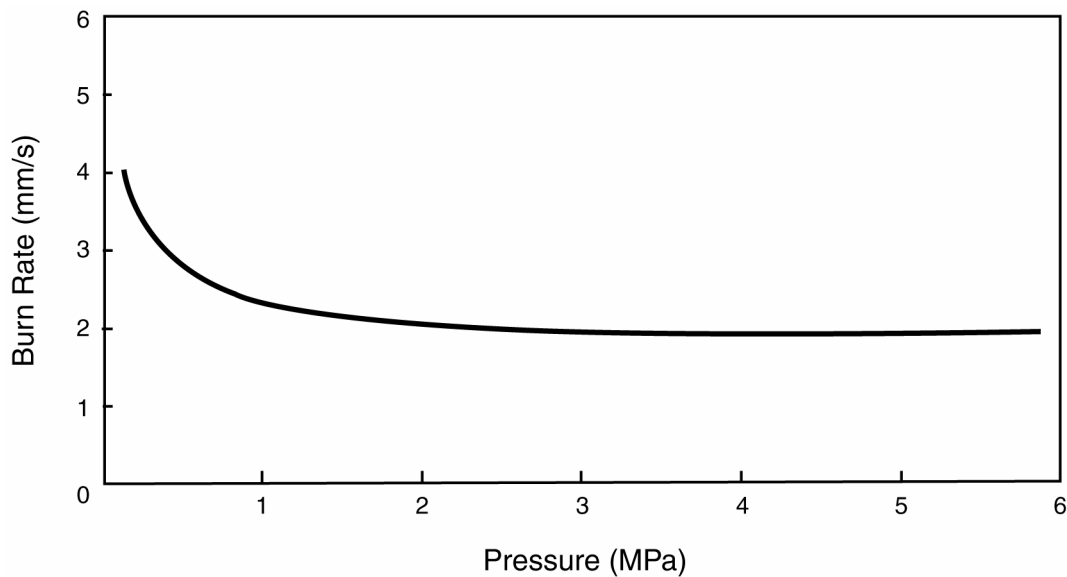
Figure 6. Burning rate vs pressure curve for B/BaCrO₄.

As examples, Figure 6 shows the experimentally determined burning rate/pressure relationship for a fast gasless delay composition containing boron and barium chromate (5/95 by weight). It can be seen that the curve, after a gradual slowing of the burning rate due to pressure increase, reaches a plateau region and further elevation of the combustion pressure to between 1.5–6 MPa has only a marginal effect on the burning rate. This classic relationship exhibits good agreement with Vieille's law over

this pressure range. This composition would be ideal for an internally pressurised delay element with a moderate free space.

The relationship in Figure 7 however, is more complex, particularly over the pressure range up to about 2 MPa. This curve is for a relatively slow burning gasless delay formulation containing boron, silicon and potassium dichromate (4/5/91), a composition that has been used in very accurate delay detonators for missiles. It can be seen that there is a sharp increase in the
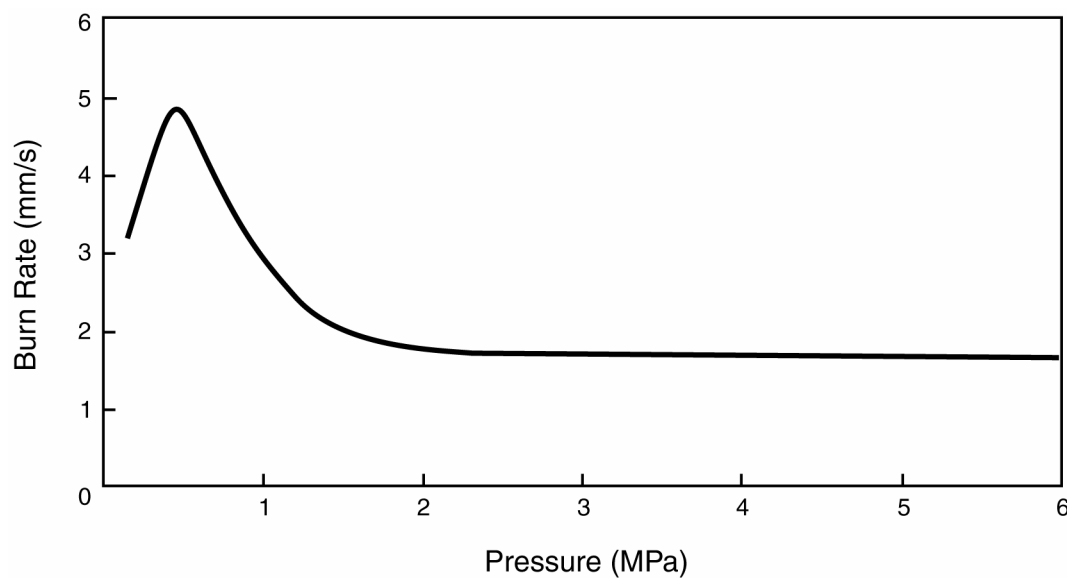
Figure 7. Burning rate vs pressure curve for B/Si/K₂Cr₂O₇.

burning rate between 0.1 and 0.4 MPa; there-upon the burning rate slows until a minimum is reached at about 2 MPa. Beyond this level, the burning rate is relatively unaffected by further pressure increase. The peculiar behaviour of this composition is thought to be caused by the sealing effect of the molten oxidiser (MP 398 °C) and the differential pressures developed within the consolidated column as a consequence.[10]

In the illustrated system, if the free space or the ignition source chosen by the designer were such that the internal pressure was between 0.1 and 2 MPa, the delay element could not be expected to yield a reproducible time interval. It is therefore important to select a gas-producing igniter or set the free space above the delay column in accordance with the burning rate/pressure relationship of the particular delay composition, or to choose a composition in which the dependence is not as critical.

The pyrotechnic composition database for the burning rate dependency on combustion pressure is very limited; therefore, each composition must usually be tested according to the intended application and evaluated according to the general principles outlined above.

The Pyrotechnic Delay Element

In its simplest form, the gassy pyrotechnic delay element may consist of a length of Bickford fuse potted for example, into a container of flash composition. The fuse may be ignited directly with a match or struck upon a matchbox if primed with a match composition. The fuse burns from one end to the other; the product gases exit the end of the fuse case, which is usually made of hemp coated with pitch or plastic. Black Powder burns at a defined RLBR (about 0.7 s/cm); therefore, the resulting delay interval is dependent upon the cut length of the fuse.

In more complex designs, the formulation of the Black Powder itself can be altered if required to slow the burning rate and produce longer times from a given column length. This can be achieved by the addition of modifiers such as excess charcoal, lactose or other sugars, or acaroid resin to the mealed form of Black Powder, which is then pressed into a tube.
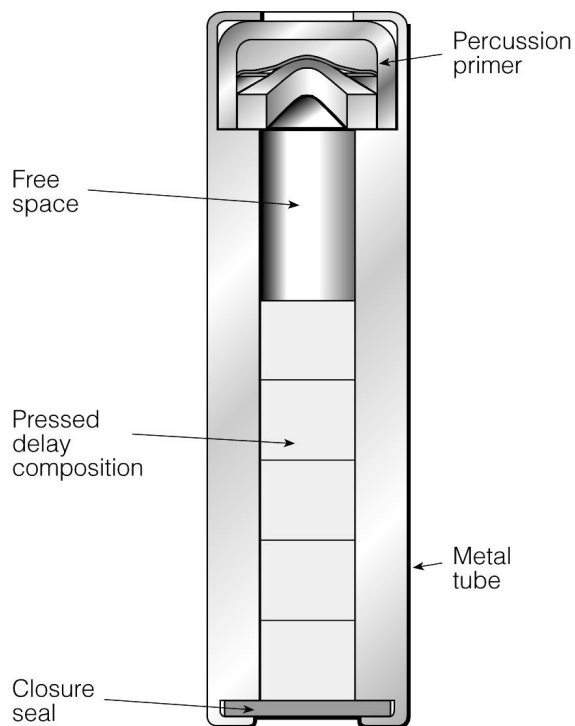
Figure 8. A typical pyrotechnic delay element.

A simple gasless delay element consists of a metal tube into which the delay composition is directly pressed at high compaction pressure to form a column. The tube is fitted at the ignition end with an ignition source (a percussion primer in the illustrated case in Figure 8). Beneath this is the free space; unless this volume is provided, combustion gases can overpressurise the system and eject the primer. A mechanical seal at the opposite end completes the assembly; this is normally designed to vent the combustion products from the tube upon delay burnout to provide an ignition transfer stimulus.

When the primer is struck, ignition is transferred to the top surface of the delay composition (which may be primed in the case of slow burning delay compositions) and it commences to burn along the length of the column. As the burning front approaches the end, the closure seal reaches a point where it can no longer withstand the internal pressure and temperature. It fails and the hot combustion products, which are usually molten or incandescent species, are ejected from the tube. The time between primer strike and the ignition transfer stimulus is the delay interval, which is mainly determined by

the type of composition and the length of the column.

Thermal Sources

Pyrotechnic delay systems are examples of the irreversible solid-solid interactions of fuels and oxidisers that are the basis of all pyrotechnic reactions, however as has been said, other types of composition are deliberately designed to produce a hot molten slag that can be used for specific purposes. Such compositions are usually called thermites; the original thermite reaction was first patented by Goldschmidt[11] in 1895:

$$8 \, Al + 3 \, Fe_3O_4 \rightarrow 4 \, Al_2O_3 + 9 \, Fe$$

$$Q_2 = 3.68 \text{ kJ/g} \qquad (9)$$
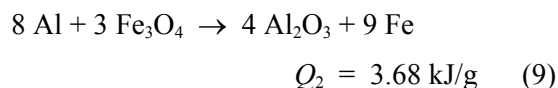
The characteristics that distinguish a thermite reaction from other pyrotechnic reactions are:

- an almost complete absence of gaseous reaction products after combustion

- a high reaction temperature (typically 2000–3000 °C)

- the formation of a molten slag that can be used to burn, cut or weld

Chemistry of Thermites

In a Goldschmidt reaction, the thermal energy produced is the total heat of formation of the products minus the total heat of formation of the reactants, minus the heat losses associated with physical effects such as latent heats of fusion and vaporisation of the products. If the heat produced is greater than about 2.23 kJ/g, the reaction is likely to go to completion.[12] While organic binders can be used in thermite compositions for special applications, some of the heat from the reaction will be lost due to the formation and ejection from the burning front of endothermic gaseous products such as carbon dioxide, water and nitrogen.

Because the basic reaction is relatively simple, it is possible to calculate the temperature of the reaction quite accurately. This is an invaluable tool because a thermite formulation can be designed to match a particular requirement. The technique is as follows:[13]

Using the reaction

$$2 \, Al_{(s)} + Fe_2O_{3(s)} \rightarrow Al_2O_{3(s)} + 2 \, Fe_{(l)} \qquad (10)$$
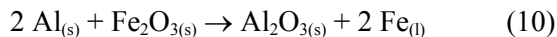
Heat of Reaction, $\Delta H°$

$$= \Delta H° \text{ (Products)} - \Delta H° \text{ (Reactants)}$$

$$= (-1675.7) - (-824.2)$$

$$= -851.5 \text{ kJ/mol}$$

It is possible to estimate the maximum theoretical combustion temperature of a thermite reaction using the equation:

$$Q = m \, S \, (T_o - T) \qquad (11)$$

where Q is the heat of the reaction, m is the number of atoms in the final product, T is the final temperature, T_o is the initial temperature and S is the specific heat at constant pressure. For the sake of simplicity, the specific heat is given a value of 27.2 J/mol/deg,[13] which corresponds to the average specific heat of the metal up to its boiling point. This means that the specific heat of the oxide formed is not considered in this calculation. Using data from equation 10

$$298 - T_{max} = -851.5 \times 1000/(27.2 \times 7)$$

therefore $T_{max} = 4770 \text{ K}$.

which is comparable to the temperature of 4382 K determined by Fischer and Grubelich.[14]

Uses for Thermites

The military uses of thermites as incendiaries have largely been superseded by liquid incendiary materials. However thermites are currently being used for the safe disposal of explosive ordnance whether used as a powder, putty, cast or pressed pellet form. Typical examples of thermite devices include incendiary grenades and the pyrotechnic torch (thermal lance).

In the industrial sphere, technology based on this reaction has been used to repair castings and to carry out butt-welding of railway lines.

Alumino-thermic reactions have also been used to produce pure carbon-free metals such as chromium and manganese by the use of the appropriate oxidiser. For example:

$$4 \, Al + 3 \, MnO_2 \rightarrow 2 \, Al_2O_3 + 3 \, Mn$$

$$Q_2 = 4.86 \text{ kJ/g} \qquad (12)$$
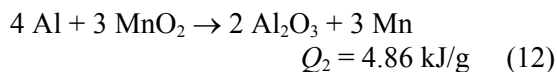
Table 6. Key Characteristics of Some Thermite Fuels.[16]

| Fuel | Melting Point of Oxide (°C) | Boiling Point of Oxide (°C) | Specific Gravity of Fuel (g/cm^3) | Formula of Oxide | Heat of Formation of Oxide (–kJ/mole) | Stoichiometric Formula of Thermite (%) | | Thermal Output (kJ/g) |
						Fuel	Oxidiser (Fe$_2$O$_3$)	
Al	2054	3000	2.7	Al$_2$O$_3$	1675.7	25	75	3.98
Mg	2826	3600	1.7	MgO	601.6	32	68	4.22
Ca	2899	> 2899	1.5	CaO	634.9	43	57	3.86
Ti	1843	> 2500	4.5	TiO$_2$	944.0	31	69	2.56
Si	1713	2950	2.3	SiO$_2$	910.7	21	79	2.68
B	450	~ 1860	2.3	B$_2$O$_3$	1273.5	12	88	2.48

Recently this technology has been expanded to include not only the manufacture of pure metals but also alloys (aluminides, nickelides), refractories (borides, carbides, nitrides, silicides), complex oxides (niobates, tantalates, ferrites, cuprates), hydrides and phosphides. The process is called self-propagating, high-temperature synthesis (SHS).[15] The few examples following demonstrate the versatility of the SHS process:

$$2\ B_2O_3 + C + 6\ Mg \rightarrow B_4C + 6\ MgO + \text{heat} \quad (13)$$

$$3\ NiO + 5\ Al \rightarrow 3\ NiAl + Al_2O_3 + \text{heat} \quad (14)$$

$$24\ Fe + 2\ BaO_2 + 17O_2 \rightarrow 2\ BaO\cdot6\ Fe_2O_3 + \text{heat} \quad (15)$$
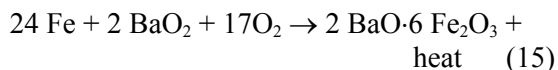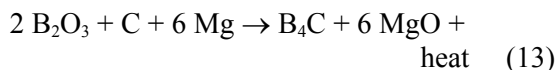
Ingredient Selection

Fuels

When designing a thermite composition it is important to select a fuel:

- with a high heat of combustion
- that forms an oxide of low melting point and high boiling point.

When chemical stability, cost and availability are considered along with the above criteria, aluminium is the optimum fuel (Table 6). However magnesium is often added to improve ignitability, and titanium or zirconium included to achieve a showering incendiary effect.

There is another class of fuel that is occasionally used for heat production, the intermetallic compounds such as: 'magnalium' (a 50/50 alloy of magnesium and aluminium), aluminium/nickel, aluminium/palladium, zirconium/nickel, titanium/boron, titanium/carbon, and calcium/silicon. The purpose of these fuels is usu-

ally system-specific and one of the alloying components usually serves a function other than as a fuel in the reaction.

Oxidisers

When choosing an oxidiser, the following characteristics are important:

- a low heat of formation
- minimum oxygen content of 25%
- a high density
- the ability to reduce to a metal with a low melting point and high boiling point

From Table 7, the best oxidisers for use in thermites are the oxides of iron, manganese and copper. Iron oxides are the cheapest to use but the slag formed in the Goldschmidt reaction has relatively low fluidity—this can be improved by the addition of sulphur or sulphides.[12]

Improvements in Ignitability

Alumino-thermic compositions have been found to be difficult to ignite and must be primed to ensure ignition transfer. There are also a number of other ways in which thermites can be made to ignite more reliably, the final choice depending on cost and the intended application.

General

The original Goldschmidt reaction was based on the use of *hammerscale*, an oxide of iron (rust) of inconsistent composition. This formulation was particularly difficult to ignite; the problem was largely overcome by the use of the well-defined forms of iron oxide (including syn-

Table 7. Characteristics of Some Oxidisers Used in Thermites.[16]

| Oxide | Heat of Formation (–kJ/mole) | Oxygen Content of Oxide (%) | Specific Gravity of Oxide (g/cm^3) | Melting Point of Metal (°C) | Boiling Point of Metal (°C) | Stoichiometric Formula of Thermite (%) | | Thermal Output (kJ/g) |
						Fuel (Al)	Oxidiser	
B_2O_3	1273.5	69	1.8	2075	4000	44	56	3.25
SiO_2	910.7	53	2.2	1414	3265	37	63	2.15
Cr_2O_3	1139.7	32	5.2	1907	2671	26	74	2.60
MnO_2	520.0	37	5.0	1246	2061	29	71	4.59
Fe_2O_3	824.2	30	5.1	1538	2861	25	75	3.98
Fe_3O_4	1118.4	28	5.2	1538	2861	24	76	3.68
CuO	157.3	20	6.4	1084	2562	19	81	4.11
Pb_3O_4	718.4	9	9.1	327	1749	10	90	2.00

thetic forms) and better control of oxidiser particle size. In recent times, most thermite applications have been limited to incendiary, explosive ordnance disposal (EOD), and cutting technology. For these alumino-thermic devices, an ignition system has often had to be developed.

Inclusion of Copper or Manganese Oxides into Iron Oxides

Experimental observations have indicated that thermite compositions containing Fe_3O_4 are easier to ignite than those containing Fe_2O_3. The reason is thought to be related to the crystal structure of the oxide, Fe_3O_4 having an inverse spinel structure of the general classification AB_2O_4.[17]

The inclusion of copper and manganese oxides as part of or all of the oxidiser content will also improve the ease of ignition of a thermite; one technique reported includes the copper oxide (CuO) and/or the manganese oxide (MnO_2) in the crystal lattice as a ferritic structure. For example, the ferrite, $CuFe_2O_4$, can be prepared by heating a mixture of $CuSO_4 \cdot 5H_2O$ and $FeSO_4 \cdot 7H_2O$ in the appropriate ratios.[18] McLain[19] reports the calorimetrically measured heat of reaction for a 50:50 mix of $CuFe_2O_4$ and Ti as 5.7 kJ/g, whereas for Fe_2O_3 and Ti, the heat of reaction was only 3.67 kJ/g.

Inclusion of Metal Oxides of High Specific Gravity

The inclusion of oxidisers such as molybdenum oxide (MoO_3), tungsten oxide (WO_3) and

lead oxide (Pb_3O_4) can be used to produce highly reactive thermite mixtures. These systems can be very expensive and there may be OH&S concerns with their preparation, but their rapid burning rate ensures their use in very fast delays and in the ignition systems of infrared decoy flares. Examples include B/MoO_3, Zr/WO_3 and Si/PbO_2.

Inclusion of Salt Oxidisers - Thermates

The addition of oxidisers such as nitrates and peroxides increases the heat of combustion and improves the mechanical strength of the pressed compositions. These oxidisers also introduce flame to the combustion (because of the amount of gas evolved) and usually make the composition more sensitive to mechanical stimuli such as impact and friction.

The inclusion of a nitrate oxidiser, usually barium nitrate, into a thermite improves both the ignitability of the formulation and increases target penetration due to gas production and the consequent projection of molten slag. Such a formulation is called a *thermate*. These have been widely used in incendiary grenades, particularly for explosive ordnance demolition (EOD) applications.

Explosives Safety Hazards

There is a misguided belief that thermite compositions are explosively insensitive. This is far from the truth and the variability of explosives hazards assessment data for a range of different types of thermite compositions is emphasised. Refer to Table 8. The burning rates of

Table 8. Explosive Sensitiveness Data for Typical Thermite Compositions.

Type of Thermite Composition (%)	Hazards Assessment Data			
	F of I [a]	T of I (°C)	Friction [b]	Ignition by electric spark
Mg/Fe$_2$O$_3$ (30/70)	> 200	> 400	0-0-0	Nil at 4.5 J
Plastic Thermite[20]	> 200	> 400	0-0-0	Nil at 4.5 J
Thermate Mg-Al/Ba(NO$_3$)$_2$ (40/60)	50	> 400	100-100-50	Nil at 4.5 J
Si/PbO/Bi$_2$O$_3$ (15/52/33)	120	> 400	0-0-0	0.01 J

a Figure of Insensitiveness (RDX = 80).

b Temperature of Ignition.

c Mallet Friction Test (Boxwood mallet on: Yorkstone-hardwood-softwood anvils, % ignitions from 10 tests).[21]

some thermite-type compositions are exceedingly rapid and the entire mass may explode upon initiation.

From the data in Table 8 a magnesium-fuelled thermite could be considered to be relatively insensitive to most stimuli but the thermate composition is friction-sensitive and by contrast, the Si/PbO/Bi$_2$O$_3$ system is electrostatically sensitive.

Conclusion

The technology associated with the design of pyrotechnic delays, which are used to provide reliable time intervals, has been described in detail. The different practical applications of the two basic types of delay composition, 'gassy' and 'gasless', have also been outlined.

The reaction chemistry of gasless delays is similar to that of thermite compositions. Both systems are based on the Goldschmidt reaction, but a thermite mixture, containing a metal and a metal oxide, is specifically formulated to burn and liberate high amounts of thermal energy.

References

1) R. Lancaster, *Fireworks—Principles and Practice*, 3rd ed., Chemical Publishing Co., New York, NY, USA, 1998.

2) T. Griffiths, *Private Communication*, DERA, U.K, 1993.

3) J. H. McLain, *Pyrotechnics from the Viewpoint of Solid State Chemistry*, Franklin Institute Press, Philadelphia, PA, USA, 1980.

4) F. S. Scanes, "Thermal Analysis of Pyrotechnic Compositions Continuing Potassium Chlorate and Lactose", *Combustion and Flame*, Vol. 23, 1974, pp 363–371.

5) H. Ellern, *Military and Civilian Pyrotechnics*, Chemical Publishing Co., New York, NY, USA, 1968.

6) H. O. Biddle & J. H. McLain, *Senior Thesis*, Washington College, Chestertown, MD, USA, 1970.

7) A. M. Scott, *A Guide to the Design of Pyrotechnic Delays*, Royal Armament Research and Development Establishment Memorandum 40/67, Fort Halstead, Kent, U.K, 1967.

8) L. V. de Yong, "Predicting the Ignition Performance of Percussion Primers", *Proceedings of the 13th International Pyrotechnics Seminar*, Grand Junction, CO, USA, 1988.

9) C. H. Bamford & C. F. H. Tipper, *Comprehensive Chemical Kinetics*, Vol. 2, Elsevier Publishing Co., Amsterdam, Holland, 1969.

10) S. L. Howlett, A. M. Scott & I. L. Chapman, *Pressure Effects in Sealed Delays Containing Boron Fuelled Gasless Compositions*, DSL Technical Note DSL-TN-258, Defence Standards Laboratories, Melbourne, Australia, 1972.

11) H. Goldschmidt, German Patent 96,317, 1895.

12) A. A. Shidlovskiy, *Principles of Pyrotechnics* 3rd ed., American Fireworks News, first printed 1964, 1997.

13) AMCP 1967, AMCP 706-185, *Engineering Design Handbook, Military Pyrotechnic Series, Part One, Theory and Application*, HQ, US Army Materiel Command.

14) S. H. Fischer & M. C. Grubelich, "A Survey of Combustible Metals, Thermites and Intermetallics for Pyrotechnic Applications", SAND95-2448C, *Proceedings of the 32nd AIAA/ASME/SAE/ASEE Joint Propulsion Conference*, July 1-3, Lake Buena Vista, Florida, 1996.

15) A. G. Merzhanov, "Pyrotechnical Aspects of Self-Propagating High-Temperature Synthesis", *Plenary Lecture of the Proceedings of the 20th International Pyrotechnics Society Seminar*, Colorado Springs, CO, USA, July 25-29, 1994.

16) D. R. Lide, *Handbook of Chemistry and Physics*, 78th ed., CRC Press, Boca Raton, NY, 1997.

17) M. J. Sienko and R. A. Plane, *Physical Inorganic Chemistry,* W. A. Benjamin Inc, New York, 1965.

18) J. H. McLain, *Process for the Preparation of Ferrites*, US Patent 3,887,479, 1973.

19) J. H. McLain, *Pyrotechnics,* Franklin Institute Press, Philadelphia, 1980.

20) R. J. Hancox, *The Development of Plastic Thermite*, Report MRL-R-868, Materials Research Laboratory, Melbourne, Australia, 1983.

21) MOD 1988, *Manual of Tests*, Sensitiveness Collaboration Committee, Procurement Executive, Ministry of Defence, Royal Armament Research and Development Establishment, Fort Halstead, Kent, UK.

Fireworks Shell Drift due to Shell-to-Bore Clearance

Randall K. Norton

35 Northwood Ct, Pittsburg, CA 94565, USA

ABSTRACT

For fireworks aerial shells, decreasing shell-to-bore clearance and increasing mortar length appear to have the effect of increasing the predictability of fireworks aerial shell trajectories, and thus dud aerial shell impact points. Some geometrical considerations are given to the influence of mortar length and shell-to-bore clearance on apparent aerial shell drift.

Keywords: fireworks aerial shell drift, mortar length, shell clearance

Introduction

There are many potential mechanisms to explain fireworks aerial shell drift. However, in the readily available literature pertaining to shell drift, very little has been said on the effects of mortar length and shell-to-bore clearance (bore windage).[1–6] While this is not surprising considering the wide variations between different shells and mortars, large shell clearances can significantly increase the error in calculations and observations of exterior ballistics.

Background

The rifled artillery piece came into general use during the US Civil War (1861–1865), and the earlier smoothbore brass and iron artillery, though still in service, was being phased out. Mortars of that era were classed as artillery and continued to be unrifled (i.e., smoothbore).

Most material on smoothbore artillery is no longer in print, but Gibbons' *Artillerists Manual*[7] is helpful in its identification of bore balloting. Balloting is the effect caused by an iron shell 'bouncing' side to side in a softer brass barrel, causing dents or "ballots" to be formed in the barrel, somewhat similar to the surface of a washboard. Repeated firing enlarged these ballots to the point where the gun's retirement from service would become necessary. The advent of the iron gun barrel, when fired with an iron shell, reduced the barrel balloting, but the term was retained to indicate the effects of excessive shell clearance that led to wild inaccuracy. Steps were taken to improve shell casting techniques, and the resulting shells were 'ring gauged' to prove size and sphericity.[7]

Experiments and Procedure

In the author's experience with some thousands of shells fired from civil war pattern mortars using solid lead ball projectiles from 2-3/4 to 5 inches in diameter, and bowling balls of 8-inch diameter, many ballistic effects were noted. Among these was the effect of bore windage causing an off-axis launch and producing apparent shell drift. These tests were performed on a nearly weekly basis from 1972 until 1980, under generally good conditions: elevation 300 feet above sea level, mild temperatures, low winds, and at ranges from 100 to 200 yards. Targets were premarked circles, 10 to 20 feet in diameter. Azimuth alignment was accomplished using fixed iron sights, and elevation was measured using a gunner's quadrant, accurate and reproducible to 1/2 degree. (This is obviously not conducive to producing the best accuracy.) After each shot, the barrel of the mortar was searched to remove debris, wet swabbed to remove powder fouling, and dried. Firing intervals were held to 5 minutes minimum. Most test firing was done by E Battery, 4th US Artillery, Civil War Skirmish Association.

The mortars used in the above tests were civil war pattern mortars made from seamless steel tube with a wall thickness equal to the bore diameter, and were proof tested with vastly increased powder and projectile loads.

Acceptable accuracy (i.e., projectiles hitting within the pre-marked circles) was found to occur only when shell clearance was reduced to within one percent of the bore diameter. No sabot or other alignment aid was used. Many experiments were made with projectiles of different shapes, densities, sizes, etc. and the minimum shell drift was accounted for using an ordinary (and simple) trigonometric relationship. This relationship is illustrated in the following example.

Two lengths of mortars are compared

Short tube: Length = 12 in. (4 calibers)
Inside diameter = 3 in.

Long tube: Length = 40 in. (13.3 calibers)
Inside diameter = 3 in.

Projectile: Shape = Spherical
Diameter = 2.5 in.

Figure 1 shows the shell in initial contact with the side of the mortar tube, probably a typical situation for a fireworks (or any other) shell. This results in an approximately 1/2-inch shell-to-mortar clearance opposite the contact point. If the shell is fired and does not contact the barrel (mortar wall) before exiting, probably an unlikely event, there is an initial angle, θ, through which it has freedom of movement. For this scenario (no balloting), θ is the maximum angle of launch that is uncontrolled by the axis of the bore of the mortar.

For the case of the short mortar, 12 inches in length, with a 1/2-inch shell-to-bore clearance,

$$\tan\theta = \frac{0.5}{12} = 0.0417 \qquad \text{and}$$
$$\theta = 2.4°$$

Accordingly, due to shell clearance in the short mortar, the launch may be anywhere from 0 to 2.4° away from the bore axis, and in any direction about the axis.

For the long mortar, 40-inches in length and 1/2-inch shell clearance,

$$\tan\theta = \frac{0.5}{40} = 0.0125 \qquad \text{and}$$
$$\theta = 0.7°$$
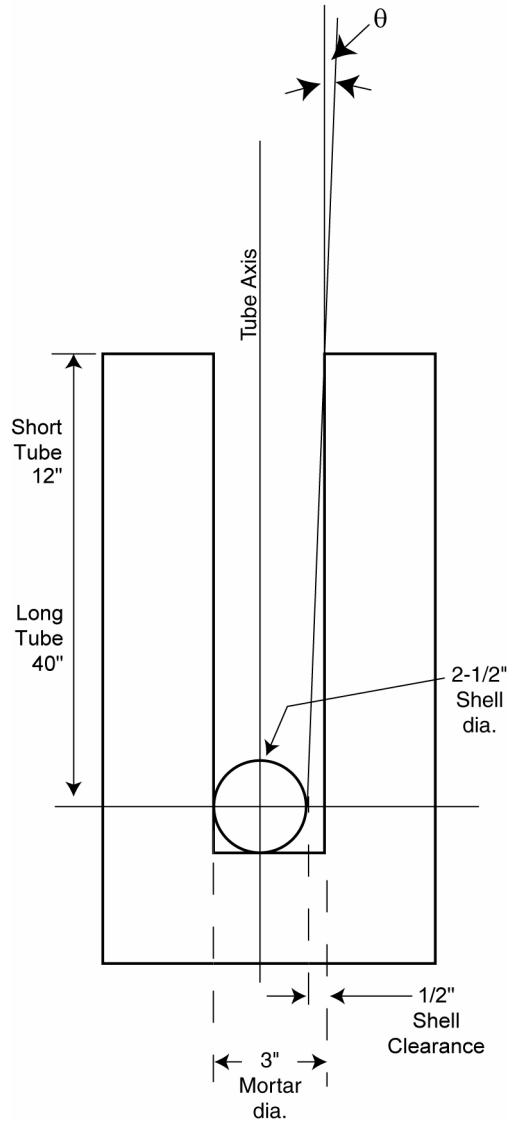
Figure 1. Sketch of the maximum projectile deviation that can occur without balloting during firing, where θ indicates the deviation from the bore axis.

Accordingly, for the long mortar, the off axis launch angle is significantly reduced—held to no more than 0.7° from the bore axis.

To calculate the potential results for fireworks aerial shells, an external ballistics computer model[8] was used. For this calculation, trajectory deviations of 2.4 and 0.7° were used for an aerial shell projected to a height of 300 feet from an otherwise vertical mortar in the absence of wind or other trajectory altering forces. This implies a trajectory uncertainty at its zenith of approximately 22 and 6 feet, for the

short and long mortar examples, respectively. If these aerial shells fail to burst (i.e., are duds), they would be expected to fall to the ground at a distance of 40 and 12 feet, respectively, from that predicted based solely on mortar angle.

As the maximum height of the shell or bore clearance increases, so will the maximum shell deviation at its zenith and upon its impact with the ground. Again, note that the above calculation is only for the scenario where the shell does not touch the side of the mortar (ballot) as it traverses the length of the mortar tube. However, if the shell does touch, the geometrical effects of bore clearance increase drastically, as shown in Figure 2.

For a shell contacting the tube wall at the halfway point of the 12 inch mortar,

$$\tan\theta = \frac{0.5}{6} = 0.0833 \qquad \text{and}$$
$$\theta = 4.8°$$

Accordingly, in this case, the result is a maximum deflection of 4.8° from the mortar axis, twice the deviation found previously when the shell did not contact the mortar wall upon exiting. In this case for an aerial shell projected to 300 feet elevation, the deviation can be approximately 44 feet at its zenith and 80 feet if it falls back to the ground. Thus, there exists a "cone of uncertainty" in the trajectory of the shell before it leaves the mortar that may amount to a significant percentage of the separation distance from spectators.

In this brief article, a number of subjects were not addressed. These include the effects of any rotational forces caused by the contact of the shell with the bore, the effects of the center of gravity not being coincident with the geometric center of the shell, the effects of surface protrusions or surface texture of the shell and mortar, and whether or not the shell or mortar is plastically or elastically deformed due to setback forces.
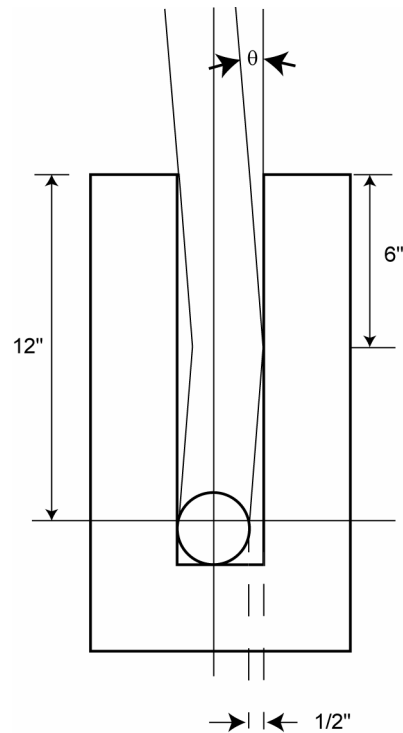
Figure 2. Sketch of projectile deviation that can occur if the projectile contacts the wall of the mortar tube at the half-way point, with θ indicating the angle of deviation from bore axis.

Conclusions

For any given amount of bore balloting, increasing mortar length to the longest convenient length will reduce the launch trajectory uncertainty resulting from shell-to-bore clearance. Similarly, for any given mortar length, keeping the shell clearance as low as possible will reduce the launch trajectory uncertainty.

Testing is planned to further study shell clearance effects. Three mortars are being constructed to fire inert fireworks shells. Results of this additional work will be reported upon its completion.

References

1) S. Yamamoto and T. Shimizu, *Studies on Precautions Against Blind Shells*, Chapter 2 "Studies to obtain a Standard of Safety Distances to Avoid Injury from Blind Shells", Tokyo University, 1959–1962.

2) T. Shimizu, *Fireworks from a Physical Standpoint, Part III*, Pyrotechnica Publications, 1985.

3) K. L. and B. J. Kosanke, "Aerial Shell Drift Effects", *Proceedings of the 1ˢᵗ International Symposium on Fireworks*, 1992. Also appeared in *Selected Publications of K. L. and B. J. Kosanke, Part 2,* Journal of Pyrotechnics, Inc., 1995.

4) K. L. and B. J. Kosanke and Al Bauer, "Aerial Shell Drift Effects (A) The Effect of Long Mortars", *Journal of Pyrotech-nics,* No. 3, 1996. Also appeared in *Selected Publications of K. L. and B. J. Kosanke, Part 4,* Journal of Pyrotechnics, Inc., 1999.

5) D. Eckhardt and H. Andre, "Results and Conclusions from the Investigation of an Accident with a Display Shell", *Proceedings of the 5ᵗʰ International Symposium on Fireworks,* 2000, pp 83–103.

6) R. L. Schneider, "Aerodynamics of Aerial Display Shells", *Proceedings of the 5ᵗʰ International Symposium on Fireworks,* 2000, pp 459–466.

7) L. Gibbons, *The Artillerists Manual*, US Ordnance Dept., 1863.

8) K.L. and B.J. Kosanke, "Computer Modeling of Aerial Shell Ballistics", *Pyrotechnica XIV,* 1992. Also appeared in *Selected Publications of K. L. and B. J. Kosanke, Part 2,* Journal of Pyrotechnics, Inc., 1995.

Pressure, Plume Flicker, and Acoustic Data Correlation in Labscale Hybrid Rockets

Mary Fran. Desrochers, Gary W. Olsen, Chris Luchini, and M. Keith Hudson
Department of Applied Science and The Graduate Institute of Technology
University of Arkansas at Little Rock, Little Rock, AR 72204 USA

ABSTRACT

The development of the hybrid rocket motor has been plagued by combustion instabilities. These are usually monitored as fluctuations in chamber pressure and are on the order of tens of Hz in frequency. Previous work using our labscale hybrid system has also indicated instabilities at these frequencies. These have been attributed to fuel chuffing or other phenomena. Additional studies, in areas such as IR and other spectral monitoring, have indicated that these oscillations are also present in the plume as light emission flicker. However, they were not investigated in the previous work.

This paper presents a study of these specific phenomena and attempts to correlate plume flicker, acoustic data, and higher speed chamber pressure monitoring. It was found that the plume flicker frequencies match those found using high speed pressure transducers, although these light intensity fluctuations demonstrate greater amplitude. Acoustic data could not be correlated, as it appears as a form of white noise. The authors feel that flicker data offers an inexpensive but sensitive alternative to high-speed pressure transducer use.

Keywords: hybrid rocket, exhaust plume, plume diagnostics, combustion diagnostics, engine health monitoring, optical emissions, acoustic emissions

Introduction

The premise for this paper was to explore combustion instabilities associated with hybrid rockets. Although the existence of these combustion instabilities is well known, they have not been well explored.[1] In this study, measurement of pressure oscillations was targeted as the best way to investigate instabilities; plume flicker data and acoustic data were recorded to examine possible correlations with the pressure oscillations.

The hybrid rocket facility at the University of Arkansas at Little Rock (UALR) consists of a labscale hybrid rocket motor, video monitor, data acquisition system, and computer control system. The facility was originally built for plume diagnostic and combustion studies. Recently, emphasis has been added to focus on physical parameters of the rocket motor.

The rocket has two main parts, a head assembly and the chamber body. Constructed of 303 stainless steel, the head assembly contains a portion of the precombustion chamber. The head also contains the igniter inlet and the pressure transducer ports, as well as inlets for the gaseous oxygen, nitrogen, and propane. The chamber body, manufactured from schedule 80, 304, stainless steel pipe, houses the rest of the precombustion chamber, the fuel grain, the postcombustion chamber and the nozzle. The hydroxyl-terminated polybutadiene (HTPB) fuel grain is 10 inches long and 2 inches in diameter (254 × 51 mm). Gaseous oxygen is used as the oxidizer. Additional information on the construction and operation of the facility can be found in previous papers.[2-4]

Experimental

The goal of the project was to reveal information relating to the combustion instabilities in hybrid rockets. The paper focuses on three measurements: pressure, plume flicker and acoustic output. All data for this paper origi-
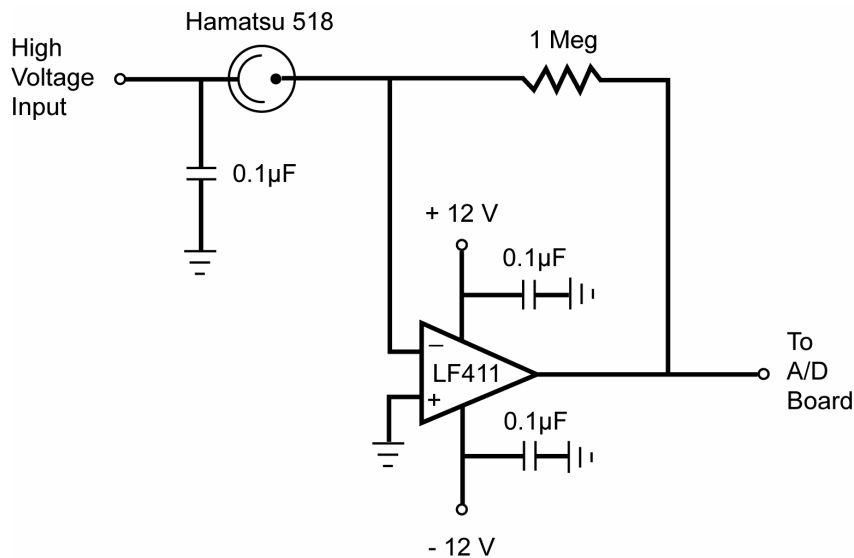
Figure 1. Schematic of phototube detector circuit.

nated from twelve rocket firings using HTPB as the fuel. The oxidizer flow was varied from 0.04 to 0.14 pounds-mass/second (18 to 64 g/s).

Pressure and plume flicker data were taken using a Computer Boards CIO-DAS-1600 12-bit data acquisition board in a 486DX-33 MHz computer. Data was sampled at 50 kHz. The rocket was equipped with two pressure transducers, both located in the pre-combustion chamber. A piezoresistive transducer manufactured by Keller PSI (series 21) capable of measuring up to 1000 psia (6890 kPa) at 1 kHz was used by the control system and sampled at 25 Hz. It was used for routine monitoring of the pressure during a firing and as a safety shutdown.[2] The second was a Kistler Model 7063A piezoelectric pressure transducer designed for use in an internal combustion engine.[5] A Kistler Model 5010 Dual Mode Amplifier, operated in charge mode, powered it. To ensure precise measurements, it was water-cooled and manufactured with an extra thermal shield to minimize errors due to hot combustion gases. Safety shutdown for the rocket occurs at 580 psi (3996 kPa), however the Kistler transducer was allowed to record to 1000 psi (6890 kPa). The charge amplifier, set at 1v/100 psi (689 kPa), was fed into the A/D board. The piezoelectric pressure transducer has minimal damping and therefore was modeled as an under-damped, spring-mass system.[5] To maintain

errors associated with the damping factor to less than 5%, the output of the pressure transducer is considered acceptable to 20% of the natural frequency, in this case to 6 kHz. A filter in the amplifier limited the bandwidth of the data to 6.8 kHz (–3 db @ 6.8 kHz). Linearity is specified to ±0.5% of full-scale output, in our case ±18 psi (124 kPa). Both transducers were calibrated using a dead weight pressure tester and tested to within 4% of each other.

The plume flicker sensor was built in our laboratory. A Hamamatsu 518 side-on type phototube was used for the sensing element.[6] The current output from the phototube was converted into voltage by the use of an LF411 op-amp. The circuit produced 1-volt output for every 1 µA produced by the phototube. This output was fed into the A/D board. Figure 1 is a schematic of the phototube circuit. The Hamamatsu literature states that vacuum phototubes can provide frequency response to 100 MHz, so our system was limited by the bandwidth of the op-amp (approximately 4 MHz). In laboratory testing and modeling, the transducer showed acceptable response from DC to 100 kHz. The phototube has an optical response from 185 to 850 nm. Testing the transducer with neutral density filters (metal film type, flat response) and various light sources proved that it had a linear response (±6% transmission from 15 to 98% transmission). The entire plume was viewed
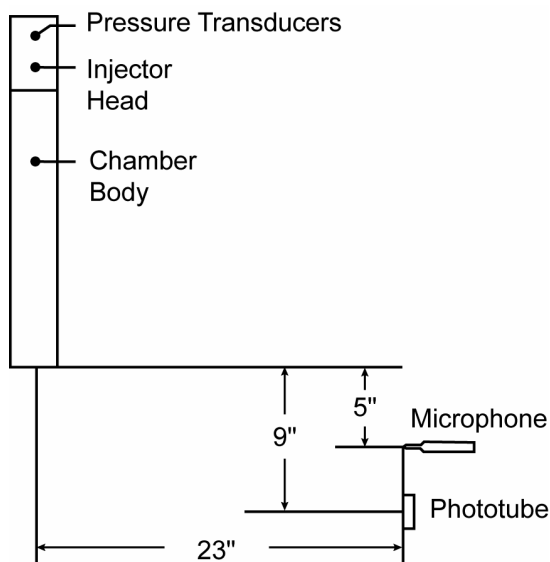
Figure 2. Top view of transducer positions.

Figure 3. Typical pressure data (data averaged for display purposes).

by the phototube. The phototube was located in the horizontal plane of the test stand, 23 inches (580 mm) from the plume and 9 inches (230 mm) from the end of the motor casing as shown in Figure 2. An iris was used to control the amount of light allowed to strike the phototube and was set to 0.094 inches (2.4 mm).

The acoustic output was sampled at 44.1 kHz by a 16-bit multimedia audio card manufactured by Turtle Beach Systems, Inc., in a 486DX2-50 MHz computer. A Bruel & Kjaer 4135 condenser microphone in conjunction with a 2801 power supply was used to record the acoustical output of the rocket. The manufacturer's calibration provided with the microphone stated acceptable response to 100 kHz. Output of the microphone was 3.39 mV/Pa. The microphone was located in the plane of the horizontal test stand, 23 inches (580 mm) from the plume centerline and 5 inches (127 mm) beyond the end of the motor as shown in Figure 2.

Results and Discussion

Fast Fourier Transforms (FFTs) of the microphone data were done using Hypersignal® for Windows. Acoustically, the rocket produces a wide band frequency spectrum within the bandwidth of our system and appears as white noise. While various frequencies appear to be emphasized at any one instant, overall no indi-

vidual frequencies stand out and certainly none correlate with the pressure data. The sound pressure level for our firings ranged from 146 to 168 dB (in reference to 2×10^{-5} Pa for 0 db).

Time and frequency domain analysis of the pressure and plume flicker data provided similar results. Figures 3, 4, and 5 are time plots of the data. The data sets were analyzed using in-house software and results are listed in Table 1. The amplitudes listed in Table 1 are maximum amplitude values expressed as a percentage of the mean value for a given data set. The frequencies are approximate center frequencies. Fast Fourier Transforms were completed on 0.16-second intervals of the data; no windowing was used. Representative FFT spectra are shown in Figures 6 and 7. The 30 Hz oscillation could be identified as the chuffing of the fuel: this oscillation is visible in the time base data for the pressure and flicker. Approximation of parameters using a 1/4-wave tube revealed an acoustic frequency of about 500 Hz. It is believed that

Table 1. Pressure and Flicker Oscillations.

Frequency (Hz)	Pressure (% of DC value)	Flicker (% of DC value)
30	6	100
450	4*	40
900	2*	20
1,800	1*	10

* Magnitude less than specified transducer linearity.
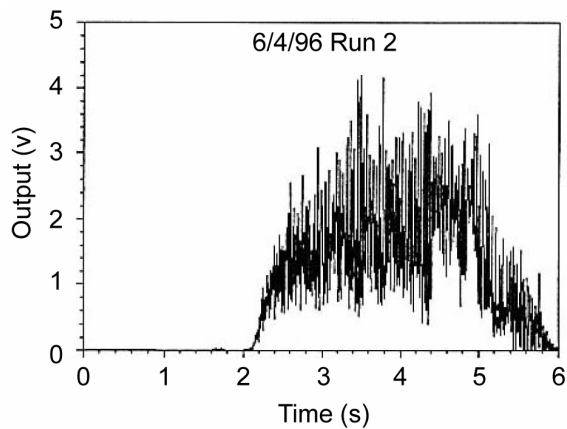
Figure 4. Typical plume flicker data (data averaged for display purposes).

the 450 Hz frequency is the fundamental longitudinal mode and the 900 and 1800 Hz frequencies are harmonics of the fundamental mode.

The Kistler pressure transducer provided the facility with new information. At ignition, there is often a short initial high-pressure spike, which the piezoresistive transducer cannot detect. The Kistler equipment, however, allowed gaining a better understanding of the start up transients. The spike is believed to be caused by slight imbalances in the propane/oxygen mixture used to ignite the fuel. The indication is that the propane pressure is too high. This phenomena has been noted in this and previous studies as an
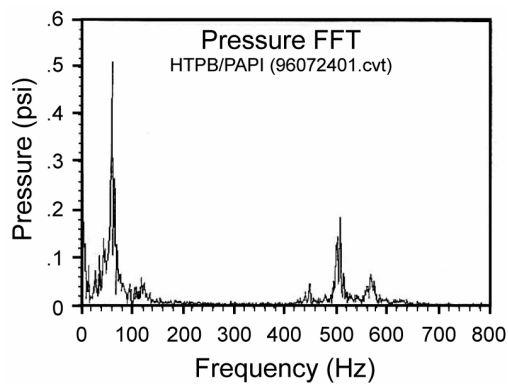
Figure 6. Frequency spectrum resulting from FFT analysis of pressure data.
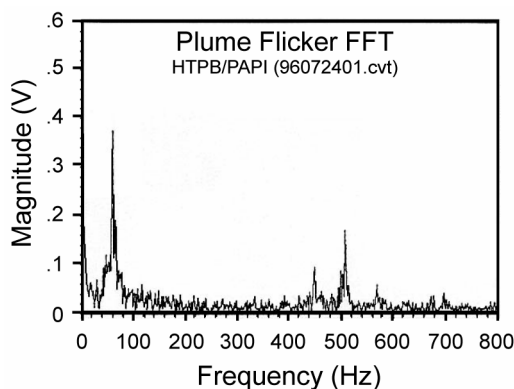
Figure 7. Frequency spectrum resulting from FFT analysis of plume optical flicker.
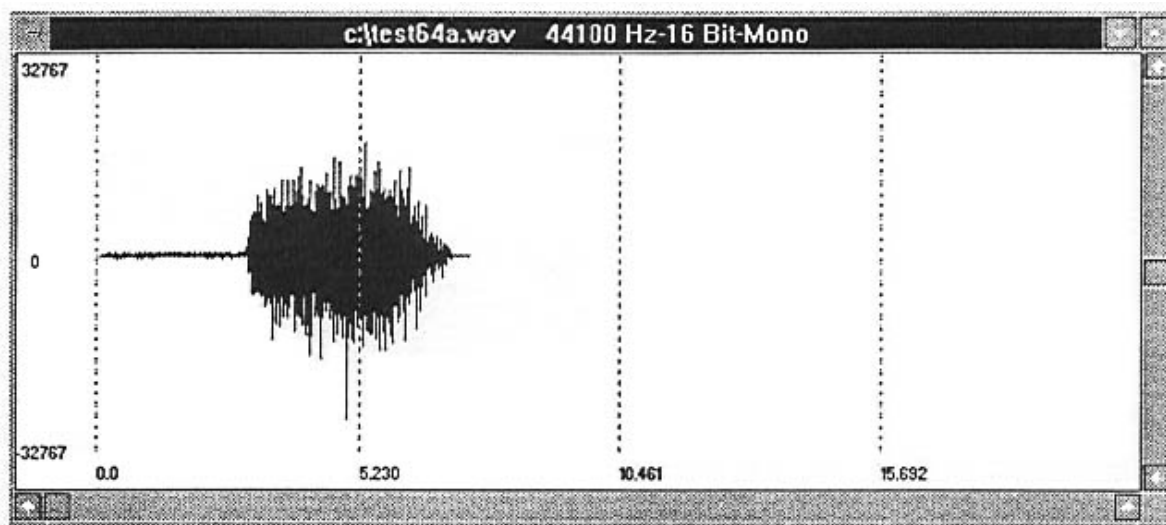
Figure 5. Typical microphone data.

audible "popping" during ignition. During the steady-state portion of the firing, slight oscillations were observed at 450, 900, and 1800 Hz. However, the magnitudes of the majority of the oscillations were lower than that of the specified linearity for the transducer, therefore, the exact magnitude is uncertain. In routine firings, the Keller transducer will continue to be used but will have its sampling rate increased in an attempt to capture the 450 Hz pressure oscillations.

Previous work on plume flicker with a different transducer exhibited frequencies at 430 Hz, therefore, there is confidence that the oscillations in the plume flicker are repeatable. The plume flicker and pressure oscillations were detected at the same points in time. The initial spike of the plume flicker data was detected 0.2 seconds after the initial pressure spike. This can be explained by considering two points. First, that the propane flame/plume is a gaseous selective radiator and that the motor may not have an actual plume at this point in time. Second, that the actual rocket plume resulting from the HTPB fuel is a particle-laden plume, with a large blackbody emission, giving significant optical radiation for monitoring plume flicker.[4] If there is, in fact, any plume resulting from the propane ignition, it will exhibit a very weak optical emission spectrum. In any case, this shows that the use of plume flicker data provides a good indicator of the pressure oscillations in a hybrid rocket motor. Flicker monitoring should also be applicable in solid propellant systems and other particle-laden plumes.

Conclusions

It was possible to detect and correlate pressure and plume flicker oscillations in our labscale hybrid motor. By using this method, future investigators may find a non-invasive alternative to the use of expensive pressure transducers for certain combustion monitoring activities. The acoustic output did not prove to be useful in this study, since it consisted of white noise. The study in this area will continue with the addition of a thrust sensor to the system. Further plume data will be taken, correlating pressure in addition to the parameters monitored here, and also focusing on particular regions of the plume.

Acknowledgments

References

1) M. J. Chiaverini, G. C. Harting, Y. Lu, K. K. Kuo, N. Serin, and D. K. Johnson, "Fuel Decomposition and Boundary-Layer Combustion Processes of Hybrid Rocket Motors", *AIAA Paper No. 95-2686*, Jul 1995.

2) R. B. Shanks and M. K. Hudson, "A Labscale Hybrid Rocket Motor for Instrumentation Studies," *Journal of Pyrotechnics*, No. 11 (2000) pp 1–10.

3) R. B. Shanks, "A Labscale Hybrid Rocket Motor and Facility for Plume Diagnostic and Combustion Studies," A Doctoral Dissertation, University of Arkansas at Little Rock, December 1994.

4) M. K. Hudson, R. B. Shanks, D. H. Snider, D. M. Lindquist, and C. B. Luchini, "UV, Visible, and Infrared Spectral Emissions in Hybrid Rocket Plumes", *International Journal of Turbo and Jet Engines*, Vol. 15 (1998) pp 71–87.

5) Kistler Instrument Corporation, General Catalog K2.006, 4th ed., May 1995.

6) Hamamatsu Photonics, Phototubes, January 1990.

Pyrotechnic Reaction Residue
Particle Identification by SEM / EDS

K. L. & B. J. Kosanke

PyroLabs, Inc., 1775 Blair Rd., Whitewater, CO 81527, USA

and

Richard C. Dujay

Mesa State College, Electron Microscopy Facility, Grand Junction, CO 81501, USA

ABSTRACT

Today the most reliable method for detecting gunshot residue is through the combined use of scanning electron microscopy (SEM) and energy dispersive spectroscopy (EDS) of the resulting X-rays. In recent years, this same methodology has found increasing use in detecting and characterizing pyrotechnic reaction residue (PRR) particles. This is accomplished by collecting particulate samples from a surface in the immediate area of the pyrotechnic reaction. Suspect PRR particles are identified by their morphology (typically 1 to 20 micron spheroidal particles) using a SEM, which are then analyzed for the elements they contain using X-ray EDS. This will help to identify the general type of pyrotechnic composition involved. Further, more detailed laboratory comparisons can be made using various known pyrotechnic formulations.

Keywords: pyrotechnic reaction residue, gunshot residue, scanning electron microscopy, energy dispersive spectroscopy, morphology, X-ray elemental analysis, forensics

Introduction

The combined use of scanning electron microscopy (SEM) and X-ray energy dispersive spectroscopy (EDS) for the use in the detection of gunshot residues (GSR) was introduced in the mid-1970's.[1] This GSR analytic method has become so well established that it has been defined through an ASTM standard.[2] In essence, the method uses SEM to identify particles with the correct morphology and X-ray EDS to determine whether those particles have the correct elemental constituents. The sought after GSR particles have a morphology that is nearly spherical in shape and range in the size from approximately 0.5 to 5 microns. These residue particles, which originate from the primer composition, are spheroidal in shape because they are formed at high temperature, where the surface tension of the molten residue droplets contracts them into spheroids before they solidify upon cooling. The particles are relatively small because they are created under near explosive conditions, first at high pressure inside the firearm, then suddenly expanding to atmospheric pressure. The sought after GSR particles most commonly have lead, antimony and barium present (or some combination thereof), often in conjunction with a small collection of other chemical elements. This is because GSR particles have essentially the same elements present as in the formulation used in the primer for the cartridge, where compounds containing lead, antimony and barium are common.[3] In addition, materials from the projectile, cartridge case and barrel of the weapon may be present in GSR particles. The chemical elements present in smokeless powder are the same as are generally present in organic matter and are thus not unique to GSR. (However, these materials can often be chemically detected by other means.[4])

The requirement for both the correct morphology and the correct elemental composition, all within the same individual particle, provides high specificity. Certainly this methodology provides much higher specificity than the previously accepted technique for GSR analysis based

on atomic absorption spectroscopy of washes taken from the hands or clothing of an individual. In fact the SEM / EDS technique is considered so specific that in a recent survey, some forensic laboratories consider finding even a single particle meeting the GSR criteria sufficient to report that a person was near a discharging firearm.[5] (Note, however, essentially all laboratories surveyed did not provide the specific number of particles required for positive GSR identification. Presumably because the answer is more complicated, requiring consideration of things such as whether there may be natural or industrial materials present that have similar attributes.) The same high degree of specificity that SEM / EDS offers in GSR detection, also applies to the identification of pyrotechnic reaction residue (PRR) particles; however, there are two important differences. First, the chemical elements present in PRR particles are mostly different (and potentially more varied) than those most commonly found in GSR. Second, generally the quantity of PRR particles produced is several orders of magnitude greater than that for GSR. The first difference makes performing PRR analysis somewhat more difficult, but the second makes it much easier.

Although using the combination of SEM / EDS is well established from decades of use in GSR analysis, and although the same methodology applies equally well to the analysis of PRR particles, relatively little information regarding its use for PRR particle analysis has appeared in the literature. Most of the articles are recent and in the context of pyrotechnic residues that may be found to meet the criteria of GSR.[6–9] The one exception known to the authors is a single article produced at the Explosive Forensic Laboratory in the UK.[10] This lack of published information is unfortunate, because this is a powerful investigative tool about which too few people are aware. Granted, the number of pyrotechnic and fireworks incidents whose investigations can benefit from this technique is not large. However, in those instances where it can be beneficial, probably no other methodology can produce comparably useful results. Accordingly, this paper was written to increase awareness of the use of SEM / EDS for the analysis of pyrotechnic reaction residues for the purpose of accident investigation. Since many investigators may not be familiar with SEM / EDS, this article includes some basic information about these techniques. However, it should be noted that many details and subtleties of SEM / EDS methodology are beyond the scope of the present article.

Basic SEM / EDS Methodology

Most of what is described in the remainder of this article is independent of the type of instrument used. However, it may be instructive to describe the instrument most often used by the authors. The SEM is a manually operated AMRAY 1000, recently remanufactured by E. Fjeld Co.[11] For this work, the instrument is most often used in the secondary electron mode, but it is occasionally used in the backscatter and spot mapping modes when that is called for. The instrument provides software driven digital imaging. The X-ray spectrometer is energy dispersive, using a Kevex Si(Li) detector[12] with a beryllium window in conjunction with an American Nuclear System[13] model MCA 4000 multichannel analyzer and its Quantum-X software (version 03.80.20). Most typically, samples are collected on conductive carbon dots and are not coated. However, to improve the image quality of some of the micrographs in this article, some specimens were lightly sputter coated with gold. Finally, it should be noted that much additional and more detailed information on the techniques used will be included in a subsequent article.[14]

Much of the information presented in this section is based on standard texts dealing with the subjects of scanning electron microscopy and X-ray energy dispersive spectroscopy.[15,16] In its simplest terms, the operation of a SEM can be described as follows. An electron gun produces high-energy electrons that are focused and precisely directed toward a target specimen in a vacuum (see Figure 1). As a result of this bombardment, among other things, low energy secondary electrons are produced through interactions of the beam electrons with the atoms in the specimen. In the most commonly used SEM mode, these secondary electrons are collected and used to generate an electronic signal. The amplitude of that signal is dependent on the nature and orientation of the portion of the specimen being bombarded at that time. The impinging electron beam can be systematically moved
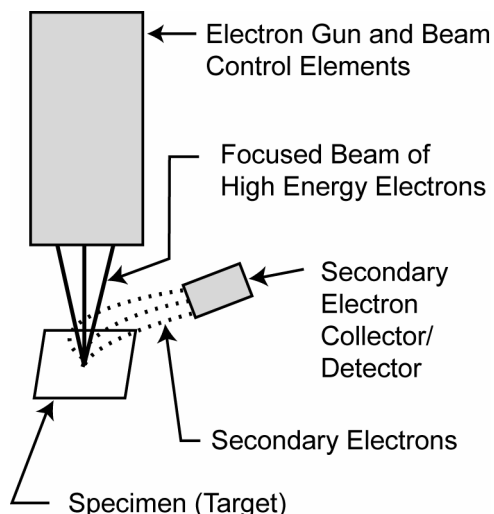
Figure 1. Illustration of some aspects of the production and collection of secondary electrons in a SEM.

Figure 2. Illustration of some aspects of rasterized SEM scanning to produce an image.

over the specimen in a rasterized pattern of scans (see Figure 2). The resulting secondary electron signal can then be used to create an overall (television-like) image of that portion of the specimen being scanned. Because the incident beam of electrons is highly focused and because the pattern of scans across the specimen can be precisely (microscopically) controlled, the image produced is of high spatial resolution and can be highly magnified (easily to 20,000 X).

Along with the production of secondary electrons, much higher energy backscatter electrons are also produced. Because of their high energy, only a relatively few will be detected and can be used for imaging. Nonetheless, there are times, discussed later in this article, when using backscatter electrons for imaging will be a useful tool in identifying the origin of some types of particles found within samples.

In addition to the production of secondary and backscatter electrons, another result of the interaction of the electron beam with the target specimen is the production of X-rays. These X-rays are uniquely characteristic of the type of atoms (the chemical elements) that produced them. By detecting and analyzing the energies of the X-rays that are generated, the identity of chemical elements in the target specimen can be determined.

The most common method for analyzing the X-rays produced by the specimen is described as energy dispersive spectroscopy (EDS). This uses a solid state [Si(Li)] X-ray detector. The output of this detector consists of voltage pulses that are proportional to the X-ray energies being deposited. Using a multichannel analyzer (MCA), the signal pulses are sorted according to voltage (energy) and the results stored for subsequent interpretation (i.e., identification of the atomic elements present). There are some limitations on the range of energies of the X-rays that are produced and detected using a SEM / EDS instrument. The maximum energy of the X-rays will be a little less than the energy of the electron beam (which typically is 20 or 30 keV). However, as a practical matter, good X-ray yields require a beam energy at least 1.5 times the X-ray energy. Further, there is an energy threshold below which the X-rays will not be detectable. For those many instruments that use a vacuum isolating beryllium window, this threshold is approximately 0.5 keV. This has the effect of preventing the detection of the X-rays from elements below oxygen in the periodic table. (As a practical matter, for such instruments, X-rays from elements below sodium are difficult to detect.)

As the primary beam of electrons penetrates and interacts with the specimen, there is a loss of their initial energy, and with that, a loss in the electron's ability to stimulate the production of higher energy X-rays. While it depends on the electron beam energy and the nature of the specimen, for the X-ray energies of interest in PRR particle analysis, the depth of interroga-

tion should be considered to be no more than approximately 5 μm.

Accordingly, the combination of SEM / EDS allows (with some limitations) the microscopic imaging of specimens and the determination of the chemical elements present in those specimens. It is this powerful combination of abilities that allows for the rapid identification and characterization of PRR particles.

Pyrotechnic Reaction Residue Particle Morphology

In essentially every case, pyrotechnic reactions produce sufficient thermal energy to produce molten reaction products. Further, in the vast majority of cases, some temporarily vaporized reaction products are also generated—usually along with some permanent gases. Assuming the pyrotechnic reaction is somewhat vigorous, the temporary and permanent gases act to disperse the molten and condensing reaction products as relatively small particles. The size of these residue particles varies from several hundreds of microns down to considerably less than one micron. The distribution of particle size depends on the nature of the pyrotechnic composition and the conditions under which they were produced. Explosions tend to produce only relatively small particles (smoke), whereas mild burning tends to produce a wider particle-size distribution, including many larger particles. Because of surface tension, those pyrotechnic reaction residue (PRR) particles that were molten and then solidified while airborne will generally be spherical (or at least spheroidal) in shape. The collection of electron micrographs in Figure 3 demonstrates the appearance of some PRR particles. The selected particles range from approximately 10 to 20 microns in diameter. These particles were collected from a surface that was one foot (0.3 m) from an explosion produced using a type of fireworks flash powder. In this same test, in addition to particles of pyrotechnic origin, soil particles are present that were mobilized as a result of the explosion. For comparison, see Figure 4, which is a collection of micrographs of typical soil particles of geologic origin. Again, all selected particles range from approximately 10 to 20 microns.
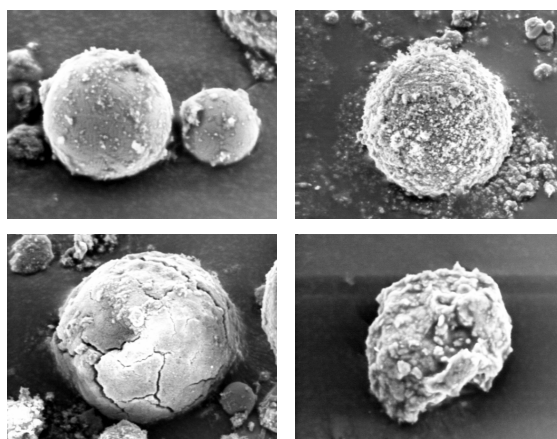
Figure 3. Examples of 10 to 20 micron spheroidal pyrotechnic reaction residue (PRR) particles.
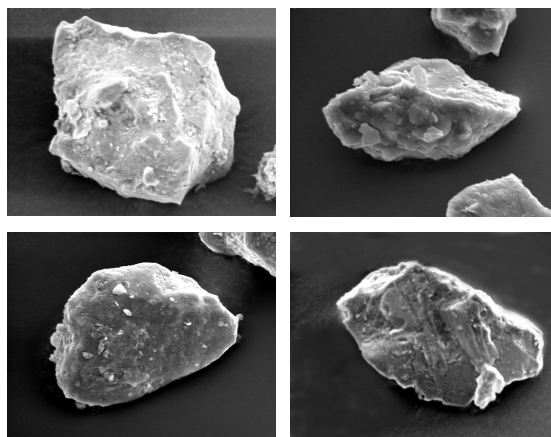
Figure 4. Examples of typical 10 to 20 micron particles of geologic origin (soil).

As illustrated in Figures 3 and 4, most often there are discernable differences between PRR particle morphologies and those of geologic soil particles; however, this cannot be absolutely relied upon. Pyrotechnic residues often include particles that are non-spheroidal, and some geologic particles can be spheroidal. The non-spheroidal particles of pyrotechnic origin can be unreacted components of the pyrotechnic composition or reaction residues that are not spheroidal, apparently the result of their still being molten when they collided with the collection surface. Occasionally soil particles appear nearly spherical in shape, apparently the result of their being mobile in the environment for a long time, during which abrasive action removed their sharp, angular features.

Another potential complication in identifying PRR particles is that occasionally particles of unreacted pyrotechnic composition can be spheroidal in shape. This can be a result of their method of manufacture or processing. For example, the left image in Figure 5 is a type of atomized aluminum occasionally used in pyrotechnic formulations. [17] The right image is a particle of potassium nitrate that has been prepared for use by ball milling to reduce its size.[18] If any particles such as these are left unreacted after an incident, it is possible a few could be found interspersed with PRR particles.
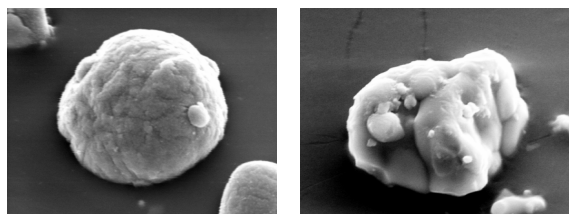
Figure 5. Examples of 10 to 20 micron spheroidal or nearly spherical particles sometimes found in pyrotechnic compositions: left, atomized aluminum; right, ball-milled potassium nitrate.

There are other types of non-pyrotechnic particles that are spheroidal and fall in roughly the same size range as PRR particles. The two images in Figure 6 are examples of spherical particles of biologic origin: blood cells and grass pollen. Although the explanation is beyond the scope of this article, the yield of secondary electrons is virtually independent of atomic number (Z), whereas the yield of backscatter electrons depends highly on the Z of the target atoms, see Figure 7. Accordingly, the use of the backscatter mode of the SEM operation is useful in differentiating between organic particles (low Z) and PRR or geologic particles (typically higher Z). Similarly, in those instances when there is sufficient difference in atomic number between PRR and geologic particles, the use of backscatter mode can be useful. The two images in Figure 8 illustrate the difference between operating in secondary and backscatter electron modes. Note how the two high Z lead particles clearly appear brighter than the many particles of organic material. Finally, Figure 9 demon-
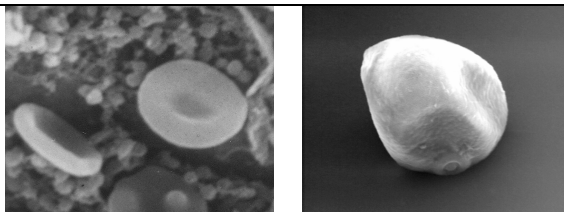
Figure 6. Examples of 5 to 20 micron spheroidal particles of biologic origin: left, red blood cell; right, grass pollen.

strates two more spheroidal particles that can be found in the environment that are of non-pyrotechnic origin. These are a particle produced by grinding metal and a cigarette smoke particle. All these various particle shapes for both PRR and non-PRR particles not withstanding, keying on spheroidal particles for analysis is still quite useful, as this fairly quickly targets those particles that have the best chance of being PRR particles.
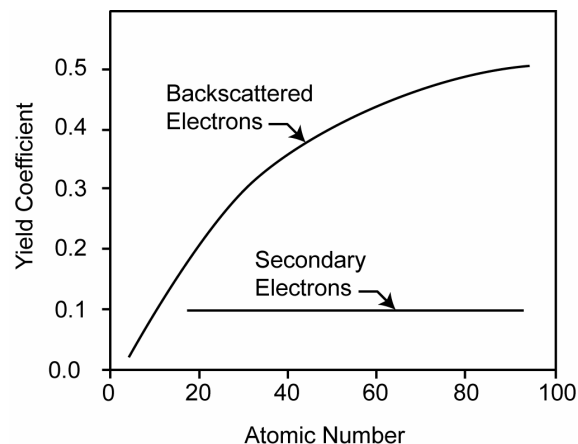
Figure 7. A graph illustrating the number of secondary and backscatter electrons produced from targets as a function of atomic number. (Based on references 15 and 16.)
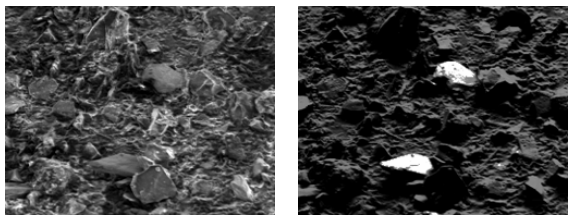
Figure 8. These two images demonstrate the difference between operating the SEM in the secondary electron and backscatter modes with a mixture of organic and high atomic number particles. (This specimen had been coated using a carbon spray.)
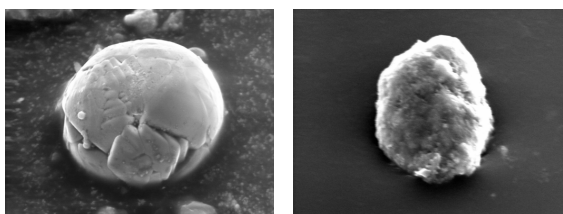
Figure 9. Examples of 10 to 20 micron spherical particles in the environment: left, particle from metal grinding and right, cigarette smoke particle.

Suspect Particle X-ray Signatures

Table 1 is a list of those chemical elements somewhat commonly found in pyrotechnic compositions. Included is an attempt to estimate the relative overall frequency of each chemical element's presence in civilian and/or military compositions. Also included are the energies of the X-ray peaks that are most often used to establish the presence of that element in PRR particles. Because many instruments commonly in use have difficulty detecting X-rays from the elements below sodium in the periodic table, those elements have not been included in Table 1.

Of course, all of the chemical elements present in the unreacted pyrotechnic composition will be present in the combustion products. However, not all of the elements will be present in the solid residues to the same degree that they were in the unreacted composition. For example, when sulfur is used as an ingredient in a high-energy flash powder, it is generally not found in the PRR particles. Most likely this is because it

Table 1. Chemical Elements Most Commonly Present in Pyrotechnic Compositions.

Element and Atomic No. (a)	Z (b)	F/P (c)	X-ray Energies (keV) (d) (e)
Sodium	11	1	1.04
Magnesium	12	1	1.25
Aluminum	13	1	1.49
Silicon	14	2	1.74
Phosphorous	15	3	2.01
Sulfur	16	1	2.31
Chlorine	17	1	2.62
Potassium	19	1	3.31, 3.59
Calcium	20	3	3.69, 4.01
Titanium	22	2	4.51, 4.93
Chromium	24	3	5.41, 5.95
Manganese	25	3	5.90, 6.49
Iron	26	2	6.40, 7.06
Copper	29	1	8.04, 8.90
Zinc	30	3	8.63, 9.57
Strontium	38	1	1.82, 14.14, 15.84
Zirconium	40	2	2.06, 15.75, 17.71
Antimony	51	2	3.60, 3.86, 4.10
Barium	56	1	4.46, 4.84, 5.16
Lead	82	2	2.36, 10.55, 12.62
Bismuth	83	3	2.44, 10.83, 13.02

a) Only those elements producing characteristic X-rays with energies above 1.0 keV are listed. The elements are listed in order of increasing atomic number.

b) Z is atomic number.

c) F/P means the frequency of presence of this element in pyrotechnic compositions. Rankings range from 1 to 3, with 1 indicating those elements most frequently present, and 3 indicating those elements only occasionally present. No attempt was made to differentiate between their presence in civilian versus military pyrotechnics.

d) Energies (in keV, reported to 0.01 keV) for the X-rays between 1 and 20 keV that are most frequently used to identify the presence of the element.

e) When using an energy dispersive X-ray spectrometer, sometimes there will be overlaps of some of the X-rays listed. However, in most instances these cases should not result in their misidentification. This will be discussed in a future article.[14]
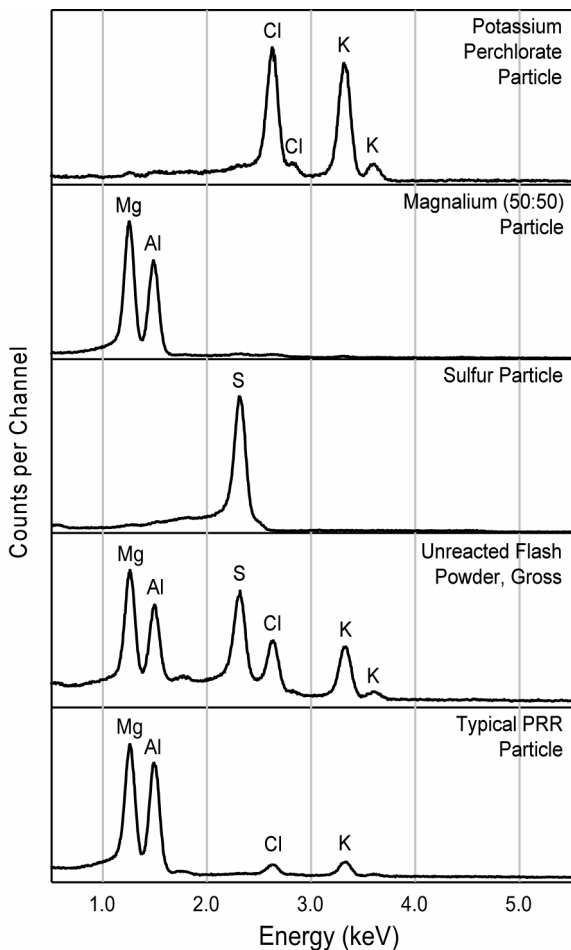
Figure 10. X-ray spectra from a pyrotechnic flash powder.

Figure 11. X-ray spectra produced during an accident investigation.

has reacted to form sulfur dioxide, a gas, which is lost.

In Figure 10, the three upper X-ray spectra are those from individual particles in an unreacted flash powder with the formulation: 60% potassium perchlorate, 30% magnesium:aluminum alloy 50:50 (magnalium), and 10% sulfur. Below them is the spectrum from a "gross" sample of the unreacted flash powder, collected such that the X-rays originate from a large collection of individual particles, and produce a spectrum representative of the average composition of the unreacted flash powder. The lower most X-ray spectrum is typical of that produced by a PRR particle. In the lower two spectra, note the difference in the sulfur peaks; while it is quite prominent in the unreacted gross spectrum, it is missing from the gross residue spectrum. The

reduction of the potassium and chlorine peaks, and a small change in the ratio of magnesium and aluminum peaks will be discussed in a subsequent article addressing some of the finer points of PRR particle analysis.[14]

The vertical scales of the spectra were normalized such that the largest X-ray peak in each spectrum has the same, full-scale height. This method was chosen because it readily facilitates the comparison of spectra collected for different lengths of time, or for which different count rates were produced. Also, while data was collected to nearly 20 keV, the horizontal (energy) axis was truncated at a point shortly above the last significant X-ray peak found in any spectrum, in this case at about 5.5 keV. This provided a clearer view of the peaks that are present. Similarly, the portion of the spectrum below approximately 0.5 keV was not included.

The X-ray spectra in Figure 11 were produced as part of an accident investigation. In this case, an individual received burns when a firework allegedly exploded and sent burning pieces of pyrotechnic composition in his direction. Uppermost is the gross spectrum of the composition taken from the firework alleged to have been responsible for the injury. In the middle is a spectrum typical of a PRR particle

produced by burning this same pyrotechnic composition under laboratory conditions. Lowermost is a spectrum typical of PRR particles taken from the clothing of the burn victim. In comparing the two lower spectra, note that the spectrum of PRR particles from the victim is consistent with having been produced by the suspect firework.

The spectra in Figure 11 were recorded for a relatively short time, approximately 1.5 minutes. It is often appropriate to use short collection times, from 0.5 to 2 minutes. Generally, data collection time only needs to be sufficient to confidently identify the significant elemental components of the particle. This allows the analysis of a greater number of PRR particles, thus increasing one's confidence in any conclusions reached. When needed, longer data collection times can be used when attempting to identify minor components of a suspect particle.

All of the spectra presented in Figure 11 (and Figure 13) use a vertical scale presenting the square root of the number of counts per channel. This scale was chosen because it readily facilitates the observation of both major and minor X-ray peaks in the spectrum (as well as giving an indication of their statistical precision). As in Figure 10, the vertical scales have been normalized to have the largest peak reach full scale, and the horizontal axis has been truncated at a point a little higher than the last peak observed.

For the most part, those particles of geologic origin, comprising the inorganic components of soil, can be eliminated from consideration based on their non-spheroidal morphology. (See again Figure 4.) In addition, those few geologic particles that appear roughly spheroidal can almost always be eliminated based on their X-ray signatures. To someone without a geochemistry and pyrotechnic chemistry background, this might not be readily apparent, especially after considering Table 2, which lists the abundance of the most prominent chemical elements in the Earth's crust. Note that of the ten most abundant crustal elements, all eight of those with atomic numbers from sodium and above also appear in the list of elements somewhat commonly present in pyrotechnic compositions. The non-morphologic basis for discriminating between geologic and PRR particles is discussed in the next few paragraphs.

Table 2. Average Crustal Abundance.[19]

Element	% (a)	Element	% (a)
Oxygen	46.6	Sodium	2.8
Silicon	27.7	Potassium	2.6
Aluminum	8.1	Magnesium	2.1
Iron	5.0	Titanium	0.4
Calcium	3.6	Hydrogen	0.1

a) Percent by weight, expressed to 0.1%.

Sometimes the presence of pyrotechnic residue is so abundant that it is clearly visible as whitish, grayish or blackish material on the surface of items exposed during the incident. In that case, the samples taken from those locations are likely to contain a relatively high proportion of PRR particles. This combined with the relatively small number of geologic particles that fit the morphology criteria for residues, often allows the tentative identification of residue particles based primarily on statistical considerations. For example, consider the case of examining a total of 50 suspect particles selected because they meet the PRR morphology requirements. Suppose that 40 of these have elemental signatures consistent with being from the same source. Whereas the 10 others have one or another of a few other general signatures. In this case, based on probability alone, it is somewhat likely that the 40 particles are of pyrotechnic origin. The level of confidence significantly increases if the X-ray elemental signature for the 40 particles is consistent with having been produced pyrotechnically (even more so if there is an absence of such particles in background samples, discussed further below). Nonetheless, it must still be considered that some of the 10 other morphologically correct particles may also be of pyrotechnic origin, such as might have been produced in another event or from a different pyrotechnic composition.

Often the exposure to pyrotechnic residues is limited, either in duration of exposure, by distance from the reaction, or both. In addition, it is possible that the surface to be sampled was dirty at the time of the exposure, has become dirty since the exposure, or is of a nature that will produce an abundance of non-pyrotechnic material. In these cases, gross statistical considerations and general pyrotechnic knowledge may

not be sufficient to produce results with a reasonable confidence level. In such cases, or to increase ones general confidence in the identification of residue particles, a combination of two other things will greatly aid in discriminating between PRR particles and those relatively few geologic particles with similar morphologies. First is the taking and analyzing of background samples, which can come from at least three different sources. Background samples can be taken of the soil (dirt) in the local area that is thought to be free of the pyrotechnic residues of interest. Background samples can be taken from the surface of items in the area of the incident, which are similar to those items of interest, but which were far enough away to be reasonably free of the pyrotechnic residues of interest. Background samples can also be taken from the primary items being sampled for PRR particles. In that case, an examination of non-spheroidal particles that clearly appear to be non-pyrotechnic in origin can also be useful in establishing the elemental signatures of geologic particles. Any of these various background samples are useful in establishing a list of elemental signatures for non-pyrotechnic particles that are likely to be found on the suspect items. Then, depending on whether the suspect particles have elemental signatures similar to background geologic particles, their origin can often be established with reasonable confidence. If not, the particles must be considered to be of indeterminate origin, at least until further information is developed.

A great aid in discriminating between geologic and PRR particles is knowledge of the likely elemental signatures for both types of particles. For example, for the most common EDS units, far and away the most abundant geologic element that can be detected is silicon, and the most common mineral is one or another form of quartz, silicon dioxide.[20a] Accordingly, it is not uncommon to find particles that produce essentially only silicon X-rays. Further, it is known in pyrotechnics that: silicon is not one of the more commonly present elements; silicon is primarily used in military formulations; silicon only tends to be used in the igniter portion of a device, which is generally only a tiny portion of the total amount of composition likely to be present; and silicon is essentially always used in combination with other readily detectable elements. Thus, when a particle is examined and found to exhibit only silicon X-rays, even when it has a morphology roughly consistent with PRR particles, one can be relatively certain that it is of non-pyrotechnic origin (especially if such particles have also been found in background samples). A similar argument can be made for particles exhibiting essentially only calcium X-rays, which may be one or another geologic form of calcium carbonate.[20b]

Geologic particles producing combinations of X-rays are a little more problematic, but most can also be identified with a reasonable degree of confidence. For example, feldspar refers to a group of minerals making up about 60% of the Earth's crust.[20c] Most commonly these are combinations of silicon, aluminum, and one or the other of potassium, sodium or calcium. While these specific combinations occur frequently in geologic particles, it would be unusual to find such combinations in PRR particles. Although a little too simplistic to make it a general rule, the most common geologic material will generally have silicon or calcium as the most prevalent X-ray peak, whereas pyrotechnic material will generally have little, if any, of these present. (For more complete information on the forensic analysis of soils using SEM, see reference 21.)

Like particles of geologic origin, those that are organic in nature (biologic or manmade) generally will not have morphologies mistakable for PRR particles. Also, similar to geologic particles, organic particles will have X-ray characteristics that greatly aid in their identification. One of these characteristics is their low rate of production of X-rays with energies greater than 0.62 keV. This is a result of biologic particles being mostly comprised of elements with elements no higher than oxygen. Thus, it is common for biologic particles to produce no more than about 1/3 the number of X-rays above 0.6 keV than will geologic or PRR particles. Further, the elemental signatures of organic particles are likely to be significantly different from PRR particles. Finally, operating the SEM in the backscatter mode offers the potential to discriminate against biologic particles because of the reduced intensity of their images. However, this generally requires applying an electrically conductive coating to the specimen. Fur-
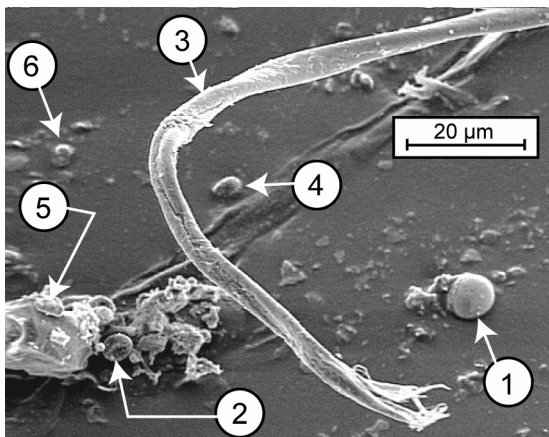
Figure 12. An electron micrograph identifying a series of particles (items) analyzed during an accident investigation. (See Table 3.)

ther, because the difference in Z between organic and geologic or PRR particles is not very great, the image intensity contrast may not be sufficient to allow their easy differentiation.

Generally, it will not be possible to establish the identity and origin of each particle analyzed, and these should be characterized as being "Indeterminate". However, in most cases the sheer number of PRR particles produced is so great (generally at least a thousand times more than for GSR) that there is no need to positively characterize each particle. Further, there is no need for the search for PRR particles to be exhaustive. Rather a statistical approach is taken in which analysis continues only until the degree of certitude reaches the level desired.

Analytical Example

This example comes from the same case mentioned earlier, wherein an individual was burned when a fireworks was alleged to have exploded sending pieces of burning pyrotechnic composition in his direction. Figure 12 is an electron micrograph of a small portion of a sample taken from the inside the individual's clothing, from the general area where the burn occurred. (This specimen was sputter coated with a thin layer of gold to help produce a satisfactory image for publication.) In this image, a series of six items are identified for use as examples of the way the analysis was performed. (In the actual investiga-
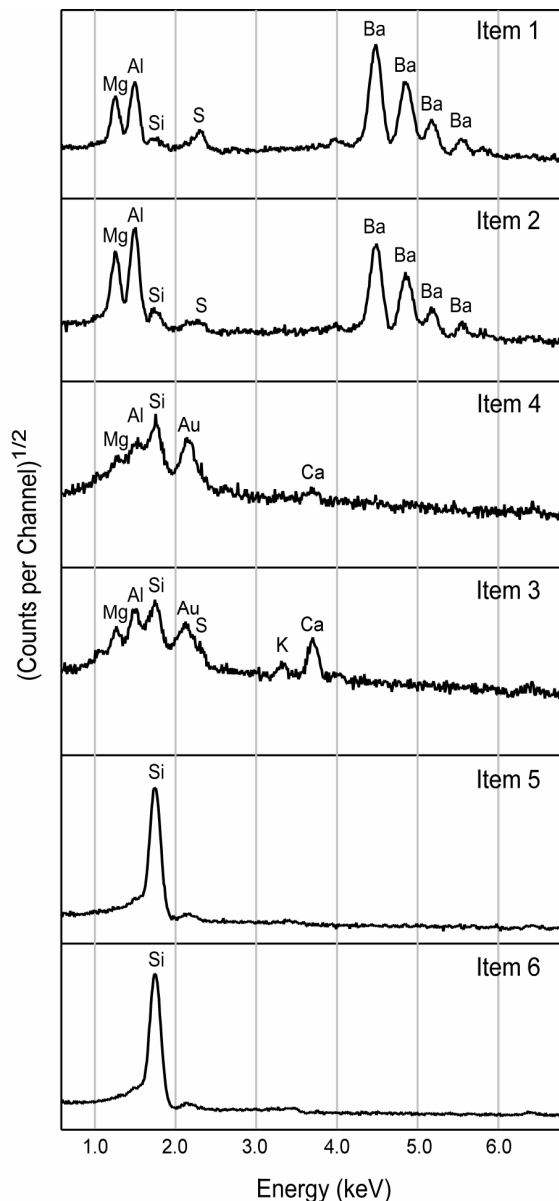
Figure 13. X-ray spectra collected from the six particles identified in Figure 12.

tion, several additional particles seen in this image were also analyzed, as well as many other particles from other portions of this and other samples.) Figure 13 is the collection of the X-ray spectra collected from the six particles (items) identified in Figure 12.

Table 3 presents the results from the analysis of the particles identified in Figure 12 and illustrates a typical methodology used in performing an analysis of PRR particles. However, the categories and classifications will often need to be

Table 3. Analytical Results for the Particles Identified in Figure 9.

Particle Number	Morphology Type	Dead Time (%)	Peak-to-Background Ratio	Chemistry Type	Particle (Item) Identification
1	Spheroidal	16	3.8	Pyrotechnic	PRR Particle
2	Spheroidal	18	3.4	Pyrotechnic	PRR Particle
3	Fibrous	4	1.0	Organic	Organic
4	Indeterminate	4	0.8	Indeterminate	Non-PRR
5	Non-Spheroidal	12	13.	Geologic	Geologic
6	Spheroidal	14	16.	Geologic	Geologic

adjusted for specific investigations. In Table 3, particle *Morphology Type* is basically divided into two categories, *Spheroidal* (in this case meaning near spherical) and *Non-Spheroidal*, with *Fibrous* as a subcategory of non-spheroidal. The reason for including the fibrous subcategory is that organic materials (both biologic and manmade) often have this appearance, while PRR particles do not. (In this example, since the specimen was taken from clothing, many fibrous items were found.) When the appropriate category for a particle is not reasonably clear, it is assigned as being *Indeterminate*.

Multichannel analyzer (MCA) *Dead Time* is the percent of time the MCA is occupied sorting the electronic pulses from the X-ray detector. All things being equal, MCA dead time is a useful indication of the rate at which X-rays from the specimen are being detected. For many systems, the X-rays from elements with atomic numbers (Z) less than approximately 11 (sodium) are essentially not detected. Nevertheless, MCA dead time will often provide a useful indication of the extent to which the specimen is composed of elements with Z less than 11. This is of interest because it will aid in determining whether a particle is organic in nature (whether manmade or biologic). Many things affect the rate of production and detection of X-rays from the specimen. However, for the instrument and the configuration used in this article to produce the spectra in Figure 13, when the dead time is less than approximately 5 percent, it is likely that the vast majority of the atoms in the portion of the specimen being scanned have atomic numbers less than 11. For this reason, spectra dead times have been included in Table 3. As further indication that a recorded spectrum is

from organic material, it will generally not contain any peaks of major intensity. Usually a visual inspection of the spectrum is sufficient to reveal this; however, for the purpose of this example, a quantitative measure of the peak-to-background ratio for the most prominent peak(s) in the spectrum was produced. For the instrument and its configuration used in this article, purely organic material generally produces peak-to-background ratios less than 2. Thus, as a further aid in characterizing particles, Table 3 includes the value for the maximum peak-to-background ratio found in each spectrum.

While the use of approximate MCA dead times to infer something about the predominant atomic numbers of a particle is useful, it is not completely reliable. Even for the same instrument, operated under the same conditions, there are a number of factors that can give false low dead times. For example, for the very smallest particles (those significantly less than the interrogation depth of the electron beam) the count rate (dead time) will be reduced. Similarly, when there is shadowing of the X-ray detector by another portion of the specimen, the count rate will be reduced. These effects are expected and manageable; however, a more complete discussion must be deferred to a subsequent article.[14] Similarly, peak-to-background ratios are not a completely reliable indicator of prevalent atomic number. When there is a mixture of several moderate to high Z materials in the particle, such that there are many prominent peaks in the spectrum, peak-to-background ratios are reduced (in Table 3, compare particles 1 and 2, with particles 5 and 6). Further, sometimes particles are mixtures of organic material with other material having higher Z components. For example, white

paper has calcium carbonate added to make it whiter and more opaque, and organic material may have inorganic material imbedded within or adhering to its surface.

Identification of organic particles can often be aided using the instrument in the backscatter electron mode. However, this is also not always reliable. If there is not a sufficient difference between the atomic number of the PRR and organic particles, the difference in the backscatter yield coefficients may not be sufficient. In that case, the contrast between PRR and organic particles may not be readily apparent given the normal variation in contrast between particles in the image (flaring or excessive contrast), especially when the sample has not been coated.

In Table 3, particle *Chemistry Type* is basically divided into two categories (*Pyrotechnic* and *Non-Pyrotechnic*, with subclasses of *Organic* and *Geologic* for non-pyrotechnic particles). Assignments are made based on the types and ratios of chemical elements present. For the most part, the basis for assigning particles (items) to these classifications was described in the previous section on X-ray signatures. Another non-pyrotechnic subclass is often used for particles that are removed from the substrate from which the sample was collected. This might include paint flecks from a painted surface or rust particles from an iron or steel surface. In the example being discussed, clothing fibers could have been assigned to that category. When the appropriate category for a particle is not reasonably clear, it is assigned as being *Indeterminate*.

Particles one and two, have the correct morphology and reasonably high count rates. Further, their chemistry is consistent with that of a PRR particle, which has been confirmed through the production of effectively identical (matching) PRR particles in the laboratory using the suspect pyrotechnic composition (see again Figure 11). Further, many more particles with the same elemental signature were found in the same area of clothing where the injury occurred. Finally, no similar particles were found on background areas of clothing remote from the area of the injury. Accordingly, with a high degree of confidence, particles one and two are identified as PRR particles.

Item three has the obvious appearance of a fiber; most likely from the individual's clothing itself. Further, its counting dead time and peak-to-background ratio are quite low, suggesting it consists mostly of low Z atoms, and its chemistry is essentially devoid of those major elements associated with geologic or pyrotechnic materials. Accordingly, with a high degree of confidence, this item is identified as being organic material. (The presence of an X-ray peak from gold is the result of the specimen having been sputter coated with gold for the purpose of facilitating the taking of a high resolution electron micrograph for this article. The same gold X-rays were produced by all of the particles being analyzed; however, when those particles produce higher X-ray count rates, the gold peak becomes much less prominent.) Particle four is roughly spheroidal, although it is elongated with a fairly pointed end. Accordingly, it has been conservatively designated as having a morphology that is indeterminate. Its counting dead time and peak-to-background ratio are quite low, suggesting it consisted of mostly of low Z atoms. While its chemistry appears to be much like that of particle (item) three, it has been conservatively designated as indeterminate because of the somewhat increased prominence of X-ray peaks most consistent with geologic material (calcium, silicon, magnesium and aluminum). Taking everything into consideration, with a reasonable degree of confidence, this particle could have been identified as being organic in nature; however, it was more conservatively designated as being *Non-PRR*.

Particle five is of non-spheroidal morphology, has a relatively high dead time, has a very high peak-to-background ratio, exhibits chemistry consistent with being silica sand, and has a chemistry that is quite inconsistent with being pyrotechnic. Further, samples taken from the cuff area of the clothing, well beyond the area of likely deposition of PRR particles contain many particles of the same chemistry. Accordingly, with a high degree of confidence, this particle is identified as being of geologic origin. Except for its spheroidal shape, particle six is like that of particle five. However, geologic particles, that have been mobile in the environment for a prolonged time, tend to become near spherical in shape. Accordingly, with a high degree of

confidence, this particle is also identified as being of geologic origin.

In the case of this example, most of the particles cataloged were not PRR particles. As a practical matter, during an investigation it would be unusual to bother to document the nature of a high percentage of non-PRR particles. Typically, only enough of these particles would be analyzed and documented such as to reasonably represent the range of different non-PRR particles found. Instead, most of the time would be devoted to finding and analyzing PRR particles. In this way, while a few particle assignments may be less than certain, collectively, conclusions can be drawn with a high degree of confidence.

Conclusion

The use the SEM / EDS methodology to analyze PRR particles in the course of investigating accidents involving pyrotechnic materials can provide information with a degree of sensitiveness and specificity that is unavailable with other commonly used techniques. Given the wide spread availability of SEM / EDS instruments and the long history of the successful use of the same methodology in GSR analysis, it is somewhat surprising that the technique is not used more often in investigating accidents involving pyrotechnics. Obviously one reason for its infrequent use is that most accident investigations would benefit little, if any, from the type of information that could be developed. However, even for those accidents where PRR particle analysis would be of great benefit, often that analysis is not performed. After speaking with pyrotechnic researchers and investigators, the authors have conclude the likely reason for its under use is simply that many investigators working outside of forensics are not sufficiently aware of the PRR particle analysis methodology and the information it can provide. Therein lies the purpose of this introductory article, to disseminate some basic information about PRR particle analysis to the scientifically oriented pyrotechnic community. Toward this same end, at least two additional articles are planned. One article will present much more information about the mechanics of specimen production, collection, and their subsequent analysis.[14] A second article will further demonstrate the nature and utility of the information produced by considering a series of investigations of actual and staged incidents.

References

1) R. S. Nesbitt, J. E. Wessel, and P. F. Jones, "Detection of Gunshot Residue by Use of the Scanning Electron Microscope", *Journal of Forensic Science*, Vol. 21, No. 3 (1976) pp 595–610.

2) ASTM: E 1588-95, "Standard Guide for Gunshot Residue Analysis by Scanning Electron Microscopy / Energy-Dispersive Spectroscopy", ASTM, 1995.

3) J. S. Wallace, "Chemical Aspects of Firearms Ammunition", *ATFE Journal*, Vol. 22, No. 4 (1990) pp 364–389.

4) H. H. Meng and B. Caddy, "Gunshot Residue Analysis—A Review", *Journal of Forensic Science*, Vol. 42, No. 4 (1997) pp 553–570.

5) R. L. Singer, D. Davis, and M. M. Houck, "A Survey of Gunshot Residue Analysis Methods", *Journal of Forensic Sciences*, Vol. 41, No. 2 (1996) pp 195–198.

6) P. V. Mosher, M. J. McVicar, E. D. Randall, and E. H. Sild, "Gunshot Residue-Similar Particles by Fireworks", *Canadian Society of Forensic Science Journal*, Vol. 31, No. 2 (1998) pp 157–168.

7) J. R. Giacalone, "Forensic Fireworks Analysis and Their Residue by Scanning Electron Microscopy / Energy-Dispersive Spectroscopy", *Scanning*, Vol. 20, No. 3 (1998) pp 172–173.

8) P. Mosher, "Fireworks as a Source of Gunshot Residue-Like Particles: An Overview", *Proceedings of the 4th International Symposium on Fireworks* (1998) pp 275–281.

9) J. R. Giacalone, "Forensic Particle Analysis of Microtrace Pyrotechnic Residue", *Scanning*, Vol. 21, No. 2 (1999) pp 100–101.

10) S. A. Phillips, "Analysis of Pyrotechnic Residues—Detection and Analysis of Characteristic Particles by SEM / EDS", *Proceedings of the 2nd European Academy of Forensic Science Meeting, Sept. 2000*.

11) E. Fjeld Co., N. Billerica, MA, USA.

12) Kevex, Inc. Foster City, CA, USA.

13) American Nuclear Systems, Inc., Oak Ridge, TN, USA.

14) K. L. & B. J. Kosanke and R. C. Dujay, "Analysis of Pyrotechnic Reaction Residue Particles Using SEM / EDS", in preparation.

15) J. I. Goldstein, D. E. Newbury, P. Echlin, D. C. Joy, A. D Roming, C. E. Lyman, C. Fiori, and E. Lifshin, *Scanning Electron Microscopy and X-Ray Microanalysis*, 2nd ed., Plenum Press (1992).

16) R. E. Lee, *Scanning Electron Microscopy and X-Ray Microanalysis*, Prentice Hall (1993).

17) K. L. & B. J. Kosanke and R. C. Dujay, "Pyrotechnic Particle Morphologies – Metal Fuels", *Journal of Pyrotechnics*, Issue 11 (2000) pp 46–52.

18) K. L. & B. J. Kosanke and R. C. Dujay, "Pyrotechnic Particle Morphologies – Low Melting Point Oxidizers", *Journal of Pyrotechnics*, Issue 12 (2000) pp 5–15.

19) D. L. Holmes, *Holmes Principles of Physical Geology*, John Wiley (1978) p 46.

20) *Van Nostrand's Scientific Encyclopedia*, 5th ed., Van Nostrand-Reinhold (1976), [a] p 1857; [b] p 400; [c] p 1012.

21) M. J. McVicar, "The Forensic Comparison of Soils by Automated Scanning Electron Microscopy", *Canadian Society of Forensic Science Journal*, Vol. 30, No. 4 (1997) pp 241–261.

Commercial Developments in Red Phosphorus Performance and Stability for Pyrotechnics

Sebastian Hoerold and Andrew Ratcliff

Clariant GmbH, Division PA, BU-Additive, D-65840 Sulzbach am Taunus, Germany

email: Andrew.Ratcliff@Clariant.com

ABSTRACT

Red phosphorus has become an essential ingredient in the production of modern smoke and obscurant devices. Nearly all multi-spectral developmental projects are being based on the new versions of red phosphorus available from Clariant.

In pyrotechnics and munitions, phosphine liberated by the traditional red phosphorus-based smoke compounds may diffuse through the device and can give rise to corrosion of essential working parts. This paper shows that surface modification treatment of red phosphorus can dramatically reduce the formation of decomposition products. New developments in coating the surface are presented and the long-term stability of various pre-treated red phosphorus powders are discussed.

The best stabilization results are found by using special combinations of precipitated inorganic salts together with special micro encapsulation systems. The use of dust suppression agents is also discussed.

The newly developed materials reduce the potential hazards that arise during the manufacturing process whilst improving the shelf life of the smoke composition.

Keywords: red phosphorus, stability, smoke, microencapsulation

Commercial Production of Red Phosphorus

White phosphorus (also known as yellow phosphorus) is produced in an electric furnace at 1,400–1,500 °C from a sintered mixture of rock phosphate (fluorapatite), coke and silica. The gaseous white phosphorus (P_4) is distilled from the furnace by condensing with water.

Red phosphorus is commercially produced from white phosphorus by a thermal conversion. The existing process has been used in Knapsack, Germany since 1953. See Figure 1. The conversion of white phosphorus to red phosphorus is performed in multi-ton batches in special sealed reactors. Each reactor consists of a rotary iron furnace resting on two hollow shafts with a drive mechanism and contains milling balls to grind the converted phosphorus to the desired particle size. The thermal conversion takes place at elevated temperatures over a period of several hours. The reactor is then cooled and filled with water, and the red phosphorus is milled to a fine-grained powder.

An aqueous dispersion of red phosphorus is pumped to stirred vessels, where remaining white phosphorus is removed with sodium hydroxide. Technical red phosphorus contains significantly less than 200 ppm white phosphorus. The phosphorus is filtered, washed and dried under nitrogen. Red phosphorus is then packed in anti-static plastic bags, steel drums or other specialized containers.

Applications for Red Phosphorus

Red phosphorus is commercially used in a wide variety of industrial applications (see Figure 2), with the classical ones being, safety matches, chemical catalyst, phosphides and pyrotechnics.

In most applications, the red allotrope is favored over the white allotrope because of its greater stability in air and its easier handling characteristics. Red phosphorus is not consid-
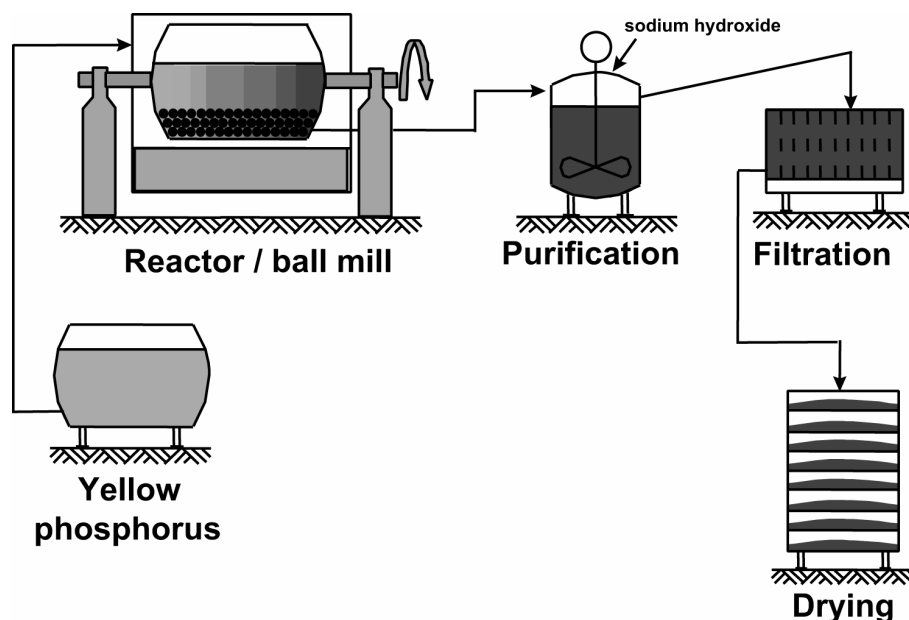
Figure 1. Production of red phosphorus.

ered problematic with regard to environmental and occupational health issues. It is not soluble in water and is considered non-toxic when pure (see Table 1). When the content of white phosphorus is less than 0.02%, the LD_{50}-value is >15,000 mg/kg (rat).

a) Safety Matches

The production of safety matches is still an important market for high-grade, fine-grained red phosphorus. The phosphorus is used on the striking surface of the matchboxes. It is typically applied by using a rotogravure printing process together with binders (e.g., polyvinyl alcohol, PVA) and special fillers (see Tables 2 and 3). The modern printing process requires especially fine-grained red phosphorus to operate efficiently and economically.
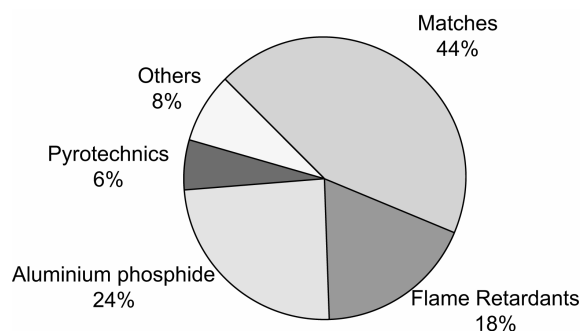
Figure 2. Application areas of red phosphorus worldwide 1999.

Table 1. Safety Data of Red Phosphorus (source: Clariant's Investigations).

Parameter	Value
Red phosphorus purity	>99%
White phosphorus (P_4) content	<0.02%
Acute oral toxicity LD50 (rat)	>15,000 mg/kg
Fish toxicity LC_{50} (*Brachidanio rerio*) Method: 92/69/EEC, C.1	>10 mg/L, 96 h exposure
Bacteria toxicity EC_{50} (activated sludge) Method: OECD 209	>1,000 mg/L, 3 h exposure

Table 2. Traditional Friction Compound Guide Formula for Safety Matches.

Ingredient	% by weight
Red phosphorus grade NF	17–24
Binder (gum Arabic/gelatin type)	10–12
Antimony sulfide	20–24
Filler*	2–6
Water	38–48

Table 3. Rotogravure-Style Friction Compound Guide Formula.

Ingredient	% by weight
Red phosphorus grade NFC	60–80
Binder (water based PVA)	40-20
Friction fillers*	0–2

* Fillers are typically mixtures of silicates and metal oxides

Although the match industry is still growing in some regions, the total quantity of red phosphorus in match making applications has been declining for some years due to the consolidation of production units, improved processing efficiency and wide spread introduction of rotogravure printing technology.

b) Flame Retardants

Red phosphorus is often used as a flame retardant additive for plastics. It is quite astonishing that red phosphorus, being a flammable powder, can act as one of the most efficient flame-retardants known for plastics. The addition of red phosphorus is typically in the range of 5 to 10%. The flame-retarded plastics are used widely in electronics, where it is replacing brominated and chlorinated flame-retardants. Red phosphorus is incorporated in plastics like polyamide, epoxy resins, polyurethanes and rubbers and is now available in a wide range of polymer carriers such as polyolefins, polyamides and special thermoplastic resins. The polymer industry is now able to obtain the red phosphorus as dispersions, pastes, pellets or prills, which eliminates the issues of handling red phosphorus powders.

c) Phosphides

A considerable portion of red phosphorus is converted to aluminium phosphide. This is applied as a fumigant for pest control purposes in grain and tobacco silos, mainly due to its ability to liberate phosphine gas. The aluminium phosphide is formulated with other additives and then pressed in small pellets. The pellets are left to react with atmospheric moisture in the silos to generate phosphine gas. The aluminium is converted into a residual slag of aluminum oxides and hydroxides. The residual phosphine in the silo is then further oxidized to phosphoric acids.

d) Pyrotechnics—Smoke and Obscurants

Red phosphorus is an essential component in the production of energetic, multi-spectral smoke and obscurant devices in both current and future applications. Red phosphorus is normally mixed with a binder and an initiator (e.g. magnesium) in a solvent. The resulting mixture is then physically processed to the required shape or form. The binder is typically a butyl rubber, fluorinated rubber or epoxy resin. However, some formulations also include magnesium in the composition. It reacts in the slag formed on the pellets to consume the slag and promote complete combustion.

When a smoke grenade is launched, the pellets are ignited and dispersed. The burning red phosphorus produces a dense white smoke, while the binder maintains the integrity of the pellets to promote duration of the smoke screen. The burning red phosphorus produces mainly phosphorus pentoxide in the presence of excess oxygen. Phosphorus trioxide is the major product when combustion is oxygen limited.[1] The phosphorus pentoxide hydrolyses to form a series of polyphosphoric acids, which are biologically degradable.

Minimal quantities of red phosphorus within the field of pyrotechnics are also used in the production of toy pistol caps.

Stability of Red Phosphorus

One significant problem with pure red phosphorus powder is that on storage, a gradual release of toxic phosphine gas occurs and various phosphoric acids are produced. This decomposition reaction takes place in the presence of oxygen and water. See Figure 3. The decomposition rate depends directly on the availability of air, moisture and temperature. In pyrotechnics and munitions, the phosphine liberated by standard red phosphorus charges may diffuse through the device and can give rise to corrosion, presumably after subsequent oxidation to phosphoric acids.

$$P_x \xrightarrow[> 50°C]{+ \ H_2O/O_2} \begin{array}{l} PH_3 \\ H_3PO_2 \\ H_3PO_3 \\ H_3PO_4 \end{array}$$
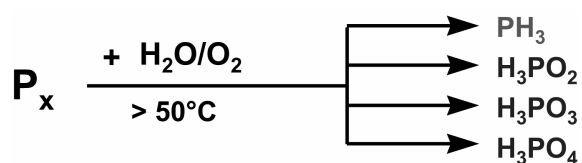
Figure 3. Red phosphorus disproportionates in the presence of moisture at elevated temperatures.

The formation of phosphine gas can be suppressed by:

- controlling the availability of moisture and oxygen

- storing at room temperature

- using stabilisers to inhibit phosphine formation

- using dust suppressants (oiling)

- coating the surface of the red phosphorus (microencapsulation)

The first generation of pyrotechnical red phosphorus basically evolved in the late 1940's and early 1950's when the US military introduced a procurement specification for red phosphorus powder. The result was the initial version of US MIL-P-211. The focus was to try to control the presence of white phosphorus and moisture. These were recognized as being key issues in the processing and stability as the white phosphorus is spontaneously combustible and the moisture specification was used to ensure that dry material was delivered.

In the following years, producers improved the stability of red phosphorus by introducing additives to the powder. Additives can be a mixture of dust suppressing agents, stabilisers or microencapsulating resins. The principle behind these additives is to reduce the sensitivity of red phosphorus to chemical influence and decomposition. It is shown in the following section how these additives reduce phosphine emission from red phosphorus powder. The major improvement was the introduction of new microencapsulation technology, a technique now regarded as being standard in the plastics industry, but not applied until now in pyrotechnic formulations.

Experimental Work

The phosphine emission of red phosphorus powder grades can be measured with Draeger tubes either at 25 °C (room temperature) and 65% humidity (vapor pressure over saturated aqueous ammonium nitrate solution), or at 80 °C and 100% humidity. Data is given in micrograms of phosphine per gram of red phosphorus powder.

a) Dust Suppression

Handling red phosphorus powder can be hazardous due to the potential for dust explosions. Dust suppressing[2] or "oiling" prevents dust explosions, improves the handling and increases its stability in air due to the reduction of the active surface of red phosphorus. In dust suppressing, the dust particles are agglomerated to form bigger particles. See Figure 4.

The 1980's saw the introduction of "oiled" red phosphorus, which basically involved the introduction of dust suppressants. In practice the
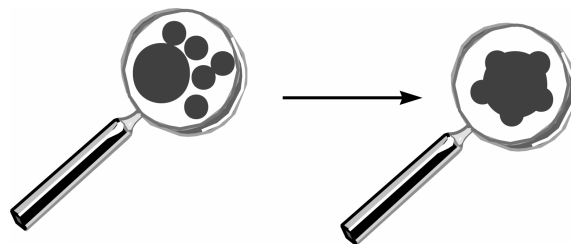
Figure 4. Effects of dust suppressant.

Table 4. PH$_3$ Generation at Room Temperature (25 °C) and 65% Humidity. A Comparison of Various Red Phosphorus Grades.

Red Phosphorus Grade	PH$_3$ Formation (µg/g RP)			
	24 hr	48 hr	14 days	28 days
Non dust suppressed *Clariant grade SF*	150	290	1300	2400
Dust suppressed *Clariant grade HB 250*	18	40	507	980
Stabilized *Clariant grade NF*	3	5	48	81
Stabilized and dust suppressed *Clariant grade NFD*	3	5	32	48
Microencapsulated *Clariant grade HB 700**	2	3	7	8
Microencapsulated *Clariant grade HB 714***	0.8	1.2	3	4

* HB 700: stabilized, dust suppressed and microencapsulated.

** HB 714: stabilized and microencapsulated.

red phosphorus producers "oiled" the material then customers remove the oil with a solvent (e.g., acetone or methylene chloride) before processing. The US MIL-P-211 specifications required 0.8–1.5% dust suppressant.

Typical dust suppressants are liquid organic compounds. The US MIL-P-211 allows the use of commercially available long-chain ethoxylates rather than the original transformer oils. Table 4 shows the reduction of phosphine emission by the addition of dust suppressant, measured at 25 °C and 65% humidity compared to non-dust suppressed red phosphorus. Note that in the first days a decrease in phosphine emission by a factor of seven is observed but after two or four weeks, the reduction is by only half the amount of phosphine observed with the untreated red phosphorus.

b) Stabilisation

Various metal oxides can be used as stabilizers[3] by precipitating them on the surface of the red phosphorus grains. Typical metal oxides are aluminium and magnesium and they work by buffering acid traces formed on oxidation of red phosphorus. Freshly prepared red phosphorus in an aqueous dispersion gives a nearly neutral pH. After storage, the pH value decreases with time from pH 7 to pH 2. Stabilized red

phosphorus keeps the neutral pH value for a longer time (approximately six months).

In the mid-1980s, the stabilizer technology for red phosphorus was improved further by the matchmaking and plastics industry. The basic idea behind the improvements can be found in the MIL-P-670A dating back to 1948 but this was mostly used for Navy markers and not for general smoke and obscurant applications. The MIL-P-670A included an aluminium stabilizer coupled with a basic particle size distribution requirement but no dust suppressant.

As shown in Table 4 (grade NF), stabilisers suppress the phosphine emission from red phosphorus powder (in addition to maintaining a neutral pH.)

c) Combination of Stabilisers and Dust Suppressants

As expected, the combination of both stabilizing metal oxides and dust suppressing oils on the red phosphorus surface gives further improved effects. See Table 4, grade NFD, as an example. Such red phosphorus is used in the match industry as the top quality red phosphorus grades.

d) Microencapsulation

Microencapsulation[4,5] of red phosphorus reduces its active surface. It is a very thin coating on the individual grains. Various resins can be used for microencapsulation with the best results obtained using selected thermoset resins, such as epoxy resins or phenolic resins.

Microencapsulation is normally combined with stabilization and dust suppression to optimize performance. See Figure 5.

The resin content can vary from 1–8% by weight of red phosphorus. Some interesting combustion characteristics can be obtained by changing the microencapsulation system.

Microencapsulated red phosphorus grades are used extensively in the plastics industry, where approximately 5–8% by weight are added to different polymers as a flame retardant. Such plastics include polyamides, polyurethanes, polyethylene, EVA (ethylene-vinyl-acetate), and epoxy resins. Microencapsulation is currently
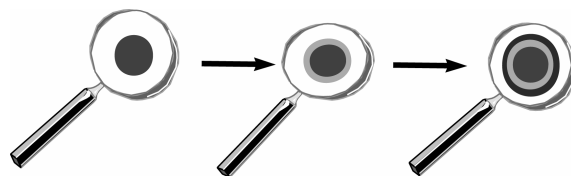
Figure 5. Stabilisation and microencapsulation of red phosphorus grains.

not included in military specifications.

As shown in Table 4 (grades HB 700 and HB 714), microencapsulated red phosphorus grades provide a significant improvement in stability. The use of red phosphorus in the plastic industry would be virtually impossible without applying these techniques.

A graphic overview of the change in phosphine generation is shown in Figure 6.
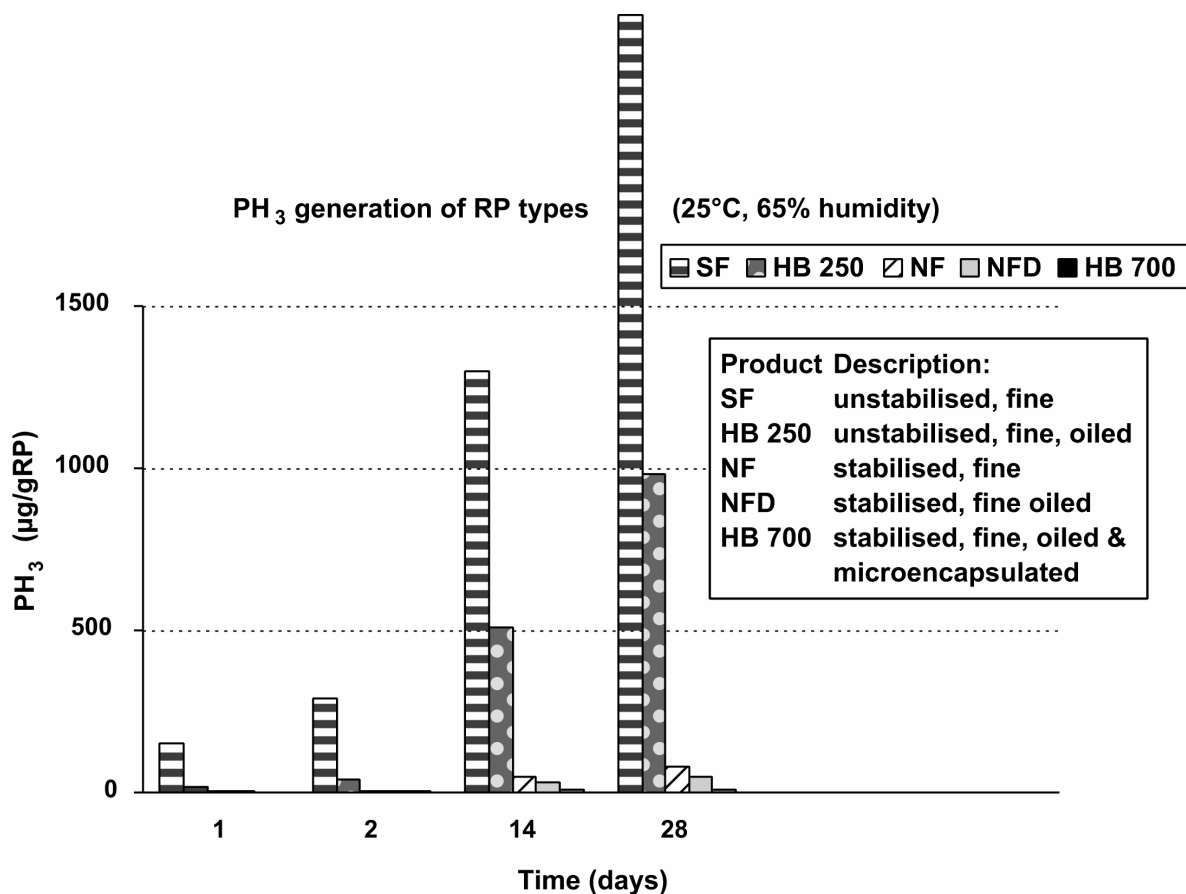
Figure 6. PH₃ generation of red phosphorus types.

Conclusion

The reported data shows that the stability of red phosphorus in air and in a humid environment can be improved by a combination of stabilisers and microencapsulation. The newly developed materials reduce the potential hazards in the manufacturing process of smoke compounds and can lead to shelf life improvements in red phosphorus-based obscurants. The development work is continuing, driven by the requirement to further improve the stability of phosphine and to produce flame-retardants with better performance characteristics. The future research and development work will continue to be focused on the technical improvements required to further penetrate the polymer industry with high performance flame-retardants.

The efforts will benefit manufacturing safety and performance of both military and civilian pyrotechnic items in the future.

Literature

1) F. G. Burton, M. L. Clark, R. A. Miller, and R. E. Schirmer, *American Industrial Hygiene Association Journal*, Vol. 43, No. 10 (1982) pp 767–772.

2) H. Staendeke, and U. Thuemmler, *EP* Vol. 176 (1985) p 836.

3) H, Staendeke, U. Thuemmler, *EP* Vol. 378 (1989) p 803.

4) H. Staendeke, U. Thuemmler, *EP* Vol. 176 (1985) p 834.

5) H. Staendeke, U. Thuemmler, *EP* Vol. 759 (1987) p 283.

Communications

Brief technical articles, comments on prior articles and book reviews

Brief Survey of Chromium Toxicity

Monona Rossol

Arts, Crafts & Theater Safety, Inc.

I recently read some information in the pyrotechnic literature[1] about chromium toxicity, which, unfortunately, was not completely correct. Since there are some serious health concerns regarding chromium, this brief article has been written to present a survey of some of what is known.[2–4]

Chromium (Cr) is probably the most complicated of the metals in terms of toxicity. To consider the toxicity of chromium compounds, the very first thing you have to do is look at the valence state of the chromium ion

Carcinogenicity by Valence State

Cr^0 metal, Cr(II) and Cr(III) have airborne threshold limit values (TLVs) of 0.5 milligrams per cubic meter (mg/m^3) and are *not* considered carcinogens. Here the TLV is set to avoid irritation, sensitivities, etc.

Cr(VI) compounds generally have a TLV of 0.05 mg/m^3 and *are* carcinogens. This group includes the chromates, dichromates, chromic acid, and chromium trioxide. However, some Cr(VI) compounds have been assigned even lower TLVs:

1) Insoluble Chromates

Certain insoluble chromates such as fume from stainless steel welding and byproducts of manufacture of chromate compounds are much more carcinogenic based on epidemiological studies. Therefore, a separate TLV is set for these compounds:

Insoluble Cr(VI) compounds: 0.01 mg/m^3

2) Individual Chromates with Separate TLVs

Various individual chromates have their own TLVs based on pretty solid data. Included are:

Calcium chromate: 0.001 mg/m^3
Lead chromate: 0.05 mg/m^3 for the lead, 0.012 mg/m^3 for the Cr
(This means that there can be no more than 0.05 mg of Pb per cubic meter, and no more than 0.012 mg of Cr per cubic meter, if these elements are present as $PbCrO_4$.)
Zinc chromate: 0.01 mg/m^3

In addition, one particular chromate, strontium chromate, is one of the most potent animal carcinogens ever tested. It has its own very special TLV:

Strontium chromate: 0.0005 mg/m^3

No one really knows exactly why this strontium compound is so toxic. Most strontium compounds are of very low toxicity, and there are no TLVs for them at all.

Sensitization Caused by Chromium

All the chromium compounds and the chromium metal appear to be skin sensitizers with the more soluble usually being more sensitizing. These compounds cause a well-known occupational disease called "chrome ulcers" (which I have had). I developed my chromium sensitivity from working with chrome compounds in pottery and now have to avoid chrome even in the metal jewelry I wear, or I will get dermatitis and/or a chrome ulcer on the site of contact. These ulcers can take up to 6 months to heal.

Sensitization of the respiratory system by chromium metal, chromium containing alloys and chromium compounds is even more relevant to pyrotechnics. Fumes from the metallic salts (which would be produced in a pyrotechnic effect containing chromium compounds) are capable of inducing bronchial reactivity (e.g.,

asthma) even in previously non-allergic individuals. Once sensitized to chromium, people usually will have allergic reactions to all forms of chromium for the rest of their lives. It is even likely they will react to smaller and smaller amounts over time. While no one should inhale pyrotechnic smoke containing chromium, it can be especially hazardous to these pre-sensitized individuals.

Other Aspects

Chromium in many forms can damage the skin and mucous membranes. This effect can range from stuff that will eat holes in you like chromic acid to stuff that will ulcerate your nasal passages like potassium dichromate. While the chromium VI compounds usually are the most damaging, some chrome III and IV compounds and even chrome metal dust will cause irritation of the nasal mucosa. Many of the compounds also stain the skin and may be a factor in causing certain adverse kidney effects.

Chromium is also essential for glucose metabolism. It is needed in *trace* amounts, as Cr(III). (Chromium is only one of many elements that are needed in the diet, but that are toxic at higher doses. Other examples include cobalt and manganese.)

Ongoing studies of chromium compounds are expected to deepen and alter our understanding of their toxicity and carcinogenicity. For example, some experts think there are circumstances under which chromium(II) and (III) compounds can be altered to the cancer causing chromium(VI) forms in the body. In any case, it is wise for us to use prudent chemical handling procedures to avoid exposure to all chromium chemicals that can be inhaled, ingested, or contact the skin in liquid or fine particulate form.

References

1) T. I. Perigrin, "Chemical Risks", *American Fireworks News*, No. 202 (1998) pp 2–3.

2) *Documentation of Threshold Limit Values and Biological Exposure Indices*, American Conference on Governmental Industrial Hygienists (ACGIH) (1997).

3) Guide to Occupational Exposure Values—2000, ACGIH, 1330 Kemper Meadow Dr, Cincinnati, OH 45240-1634, USA http://www.acgih.org

4) *Patty's Industrial Hygiene and Toxicology*, Vol. II, Part C, 4th ed., Wiley Interscience, pp 1973–1985.

Summary Report on Tests on Display Fireworks Conducted by the Bureau of Mines for the U.S. Department of Transportation Relative to Hazard Classification of Display Fireworks

J. Edmund Hay

Formerly: Supervisory Physical Scientist, Pittsburgh Research Center, U.S. Department of the Interior, Bureau of Mines, Pittsburgh, PA, USA

Introduction

The U.S. Department of Transportation (DOT) requested the U.S. Bureau of Mines to conduct tests on explosive substances and articles in support of the involvement of both agencies with the United Nations (UN) Group of Experts on Explosives pursuant to the development of an international classification system for explosive substances and articles. This request was embodied in Interagency Agreement No. DTRS 5684-X-00315. As a sub-set of the work performed under this agreement, DOT requested the Bureau to conduct special tests on samples of display fireworks (classified as class B fireworks at the time that the tests were done) in their normal shipping cartons. These tests included tests conducted according to the specifications of UN test series 6, and an additional test to determine the consequences of a fire involving a truck loaded with 500 pounds of class B Fireworks. Test procedures and results are reported herein. These tests were performed at a site leased by the Bureau from Consolidation Coal Co. in Harrison County, Ohio, during the period May 28–31, 1985.

The Department of Transportation (DOT) Hazardous Materials Regulations (HMR) published in title 49 Code of Federal Regulations (49 CFR) defines six classes of explosives consistent with the UN classification scheme, of which three are of relevance here, viz. class 1.1, class 1.3, and class 1.4. The general hazards of each class are (49 CFR 173.52):

Class 1.1 explosives — detonation or mass explosion hazard; generally corresponds to the former DOT class A.

Class 1.3 explosives — fire/minor explosion hazard, generally corresponds to the former DOT class B.

Class 1.4 explosives — minimum hazard, generally corresponds to the former DOT class C.

Throughout the text of this report the terms 'Class A', 'Class B', and 'Class C' are used even though no longer applicable, since they were correct at the time that the tests were done, whereas it would not be correct to use the UN terminology since the UN scheme was not in effect at the time the tests were performed and criteria applied were not completely in accordance with UN specifications.

i. Class 1 / Division 1.1 consists of explosives that have a mass explosion hazard. A mass explosion is one that affects almost the entire load instantaneously.

ii. Class 1 / Division 1.3 consists of explosives that have a fire hazard and either a minor blast hazard or minor projection hazard or both, but not a mass explosion hazard.

Table 1. Contents of Package of Ship and Show Fireworks.

(DOT Specification 12B65 fiberboard box 13"×13"×18-½"; Gross Weight 32 pounds)

Manufacturer	Size (diameter, in.)	Identification	Quantity
A	6	Green and silver	1
B	6	Green and silver	1
C	5	Color pearl	1
A	5	Red and green	1
D	5	#403	1
E	4	Red flitter	2
A	4	Blue and silver	2
D	4	#251	1
A	3	Red and green	4
F	3	Red, green and yellow	4
B	3	Green to red peony	2
B	3	Bright red and gold	2
G	3	Red rose	2
H	3	#378	1
C	3	Red and green	2
E	4	Blue and flitter	1
E	4	Red	1
G	4	White rose	2
B	3	Variegated peony	1

iii. Class 1 / Division 1.4 consists of explosives that present a minor explosion hazard. The explosive effects are largely confined to the package and no projection of fragments of appreciable size or range is to be expected. An external fire must not cause virtually instantaneous explosion of almost the entire contents of the package.

The test procedures employed (except for Test 4) represent versions of UN test series 6(a), 6(b) and 6(c); even though the UN classification scheme for explosives was not yet in effect in the U.S. at the time that the tests were done, its adoption was imminent and it was felt that these would be the appropriate test methodologies.

One purpose of the tests described in this report was to determine which of the above explosives classes, if any, should be assigned to the devices known as special fireworks. Another purpose was to evaluate the hazard of 500 pounds of certain fireworks (ship and show) when deliberately ignited in a motor vehicle. With the exception of the salute shells, all the fireworks tested were what is called in the fireworks industry "ship and show" fireworks. "Ship and show" fireworks are packaged fireworks designed for organizations such as Chambers of Commerce who wish to put on a relatively small display. Restrictions placed on these shipments by the industry are:

1) No salute shells.

2) No shells larger than 6 inch diameter.

3) No multi-break shells.

4) No more than 500 pounds gross weight in one vehicle.

Table 1 shows the shells making up a typical "ship and show" package. It is reasonable to assume that, if shells larger than 6 inch had been tested, the explosions and fires observed would have been larger.

Description of Tests

The test procedures and their results are described below.

Test No. 1: This was a test on a single package of assorted display (DOT class B) fireworks. The package was a DOT specification 12B fiberboard container measuring 12.5×13×19 inches, one of the cartons in which the fireworks were originally shipped from the manufacturer. The as-received cartons were not used for the test however, since each one contained fireworks of a different type (star shells, special effects shells, etc.), size, and manufacturer. The as-received cartons were opened and the individual shells were repacked in the carton used for the test so that this carton contained a representative assortment of each of the individual types, sizes, and makers. A list of the types of shells is given in Table 1.

The net weight of the fireworks in the carton was 32 pounds. Two ignitors each consisting of a small plastic bag containing 2 grams of grade FFFg Black Powder and an electric match-head were placed in the center of the carton. The carton was then sealed and laid on a 0.125-inch thick, mild steel witness plate 48×48 inches and was then surrounded and covered by a pile of sand-bags (100 pounds each) so that the thickness of the sand on all sides of and on top of the package was at least 20 inches (.508 meters). The resulting pile measured 53 inches wide × 59 inches long × 33 inches high.

Although not strictly required by the test procedure, four pressure gages (PCB Piezotronics type 112A21) were deployed at a distance of 50 feet in various directions.

Result: The ignitor was fired and a series of small, muffled explosions began inside the sandbag stack which displaced or destroyed some of the bags so that some of the remaining fireworks exploded under little if any confinement. Burning stars were projected as far as 200 feet from the package.

There was no evidence of detonation: no crater was observed and the witness plate under the carton was neither punched nor dented. The entire contents of the package were consumed, the process taking about 8 seconds. About 15

separate reports could be resolved; considering that reports and flashes from explosion of articles occurring before the sand pile was disrupted would be muffled and obscured respectively, it is not possible to conclude that the greater part of the articles exploded virtually simultaneously.

At this point one of the oscilloscopes was found to be triggering erratically, and two of the pressure gage records were lost. The remaining pressure gages recorded pressures of 0.38 and 0.36 psi, or an average pressure of 0.37 psi at 50 feet.

Test No. 2: This test was conducted on a stack of four packages, each 24×20×13 inches, and identical in contents to the one described in Test No. 1. The four packages were stacked in two layers consisting of two cartons side by side, the total contents were 128 pounds net of miscellaneous class B fireworks, the total volume of the stack was 10,800 cubic inches or 0.177 cubic meters. As in Test No. 1, two ignitors each consisting of 2 grams of grade FFFg Black Powder in a small plastic bag containing an electric match-head, were placed in one of the cartons near the center of the stack. The stack of packages were laid on a 0.125-inch thick mild steel witness plate, as in Test No. 1, and surrounded by a layer of 100-pound sand bags at least 40 inches (1.016 meters) thick on all sides including the top. (A layer of 0.25-inch thick plywood had to be laid over the top of the stack of cartons to keep the weight of the sand from crushing them. The final dimensions of the sand-bag pile were 104 inches wide × 120 inches long × 66 inches high, estimated to be 15 tons of sand. As in shot No. 1, pressure gages were deployed at a distance of 50 feet.

Result: The ignitors were fired and the contents of the stack began to explode, blowing away some of the sand bags, allowing the remainder of the fireworks to explode under little confinement. Burning stars were projected as far as 200 feet from the stack. The entire process consumed about 15 seconds. No crater was formed, the witness plate was found undamaged, and all the fireworks were consumed, as in Test No. 1. Only one pressure gage trace was obtained on this shot recording a pressure of 0.38 psi, virtually identical to that in shot No. 1.

The principal result is that the explosion did in fact propagate throughout the stack, but as in Test No 1, the muffling and obscuration of the explosions by the sand bags made it difficult to establish definitely whether the greater part of the articles exploded virtually simultaneously.

Test No. 3: This test was identical to Test No. 1 in all respects except that the contents of the carton were exclusively 3-inch salute shells, rather than assorted fireworks. Seventy-five shells were placed in the carton which measured 24×20×13 inches, which was provided with ignitors, placed on a 48×48×0.125-inch mild steel witness plate and confined with a 20-inch thickness of sand bags on all sides and the top, as in Test No. 1; two pressure gages were also deployed at a distance of 50 feet as in Test No. 1.

Result: The ignitor was fired and the contents of the carton exploded within about 4 seconds. Almost all of the sandbags were blown away and the witness plate was found to have a depression about 6 inches in diameter and about 0.5 inches deep; the pressure gages recorded lower pressures than expected considering the violence of the reaction relative to Test No. 1, viz., 0.42 and 0.24 psi, or an average of 0.33 psi. All of the fireworks were consumed. Only 8 individual reports could be resolved, out of the 75 expected. Considering the short interval of time involved, and the violence with which the sand pile was disrupted, it is not reasonable to suppose (as might have been the case in Tests 1 and 2) that the other 67 explosions might have occurred one at a time and were muffled. It is concluded that most of the items exploded virtually simultaneously and that a class C classification for salute shells would be entirely inappropriate. Indeed, it is our opinion that if the witness plate had not been used, a crater would have been formed; this, if it had occurred would be evidence suggestive of class A classification.

Test No. 4: This test was designed to determine the consequences of a small load of class B display ("ship-show") fireworks in a small truck being exposed to an external fire. Five hundred pounds of assorted ship-show fireworks in their shipping cartons were placed in the cargo compartment of a small delivery van of about 18 feet overall length. The specific fireworks used in the test are shown in Table 2 (located at the end of this article). The stack of cartons was placed in the left rear corner of the cargo compartment and the exposed (front, right, and top) sides of the stack were surrounded with sand bags to a thickness of 14 inches, to simulate the confinement provided by additional packages. The truck was jacked up so that the floor of the cargo compartment was about 3 feet off the ground. At the request of DOT, one of the pressure gages was placed inside the truck body about 3 feet from the stack of packages; another was deployed at a distance of 100 feet. The space under the truck beneath the stack of packages in the cargo compartment was filled with randomly piled pine blocks approximately 6 inches wide × 16 inches long × 1.5 inches thick, soaked with kerosene and ignited with a small bag of Black Powder containing an electric match-head.

Result: The fire burned for approximately 12 minutes before the packages began to explode. Unfortunately, after 9 minutes the internal pressure gage became inoperative, despite the brass cylinder in which it was inserted which was thought to provide enough thermal inertia to protect it. The explosion of the truck contents proceeded slowly over a period of about 20 seconds, with numerous flaming particles being ejected from the open doors and windshield for distances estimated to be about 150 feet. At the height of the event the truck seemed to be engulfed in flames. All of the fireworks were consumed. Damage to the truck included breakage of glass, numerous indentations of the inner walls, the melting of plastic parts, the thermal buckling of and springing of some seams in the sheet metal, and the scorching of paint. The external gage did not record pressure peaks that could be distinguished from the background noise, an upper limit would be about 0.08 psi. As in Tests 1 and 2, the explosion of the articles proceeded over an extended period of time, and it is not possible to state that the greater part of the articles exploded virtually simultaneously.

Test No. 5: This was a test of 4 cases of assorted class B fireworks packages as in Tests 1 and 2, exposed to an external fire. The four packages containing 128 pounds net weight were stacked on a steel grid about 18 inches off the ground. Beneath this grid, pine blocks ap-

proximately 6 inches×16 inches×1.5 inches were stacked. Aluminum witness plates 48 inches × 96 inches × 0.08 inches thick were set up on frames on 3 sides of the stack of packages, approximately 120 degrees apart; the plates were 13.3 feet (≈4 meters) from the stack and were oriented vertically, facing the stack with their lower edges approximately 2 feet off the ground. Two pressure gages were deployed at a distance of 50 feet and a pyrometer was also deployed at a distance of 50 feet. The wood under the stack was soaked with kerosene, provided with an ignitor as used in Test No. 4, and ignited.

Result: The stack of packages began to explode after about 80 seconds. The explosion of the contents proceeded over a period of about 11 seconds. All of the contents were consumed. The witness plates had numerous impact marks, probably from stars, but no significant indentations — they remained standing after the event. Burning stars were projected as far as 150 feet. The pressure gages recorded pressures of 0.19 and 0.56 psi. The pyrometer recorded a peak thermal flux of 0.12 cal/cm^2/sec of about one second duration, with a 5-second average value of 0.063 cal/cm^2/sec; the period of measurable thermal radiation was about 8 seconds. The pyrometer record also exhibited 3 spikes of short (less than 0.01 second) duration which exceeded the limits of the pyrometer at 1 cal/cm^2/sec; these may have been due to shells ejected from the stack exploding near the pyrometer; they may also represent electrical noise. It was quite evident that, although many individual reports and flashes were heard, the bulk of the items exploded in such a fashion that the individual flashes and reports blended together.

Following this test some unburned stars were found widely scattered around the test site. No intact shells were found however, and the presence of such relatively small amounts of unreacted material does not alter the conclusion that virtually all of the shells exploded.

Test No. 6: This was a repetition of Test No. 3, except that the box contained 73 rather than 75 three-inch salutes; the dimensions of the box were 12.5×13×26 inches. In all other respects the setup was identical.

Result: The result was very nearly the same as in Test No. 3 except that the explosion of the

contents proceeded over a period of about 5 seconds, no indentation of the witness plate was observed, and the maximum blast pressures recorded were 0.48 and 0.37 psi for an average of 0.43 psi. The same conclusions as those for Test No. 3 may be drawn here, viz. the overwhelming majority of the items exploded in a period of time too short to resolve, except that the lack of damage to the witness plate did not suggest that the result might have been a detonation.

Conclusions

In every case, complete propagation of explosion throughout the sample, whether in one package or many, was observed. In the case of one of the two tests involving salute shells, there was evidence (i.e., damage to the witness plate) suggesting that the result might have involved a detonation.

The results of the internal ignition tests and the external fire test indicate that a class C explosive classification would not be appropriate for assorted display fireworks. Since these items do not function by detonation, a class A explosive classification is also not appropriate for most of the fireworks tested, and since they function primarily by rapid combustion, it is concluded that a class B explosive classification is appropriate. A question arises as to whether salute shells are ever shipped as they were tested here (i.e., unmixed with other types of shells), and if so whether a class A explosive classification should be considered. In this respect, the results of the testing described above were not completely conclusive.

Summary

This report details tests conducted by the Bureau on class B (display) fireworks for single package, stacked package and bonfire tests, in addition to a special test involving a truck partially laden with fireworks exposed to an external fire. In no case involving ship-and-show fireworks did detonation result, but in all cases explosion propagated to and consumed the entire sample and burning stars were projected for considerable distances. It is concluded that a

proper classification for the fireworks tested, according to DOT specifications, would be class B Explosive, based on the tests performed, although there is a possibility, requiring additional testing to resolve, that salute shells, unmixed with other types of shells in the same package, might be properly classified as class A explosives.

Table 2. Fireworks Used in Truck Fire Test.

	Manufacturer	Size (diameter, in.)	Identification	Quantity
Box 1 (37 lbs)	C	5	Color pearl	3
	C	3	Assorted color	32
	D	6	#241, #243	2
	D	4	#337	3
	E	3	#578	20
Box 2 (32 lbs)	D	6	#254	1
	D	4	#553	1
	A	3	Red and green	12
	E	4	Red flitter	6
	C	5	Color pearl	2
	E	4	Blue flitter	6
	B	3	Variegated peony	14
Box 3 (40 lbs)	G	6	Blue diamond	2
	A	6	Green and silver	1
	A	5	Red and green	2
	A	4	Blue and silver	4
	A	3	Red and green	12
	B	3	Glittering silver chrysanthemum	17
Box 4 (32 lbs)	F	3	Assorted color	13
	B	3	Variegated peony	2
	G	6	Blue diamond	2
	E	4	Red flitter	7
	G	3	Red rose	10
Box 5 (42 lbs)	A	5	Red and green	7
	E	4	Blue flitter	12
	G	3	White rose	24
Box 6	C	5	Pearl comet	6
	E	4	Red	6
	G	3	White rose	18
Box 7 (39 lbs)	E	4	Red and flitter	31
Box 8 (35 lbs)	C	5	Color pearl	4
	E	4	Blue flitter	12
	G	3	Red rose	28

Table 2. Fireworks Used in Truck Fire Test (Continued.).

	Manufacturer	Size (diameter, in.)	Identification	Quantity
Box 9 (37 lbs)	D	6	#428, #345	2
	D	5	#403	2
	D	4	#254	2
	D	4	#364	3
	D	4	#327	1
	D	4	#254	1
	D	4	#338	1
	H	3	#578	25
	E	4	Blue and flitter	8
	G	3	Red rose	4
	B	3	Bright red to golden peony	7
Box 10 (38 lbs)	D	6	#243	1
	D	6	#245	1
	D	5	#345	1
	D	5	#392	1
	D	5	#241	1
	D	5	#381	1
	D	5	#403	1
	D	5	#357	1
	H	3	#578	19
	D	4	#365	2
	D	4	#252	2
	F	4	Assorted colors	13
Box 11 (42 lbs)	B	2	Variegated peony	25
	B	3	Blue peony	25
	B	3	Bright red to gold	25
Box 12 (40 lbs)	D	6	#245	1
	D	6	#241	1
	D	6	#344	1
	D	6	#521	1
	D	5	#392	1
	D	5	#391	1
	D	5	#389	
	D	5	#245	1
	D	4	#245	1
	D	4	#245	1
	D	4	#245	1
	D	4	#338	1
	D	4	#363	1
	D	4	#338	1
	D	4	#553	1
	D	4	Green peony	1
	D	4	#363	1
	D	4	#344	1
	H	3	#378	25
	B	3	Bright red to gold peony	20

Table 2. Fireworks Used in Truck Fire Test (Continued.).

	Manufacturer	Size (diameter, in.)	Identification	Quantity
Box 13 (42 lbs)	G	6	Blue diamond	4
	F	4	Assorted colors	12
	B	3	Red, green and gold peony	5
	B	3	Blue	12
	B	3	Glittering silver to variegated chrysanthemum	4
Box 14 (15 lbs)	G	6	Blue diamond	2
	C	5	Color pearl	1
	B	3	Blue peony	9
	B	3	Glittering silver variegated chrysanthemum	4

Future Events Information

If have information concerning future—explosives, pyrotechnics, fireworks, or rocketry—meetings, training courses or other events that you would like to have published in the *Journal of Pyrotechnics*, please provide the following information to the publisher of the Journal of Pyrotechnics:

Name of Event / Date and Place of Event / Contact information — including, if possible, name of contact person, address, telephone and fax numbers, email address and web site information.

This information will also be published on the Journal of Pyrotechnics Web Site: http://www.jpyro.com

Events Calendar

Pyrotechnics and Fireworks

Pyrotechnic Chemistry Course

30 April to 2 May 2001, Fort Halstead, UK
9 to 11 May 2001, Buxton, Derbyshire, UK

Contact: Ken Kosanke
PyroLabs, Inc.
1775 Blair Road
Whitewater, CO 81527, USA
   Phone/FAX: +1-970-245-0692
   email: ken@jpyro.com
   web: www.jpyro.com

Concours int'l d'art pyrotech. d Montréal 2001
Montréal Int'l Fireworks Competition 2001

June 20   La Ronde (Opening)
June 27   NICO-Lünig Event GmBH (Germany)
June 30   Pirotécnia Minhota Lda (Portugal)
July 7   San Tai Fwks, Ind. Co., Ltd. (Taiwan)
July 11   Pirotécnia Igual S.A. (Spain)
July 14   Pyro Spectaculars by Souza (USA)
July 18   Concept Fiatlux, Inc. (Canada)
July 21   Brezac Artifices (France)
July 25   Foti Int'l Fwks Pty. (Australia)
July 28   La Ronde (Closing)

Les Grands Feux Loto-Québec
Quebec Int'l Fireworks Competition 2001

July 21   A.P.E. Pirotecnia(Italy)
July 25   Flash Barrandov (Czech Republic)
July 28   Antonio Caballer (Spain)
Aug. 1   Pyro Spectacular (Africa)
Aug. 4   Beijing Zhong FA Fireworks (China)
Aug. 8   Finale
web: www.lesgrandsfeux.com

Les Grands Feux du Casino
Hull City Int'l Fireworks Competition 2001

July 28   A.P.E. Pirotecnia(Italy)
Aug. 1   Flash Barrandov (Czech Republic)
Aug. 4   Pyro Spectacular (Africa)
Aug. 8   Beijing Zhong FA Fireworks (China)
Aug. 11   Finale
For more info email: furtado@pyrocomp.com

Chemistry of Pyrotechnics & Explosives

July 29– Aug 3, 2001, Chestertown, MD, USA
Contact: John Conkling
PO Box 213
Chestertown, MD 21620, USA
   Phone: +1-410-778-6825
   FAX: +1-410-778-5013
   email: John.Conkling@washcoll.edu
   web: www.John.Conkling.washcoll.edu

Pyrotechnics Guild Int'l Convention

Aug. 4–10 2001, Appleton, WI, USA

Contact:, Ed Vanasek, Sec. Treas.
18021 Baseline Avenue
Jordan, MN 55352, USA
   Phone: +1-952-492-2061
   e-mail: edvanasek@aol.com
   web: www.pgi.org

4th Int'l Autumn Seminar on Propellants, Explosives and Pyrotechnics

Oct. 25–28 2001, Shaoxing, China

Contact: Dr. Chen Lang
Mechanics & Engineering Department
Beijing Institute of Technology
P O Box 327
Beijing 100081, China
   FAX: +86-10-6891-1849
   email: webmaster@iaspep.com.cn
   web: www.iaspep.com.cn

28th Int'l Pyrotechnics Seminar

Nov. 4–9 2001, Adelaide, Australia

Contact: Ken Smit, 28th IPS Coordinator
DSTO, Bldg 307 EOP
PO Box 1500
Salisbury, SA 5108, Australia
   Phone: +61-8-8259-6737
   FAX: +61-8-8259-6585
   e-mail: Adelaide.ips@dsto.defence.gov.au
   web: www.intlpyro.org/IPS28/

6th Int'l Symposium on Fireworks

Dec. 3–7 2001, Orlando, FL, USA

Dawn Stewart
Canadian Explosives Research Laboratory
555 Booth St.
Ottawa, ON K1A 0G1, Canada
  Phone: +1-613-995-1026
  Fax   +1-613-995-1230
  email: dstewart@nrcan.gc.ca
  web: fireworksfx.com/symposium.html

Energetic Materials

Computational Mech. Assoc. Courses–2001

Contact: Computational Mechanics Associates
PO Box 11314,
Baltimore, MD 21239-0314, USA
  Phone: +1-410-532-3260
  FAX: +1-410-532-3261
  web: www.compmechanics.com

19th Int'l Symp. on Ballistics

May 7–11 2001, Interlaken, Switzerland

Contact: Dr. Iris Crewther
Swiss Defense Procurement Agency
Feuerwerkerstrasse 39
CH – 3602 Thun, Switzerland
  Phone: +41-33-228-3058
  FAX: +41-33-228-3039
  email: i.crewther@ibs2001.org
  web: www.ibs2001.org

12th Int'l Symp. on Chemical Problems Connected with the Stability of Explosives

May 13–17 2001, Sweden

Contact: Stig Johansson
Johan Skyttes väg 18, SE 55448
Jönköping, Sweden
  Phone/FAX: +46-3616-3734
  email: srj@telia.com

32nd Int'l Annual Conf. ICT "Energetic Materials – Ignition, Combustion and Detonation**"**

July 3–6 2001, Karlsruhe, Germany

Contact: Manuella Wolff
Fraunhofer-Inst. für Chem. Technologie (ICT)
P. O. Box 1240
D-76318 Pfinztal (Berghausen), Germany

  Phone: +49-(0)721-4640-121
  FAX: +49-(0)721-4640-111
  email: mw@ict.fhg.de
  web: www.ict.fhg.de

3rd Int'l Symp. on Heat Flow Calorimetry for Energetic Materials

18–20 September 2001, French Lick, IN, USA

Contact: Mr JamesWilson
Naval Surface Warfare Centre
Code 4051, Bldg 108, 300 Highway 361,
Crane IN, 47522, USA
  FAX   +1-812-854-2890
  email: wilson_jim@crane.navy.mil

2001 Insensitive Munitions & Energetic Materials Technology Symp. (NDIA)

Oct. 8–11 2001, Bordeaux, France

Contact:Club MURAT
7 rue Latécoère, BP129
FR-78148 Velizy Cedx, France
  FAX: +33-139-46-1538
  email: imemts@clubmurat.com

ISEE's 28th Annual Conference on Explosives and Blasting Technique

February 10-13, 2002

Contact: Lynn Mangol
Las Vegas, NV, USA
  Phone: +1-440-349-4004

High Power Rocketry

LDRS 2001

Contact: see web site
    www.tripoli.org/launchpad/LDRS2001.html

Model Rocketry

NARAM 2001

Contact: — see web site for details:
web: www.naram2001.org
For launch information visit the NAR Web
site: www.nar.org

Keyword Index

The following list of keywords refers to articles that have appeared in Issues 1-12 of the *Journal of Pyrotechnics*. The numbers are paired. The first number is the Issue Number. The second number is the page number. For example, 10-17 means Issue 10, page 17. Following this is a listing of the article titles and beginning page. We hope that you find this list useful. For full abstracts and author names, refer to the JPyro Web Site: http://www.jpyro.com

Titles of Articles and Page Numbers for Issues 1 to 12

Journal Sponsors

Journal of Pyrotechnics wishes to thank the following Sponsors for their support.

Individual Sponsors:

Ed Brown
P.O. Box 177
Rockvale, CO 81244, USA
Phone: 719-784-4226
email: edwinde@cs.com

Larry Crump
2001 SE 11th Street
Mineral Wells, TX 76067, USA
Phone: 940-325-1517
FAX: 972-323-2252
email: lcrump1@wf.net
web: www.wf.net/~lcrump1

Sgt. John Giacalone
725 Jefferson Rd
S. Charleston, WV 25309, USA
Phone: 304-746-2242
FAX: 304-746-2174

Gerald Laib
Gerald Laib
17611 Longview Lane
Olney, MD 20832, USA
Phone: 301-744-4358
FAX: 301-744-4784

Corporate Sponsors:

Allied Specialty Insurance
David H. Smith
10451 Gulf Blvd.
Treasure Island, FL 33706, USA
Phone: 800-237-3355
FAX: 727-367-1407
email: info@alliedspecialty.com
web: www.alliedspecialty.com

American Fireworks News
Jack Drewes
HC 67 Box 30
Dingmans Ferry, PA 18328, USA
Phone: 570-828-8417
FAX: 570-828-8695
email: afn@98.net
web: www.fireworksnews.com

Astro Pyrotechnics
Leo Autote
2298 W. Stonehurst
Rialto, CA 92377, USA
Phone: 909-822-6389
FAX: 909-854-4749
web: www.astropyro.com

**Canadian Explosives
Research Laboratory**
Ron Vandebeek
CANMET - 555 Booth St.
Ottawa, ON K1A 0G1, Canada
Phone: 613-995-1275
FAX: 613-995-1230
email: rvandebe@nrcan.gc.ca
web: www.nrcan.gc.ca

Daveyfire, Inc.
Alan Broca
500 Ygnacio Valley Rd – Ste. 250
Walnut Creek, CA 94596, USA
Phone: 925-926-6414
FAX: 925-926-6439
email: daveyfire@msn.com

Delcor Industries Inc.
Sam Bases
19 Standish Ave.
Yonkers, NY 10710, USA
Phone: 914-779-6425
FAX: 914-779-6463
email: delcor@hotmail.com
web: www.delcorind.com

Dolliff, Inc. / Insurance
John Allen
6465 Wayzata Blvd. - Suite 850
St. Louis Park, MN 55426, USA
Phone: 800-338-3531/612-593-7418
FAX: 612-593-7444
email: JAllen@dolliff.com
web: www.dolliff.com

**European Pyrotechnic Arts
Newsletter**
Rob Driessen
Van Hoensbroekstraat 16
Swalmen, NL 6071 CN
The Netherlands
Phone: 31-475-501-711
FAX: 31-475-501-711
email: driessen@cuci.nl

Fawkes Fireworks
Tony Cardell and David Watts
89 Lingfield Road
Edenbridge, Kent TN8 5DY, UK
Phone: 44-1732-862-862
FAX: 44-1342-317-818
email: Tony@fawkes.co.uk

Fire One
Dan Barker
863 Benner Pike
State College, PA 16801, USA
Phone: 814-238-5334
FAX: 814-231-0799
email: info@fireone.com
web: www.fireone.com

Firefox Enterprises Inc.
Gary Purrington
11612 N. Nelson
Pocatello, ID 83202, USA
Phone: 208-237-1976
FAX: 208-237-1976
email: custserv@firefox-fx.com
web: www.firefox-fx.com

Fireworks Professionals
Anthony Lealand
PO Box 17-522
Christchurch, 8030, New Zealand
Phone: 64-3-384-4445
FAX: 64-3-384-4446
email: anthony@firework.co.nz

Fireworks
John Bennett
68 Ridgewood Gardens
Bexhill-in-Sea
East Sussex, TN40 1TS, England
Phone: 44-1424-733-050
FAX: 44-1424-733-050
email: JFBen@netcomuk.co.uk
web: fireworks.co.uk/fireworks-journal

**Fireworks and Stage FX
America**
Kevin Brueckner
P.O. Box 488
Lakeside, CA 92040-0488, USA
Phone: 619-596-2800
FAX: 619-596-2900
email: go4pyro@aol.com
web: www.fireworksamerica.com

Fireworks Business

Jack Drewes
HC 67 Box 30
Dingmans Ferry, PA 18328, USA
Phone: 717-828-8417
FAX: 717-828-8695
email: afn@98.net
web: www.fireworksnews.com

Fullam's Fireworks, Inc.

Rick Fullam
P.O. Box 1808 CVSR
Moab, UT 84532, USA
Phone: 435-259-2666

Goex, Inc.

Mick Fahringer
PO Box 659
Doyline, LA 71023-0659, USA
Phone: 318-382-9300
FAX: 318-382-9303
email: email@goexpowder.com
web: www.goexpowder.com

Harvey Productions. Inc.

Jack Harvey
2335 South 147th Street
Omaha, NE 68144-2047, USA
Phone: 402-681-5822
FAX: 402-333-9840

High Power Rocketry

Bruce Kelly
PO Box 970009
Orem, UT 84097-0009, USA
Phone: 801-225-3250
FAX: 801-225-9307
email: 71161.2351@compuserve.com
web: www.tripoli.org

Industrial Solid Propulsion Inc.

Gary Rosenfield
1955 S. Palm St. - Ste. 6
Las Vegas, NV 89104, USA
Phone: 702-641-5307
FAX: 702-641-1883
email: garyr@powernet.net
web: aerotech-rocketry.com
rocketmotorparts.com

Iowa Pyro Supply

Mark Mead
1000 130th St.
Stanwood, IA 52337, USA
Phone: 319-945-6637
FAX: 319-945-0007
email: iowapyro@netins.net
web: www.iowapyrosupply.com

Island Fireworks Co. Inc.

Charles Gardas
N735 825th St.
Hager City, WI 54014, USA
Phone: 715-792-2283
FAX: 715-792-2640
email: islndfwk@pressenter.com
web: www.pyro-pages.com/island

Kastner Pyrotechnics & Fireworks Mfg. Co

Jeri Kastner
Rt 3 938 Logtown Rd.
Mineral Point, WI 53565, USA
Phone: 608-987-4750
FAX: 608-987-4750
email: kastner@mhtc.net

Lantis Fireworks & Lasers

Ken Lantis
PO Box 491
Draper, UT 84020, USA
Phone: 801-768-2255
FAX: 801-768-2433
email: info@fireworks-lasers.com
web: www.fireworks-lasers.com

Luna Tech, Inc.

Tom DeWille
148 Moon Drive
Owens Crossroads, AL 35763, USA
Phone: 256-725-4225
FAX: 256-725-4811
email: PyropakUSA@aol.com
web: www.pyropak.com

Marutamaya Ogatsu Fireworks Co., Ltd.

1-35-35 Oshitate Fuchu
Tokyo, 183-0012, Japan
Phone: 81-42-363-6251
FAX: 81-42-363-6252
email: moff@za2.so-net.ne.jp

Mighty Mite Marketing

Charlie Weeth
122 S. 17th St.
LaCrosse, WI 54601-4208, USA
Phone: 608-784-3212
FAX: 608-782-2822
email: chzweeth@pyro-pages.com
web: www.pyro-pages.com

MP Associates Inc.

P.O. Box 546
Ione, CA 94640, USA
Phone: 209-274-4715
FAX: 209-274-4843

Ontos Pyrotechnics, Inc.

John and Karin Driver
1059 Carter Road
DeLand, FL 32724, USA
Phone: 904-736-8996
FAX: 904-740-0555
email: JWDriver@worldnet.att.net

Orbital Dynamics, Inc.

David F. Johnson
P.O. Box 45375
Rio Rancho, NM 87174, USA
Phone: 505-994-4000
FAX: 505-994-1000
email: rockettech@OrbitalDynamics.com
web: www.OrbitalDynamics.com

OXRAL, Inc.

Tom DeWille
P.O. Box 160
Owens Crossroads, AL 5763, USA
Phone: 256-725-4225
FAX: 256-725-4811
email: oxral@pyropak.com
web: www.oxral.com

Precocious Pyrotechnics, Inc.

Garry Hanson
4420 278th Ave. N.W.
Belgrade, MN 56312-9616, USA
Phone: 320-346-2201
FAX: 320-346-2403
email: ppinc@midstate.tds.net
web: www.pyro-pro.com

Pyro Shows, Inc.

Lansden Hill
P.O. Box 1406
LaFollette, TN 37766, USA
Phone: 800-662-1331
FAX: 423-562-9171
email: pyroshow@icx.net
web: www.pyroshowsusa.com

Pyrodigital Consultants

Ken Nixon
1074 Wranglers Trail
Pebble Beach, CA 93953, USA
Phone: 831-375-9489
FAX: 831-375-5225
email: pyrodig@aol.com
web: www.infinityvisions.com/pyrodigital

PyroLabs, Inc.
Ken Kosanke
1775 Blair Road
Whitewater, CO 81527, USA
Phone: 970-245-0692
FAX: 970-245-0692
email: ken@jpyro.com

RES Specialty Pyrotechnics
Camille Coman 1st VP
Route 1 Box 7601
Belle Plaine, MN 56011, USA
Phone: 612-447-7976
FAX: 612-447-0065
email: respyro@minn.net

Pyrotechnics Guild Int'l., Inc.
Ed Vanasek Treas.
18021 Baseline Avenue
Jordan, MN 55352, USA
Phone: 612-492-2061
FAX:
email: edvanasek@aol.com
web: www.pgi.com

RES Specialty Pyrotechnics
Steve Coman
Route 1 Box 7601
Belle Plaine, MN 56011, USA
Phone: 612-873-3113
FAX: 612-873-2859
email: respyro@minn.net

Service Chemical, Inc.
Ben Cutler
2651 Penn Avenue
Hatfield, PA 19440, USA
Phone: 215-362-0411
FAX: 215-362-2578

Skylighter, Inc.
Harry Gilliam
PO Box 480
Round Hill, VA 20142, USA
Phone: 540-554-2228
FAX: 540-554-2849
email: custservice@skylighter.com
web: www.skylighter.com

Starburst Pyrotechnics & Fwks. Displays (Pty) Ltd
Bonnie Pon
2nd Fl-Sui Hing Hong Bldg
17 Commissioner St
Johannesburg, Gauteng 2000
South Africa
Phone: 27-11-838-7704
FAX: 27-11-836-6839
email: starbrst@global.co.za
web: www.artslink.co.za/starburst

Sunset Fireworks Ltd.
Gerald Walker
10476 Sunset Drive
Dittmer, MO 63023, USA
Phone: 636-274-1500
FAX: 636-274-0883
web: www.sunsetfireworks.com

Syd Howard Fireworks International
Syd Howard
420 Halcrows Road - Glenorie
Sydney, NSW 2157, Australia
Phone: 61-29-652-2244
FAX: 61-29-652-1581
email: mail@sydhowardfireworks.com.au
web: www.sydhowardfireworks.com.au

The Show Factory Pty. Ltd.
Jack Moeller
Factory 3 / 21 Church Street
Abbotsford-Melbourne, VIC 3067
Australia
Phone: 61-3-9428-7710
FAX: 61-3-9428-0901
email: pyrohead@onthe.net.au

Western Pyrotechnics, Inc.
Rudy Schaffner
2796 Casey Road
Holtville, CA 92250, USA
Phone: 760-356-5426
FAX: 760-356-2051
email: renitad@thegrid.net

Sponsorships

No advertising as such will be printed in the *Journal of Pyrotechnics*. However, a limited number of sponsors will be sought so that the selling price of the Journal can be reduced from the listed cover price. The cost of helping sponsor an issue of the *Journal of Pyrotechnics* is $70 per issue for company sponsors. In addition to a listing in the Sponsor section of the Journal, the sponsor receives two complimentary copies of the sponsored Journal and a brief listing on a flyer inserted under the transparent cover of the Journal.

We recently introduced "Individual Sponsorships". The cost of an individual sponsorship is $35 per issue. In addition to a listing in the "Individual Sponsor" section of the Sponsor page, the sponsor receives one complimentary copy of the sponsored Journal and a brief listing on the s flyer inserted under the transparent cover of the Journal.

Additionally, if the sponsor so desires, we will provide a link from the Journal of Pyrotechnics Web Site to sponsor's web site, e-mail address or simply list a company name, address and phone information.

If you would like to be a sponsor contact the publisher.

Guide for Authors

Style Guide

The *Journal of Pyrotechnics* has adopted the *ACS Style Guide* [ISBN 0-8412-3462-0]. It is not necessary that authors have a copy; however, a copy can be ordered through a local bookstore.

Subject Areas

Fireworks, Pyrotechnic Special Effects, Propellants, Rocketry and Civilian Pyrotechnics

Manner of Submission

Submissions should be made directly to the publisher at the address at bottom of page. Upon receipt of an article, the author will be sent an acknowledgment and a tentative publication date. For specific requests regarding editors, etc. please include a note with that information. Preferably the text and graphics will be submitted electronically or on a 3-1/2" diskette or CD in IBM format with a print copy as backup. The Journal is currently using Microsoft Word 2000, which allows for the import of several text formats. Graphics can also be accepted in several formats. Please inform us if any materials need to be returned to the author.

General Writing Style

- The first time a symbol is used, it is preferred to write it out in full to define it [e.g., heat of reaction (ΔH_r) or potassium nitrate (KNO_3)].

- Avoid slang, jargon, and contractions.

- Use the active voice whenever possible.

- The use of third person is preferred; however, first person is acceptable where it helps keep the meaning clear.

Format

In addition to the authors' names, please include an affiliation for each author and an address for at least the first author.

A short abstract is needed. (An abstract is a brief summary of the article, not a listing of areas to be addressed.)

Include 3 to 7 keywords to be used in a reference database: However, multi-word names and phrases constitute only one keyword (e.g., potassium nitrate and heat of reaction are each one keyword).

Use of SI units is preferred. If English units are used, please provide conversions to SI units.

Figures, and Tables are numbered consecutively. For submission, place them at the end of the text or as separate files. During page composition, they will be inserted into the text as appropriate. For graphs, please also submit "raw" X–Y data.

References cited in the text are referred to by number (i.e., "Smith[1] states"; or "the research[2,3] shows ..."). In the reference section, they will be ordered by usage and not alphabetically. It is preferred that a full citation, including author, article title or book title, journal title or book publisher, and volume and pages for journals, etc. be provided. Examples:

1) A. E. Smith, *Pyrotechnic Book of Chemistry*, XYZ Publishers (1993) p nn–nn.

2) A. E. Smith, R. R. Jones, "An Important Pyrotechnic Article," *Pyrotechnic Periodical*, Vol. 22, No. 3 (1994) p n–n.

Editing

The *Journal of Pyrotechnics* is refereed. However, the editing style is friendly, and the author makes the final decision regarding what editing suggestions are accepted.

More Information

Contact
Bonnie Kosanke, Publisher,
Journal of Pyrotechnics, Inc.
1775 Blair Road
Whitewater, CO 81527, USA.
Or email: bonnie@jpyro.com